Studying Neuronal Connectivity in the Mouse Brain
in Normal Condition and Fragile X Syndrome

Dissertation

zur

Erlangung der naturwissenschaftlichen Doktorwürde
(Dr. sc. nat.)

vorgelegt der

Mathematisch-naturwissenschaftlichen Fakultät

der

Universität Zürich

von

Matthias Georg Haberl

aus

Deutschland

Promotionskomitee

Prof. Dr. Kevan Martin	(Vorsitz)
Dr. Andreas Frick	(Leitung der Dissertation)

Zürich, 2014

Acknowledgments

I am very grateful to my supervisor Andreas Frick for giving me the opportunity to work in his lab, for helping, guiding and supporting me throughout my PhD and I am very happy that I had the chance to be there during the establishing and growth of the Cortical plasticity lab. I would like to specially thank all the team members of the Frick lab: Melanie Ginger, Elisabetta Aloisi, Maria Szlapczynska, Guillaume Bony, Katy LeCorf, Virginie Labrousse, Vladimir Kouskoff, Elian Botelho, Audrey Bonnan, Yu Zhang – for their help, for providing a stimulating and fun environment for me to learn and grow. It has been a great pleasure to work with you.

I want to thank my co-supervisor Kevan Martin (Institute for NeuroInformatics Zurich) and all his lab members, in particular Nuno da Costa, for the time I could spend with them at the INI, for their thoughtful insights and the support they provided.

I wish to thank Karl-Klaus Conzelmann (LMU Munich) and the members of his team for the fruitful long-term collaboration and their expertise.

I would like to thank Arend Heerschap, Valerio Zerbi and Andor Veltien (UMC Radboud) for working with me for the magnetic resonance imaging measurements, it was a great pleasure and I really enjoyed my stay in Nijmegen and special thanks to Andor for all the time you spent.

I wish to thank also Marcel Oberlander and Mike Guest for the successful collaboration on the computational reconstruction of long-ranging axons.

I also want to thank Christophe Mulle for his support during the last years and for his advice, which was indispensable for the ENCODS organization.

I am grateful to all my friends in- and outside the lab for their every-day support and encouragement, Filipa, Sam, Nelson, Jo, Mario, Adam, Marilena, Joana, the soccer guys and many others, thank you for your moral support.

Above all, I would like to thank my parents for the constant support they gave me on this journey and for their constant inspiration that led me towards science. Without them I would not have achieved any of this. I would also like to thank my brothers and my entire family for being there for me anytime.

For your time, for your dedication, for your support, for being there during joy and misery, for being the kind person you are, everyday, I thank you, Silvia!

This work was supported with fellowships by the European Neuroscience Campus Network (ENC Network) Erasmus Mundus FP7 Program and a 4th year PhD extension grant Brain/LabEX and furthermore with a PhD Training provided by the SyMBaD – Marie Curie Initial Training Network (ITN).

The work for this thesis was carried out as a European Joint-Ph.D. in the labs of:

Home Institute
Dr. Andreas Frick
Neurocenter Magendie
University of Bordeaux
146 Rue Leo-Saignat
33000 Bordeaux
France

Guest Institute
Dr. Kevan Martin
Institute for NeuroInformatics
UZH/ETH Zurich
Winterthurerstrasse 190
8057 Zürich
Switzerland

Summary

The goal of this work was the investigation of the anatomical and functional connectivity of neuronal networks and the development of novel tools for this purpose. Since the latter aspect is a major focus of current neuroscience, we first sought a novel viral tracer enabling sparse neuronal reconstruction and neuron classification. We then applied this and other techniques to probe neuronal connectivity defects in Fragile X Syndrome.

In the first part we discussed the merits and drawbacks of a emerging technique using a new type of viral vector that allows in a unique manner mapping of the input of a given brain area.

In the second part we developed, departing from this viral vector, a new variant to facilitate the tracing and reconstructing of morphologic features of neurons. We showed the strength of this anterograde variant of the recombinant glycoprotein-deleted rabies virus for computational reconstruction of all key morphological features of neurons: dendrites, spines, long-ranging axons throughout the brain and bouton terminals.

In the third part we examined alterations in the wiring of brain structures in the Fragile X Syndrome (FXS). FXS is the most common inherited mental retardation and most frequent genetic form of autism, leading to learning and memory deficits, repetitive behavior, seizures and hypersensitivity to sensory (e.g. visual) stimuli. One of the eminent hypotheses in the autism field assumes a local hyper- connectivity phenotype but hypo-connectivity for long-ranging connections. To test this hypothesis in a FXS mouse model we used magnetic resonance imaging, to scan the entire brain and measure the anatomical and functional connectivity. This allowed us to identify connectivity alterations in several areas that we further explored using viral tracers. Using retrograde rabies virus to count the number of neurons projecting to such areas we confirmed an altered input connectivity to the primary visual cortex, which could contribute to the altered visual information processing. We discovered an overall reduced anatomical and functional long-range connectivity between several brain areas, identifying FXS as pathology of neuronal connectivity, which might explain the difficulties several rescue strategies aiming at molecular targets are currently facing.

Keywords: Viral tracing, Fragile X Syndrome, Connectivity

Titre en français:

Neuronale connectivité dans le cerveau de souris en condition normale et en syndrome du X fragile

Résumé en français:

Le but de ce travail est l'étude de la connectivité anatomique et fonctionnelle des réseaux neuronaux et le développement des nouveaux outils à cet effet. Car le dernier aspect est une préoccupation majeure de la neuroscience actuelle, nous avons developpé d'abord un nouveau traceur virale permettant la reconstruction neuronale. Nous avons ensuite appliqué cet et d'autres techniques pour sonder les défauts de connectivité neuronale dans le syndrome de l'X fragile.

Dans la première partie, nous avons discuté les avantages et inconvénients d'une technique émergente en utilisant un nouveau type de vecteur viral qui permet une unique application pour l'étude du cerveau.

Dans la deuxième partie, nous avons développé, au départ de ce vecteur viral, une nouvelle variante de faciliter le traçage et reconstruction des caractéristiques morphologiques de neurones. Nous avons montré la force de cette variante antérograde du virus de la rage recombinant glycoprotéine supprimé pour la reconstruction de calcul de toutes les caractéristiques morphologiques clés de neurones: les dendrites, épines, les axones longs envergure dans tous les terminaux du cerveau et les boutons.

Dans la troisième partie, nous avons examiné les modifications dans la connectivité des structures cérébrales dans le syndrome du X fragile (FXS). FXS est le retard mental héréditaire la plus fréquente et la forme génétique la plus fréquente de l'autisme, ce qui conduit à l'apprentissage et de la mémoire des déficits, les comportements répétitifs, des convulsions et une hypersensibilité à des stimuli sensoriels (visuels). Une des hypothèses éminents dans le domaine de l'autisme suppose une phénotype de hyper-connectivité locale mais de hypo-connectivité pour les connexions longue portée. Pour tester cette hypothèse dans un modèle de souris FXS nous avons utilisé l'imagerie par résonance magnétique, pour balayer la totalité du cerveau et de mesurer la connectivité anatomique et fonctionnel. Cela nous a permis d'identifier des altérations de connectivité dans plusieurs domains. Après nous

avons utilisé des traceurs viraux pour explorer un de ceux domains plus detaillé. En utilisant le virus de la rage rétrograde à quantifier le nombre de neurones projetant vers ces zones, nous avons confirmé une connectivité d'entrée modifié pour le cortex visuel primaire, ce qui pourrait contribuer au traitement visuel altéré de l'information. Nous avons découvert une connectivité réduite à longue portée globale anatomique et fonctionnelle entre plusieurs régions du cerveau, l'identification FXS comme une pathologie de la connectivité neuronale, ce qui pourrait expliquer les difficultés de plusieurs stratégies de sauvetage visant des cibles moléculaires sont actuellement confrontés.

Mots clés en français: Traçage Virale, Syndrome du X Fragile, Connectivité

Titel:

Studie der neuronaler Konnektivität des Gehirns der Maus im normalen Zustand und im Fragilen X-Syndrom

Zusammenfassung:

Das Ziel dieser Arbeit war die Untersuchung der anatomischen und funktionellen Konnektivität neuronaler Netze und die Entwicklung neuer Werkzeuge für diesen Zweck. Da der letztgenannte Aspekt ein wichtiger Schwerpunkt der aktuellen neurowissenschaftlichen Forschung ist haben wir zuerst einen neuartigen viralen Tracer entwickelt der die neuronale Rekonstruktion erleichtert. Des weiteren haben wir dieses Virus zusammen mit anderen Techniken angewendet, um Änderungen der neuronalen Konnektivität im Fragilen-X-Syndrom zu untersuchen.

Im ersten Teil erörterten wir die Vorteile und Nachteile einer Schwellentechnik, die es mit Hilfe eines neuen viralen Vektors in einzigartiger Weise erlaubt, die Eingänge in bestimmte Hirnregion zu bestimmen.

Im zweiten Teil haben wir, ausgehend von diesem viralen Vektor, eine neue Variante entwickelt, um die Sichtbarmachung und Rekonstruktion von morphologischen Eigenschaften von Neuronen zu erleichtern. Wir zeigten die Stärke dieser anterograde Variante des rekombinanten Tollwut-Virus für die Rekonstruktion aller wichtigen morphologischen Merkmale von Neuronen: Dendriten, Spines, lange Axone durch das Gehirn und axonale Boutons.

Im dritten Teil untersuchten wir Veränderungen in der Verdrahtung von Hirnstrukturen im Fragilen X Syndrom (FXS). FXS ist die häufigste vererbte geistige Behinderung und häufigste genetische Form des Autismus. FXS führt zu Lern-und Gedächtnisdefiziten, repetitiven Verhaltensweisen, Epilepsie und Überempfindlichkeit auf Sinnesreize (z.B. visuell). Eine der bedeutendsten Hypothesen in dem Gebiet des Autismus geht von einer lokalen hyper-Konnektivität aber einer hypo-Konnektivität für weit enfernte Verbindungen aus. Um diese Hypothese in einem FXS-Mausmodell zu testen verwendeten wir Magnetresonanztomographie, um das gesamte Gehirn zu scannen und die anatomischen und funktionellen Konnektivität zu messen. Dies erlaubte uns, in mehreren Bereichen, Konnektivitätsänderungen zu identifizieren. Diese Änderungen konnten wir anschließend unter Verwendung von viralen Tracern weiter untersuchen.

Durch das Verwenden eines retrograden Tollwutvirus konnten wir die Anzahl von Eingangsverbindung von Neuronen zu einem dieser Bereiche, dem primären visuellen Kortex, quantifizieren. Wir entdeckten insgesamt eine Reduktion der anatomischen und funktionellen Langstrecken-Verbindungen zwischen mehreren Hirnarealen. Dies identifiziert FXS als eine Pathologie der neuronalen Konnektivität, und bietet eine Erklärungsmöglichkeit für die Schwierigkeiten der zur Zeit getesteten Medikamente im FXS.

Schlüsselwörter: Virales Tracing, Fragiles-X-Syndrom, Konnektivität im Gehirn

Publications

The present study consists of work that has been published or is submitted for publication in international peer-reviewed journals:

Publication N. 1 Revealing the secrets of neuronal circuits with recombinant rabies virus technology Melanie Ginger*, **Matthias Haberl***, Karl-Klaus Conzelmann, Martin K. Schwarz and Andreas Frick. *Equal contributions. Frontiers in Neural Circuits, Published online January 24, 2013

Publication N. 2 An anterograde rabies virus vector for high-resolution large-scale reconstruction of 3D neuron morphology**. Matthias Georg Haberl***, Silvia Viana da Silva*, Jason M. Guest, Melanie Ginger, Alexander Ghanem, Christophe Mulle, Marcel Oberlaender, Karl-Klaus Conzelmann and Andreas Frick. *Equal contributions. Brain Structure and Function, Published online April 11, 2014

Manuscript N. 3 Structural and functional connectivity deficits of the neuronal circuits in Fragile X Syndrome. **Matthias Georg Haberl**, Valerio Zerbi, Andor Veltien, Melanie Ginger M, Arend Heerschap, Kevan Martin and Andreas Frick. Manuscript in preparation for submission

Bookchapter:
Manuscript N. 4 Use of Rhabdoviruses to Study Neural Circuitry. Melanie Ginger*, Guillaume Bony*, **Matthias Haberl** and Andreas Frick. *Equal contributions. (Appearing in Biology and Pathogenesis of Rhabdo- and Filoviruses by World Scientific Publishing Co.).

List of Abbreviations

AAV	Adeno-Associated Virus
ADHD	Attention Deficit Hyperactivity Disorder
Am	Amygdala
ASD	Autism Spectrum Disorder
Au	Auditory Cortex
BOLD	Blood Oxygen Level Dependent Signal
CA1, CA3	Hippocampal regions: Cornus Ammonis 1 and 3
CAV	Canine Adeno-Virus
CNS	Central Nervous System
CPu	Caudate Putamen
DH	Dorsal Hippocampus
DLG	Dorsal Lateral Geniculate Nucleus
DT-MRI; DTI	Diffusion Tensor Magnetic Resonance Imaging
DG	Hippocampal region: Dentate Gyrus
EC	Entorhinal Cortex
EEG	Electroencephalography
FA	Fractional Anisotropy
FLN	Fraction of Labeled Neurons
***Fmr1*KO**	*Fmr1* Gene Knock out
FMRP	Fragile X Mental Retardation Protein
FXS	Fragile X Syndrome
GABA	Gamma-Aminobutyric Acid
GFAP	Glial Fibrillary Acidic Protein
LGP	Globus Pallidus
GM	Grey Matter
L 1-6	Layers 1-6 of the cortex
LGN	Lateral Geniculate Nucleus
LTD	Long-Term Depression
L	Gene encoding the Polymerase of the Rabies Virus
LV	Lentivirus
M	Gene encoding the Matrixprotein of the Rabies Virus

MBP	Myelin Basic Protein
MD	Mean Diffusivity
mGluR5	Metabotrobic Glutamate Receptor 5
Mo	Motor Cortex
MRI	Magnetic Resonance Imaging
NA	Numerical Aperture
PF	Parafascicular Nucleus
PFA	Paraformaldehyde
Pi	Piriform Cortex
PtA	Pretectal Area
RABV	Rabies Virus
ROI	Region of Interest
RS	Retrosplenial Cortex
rs-fMRI	resting state functional MRI
S1	Primary Somatosensory Cortex
SAD	Street Alabama Dufferin B19 strain of rabies virus
SADΔG	Glycoprotein deleted variant of SAD
SADΔG-eGFP	Glycoprotein deleted variant of SAD, expressing enhanced green fluorescent protein
SADΔG-eGFP (EnvA)	Glycoprotein deleted variant of SAD, enveloped with a surface protein derived from the subgroup A avian sarcoma and leukosis virus
SADΔG-mCherry (VSV^{Ctm})	mCherry expressing Glycoprotein deleted variant of SAD, enveloped with a vesicular stomatits virus derived surface protein
T	Tesla
UTR	Untranslated Region
V1	Primary Visual Cortex
VH	Ventral Hippocampus
VPN	Ventral Posterolateral Nucleus and Ventral Posteromedial Nucleus
WM	White Matter
WT	Wild type

1. General Introduction

The brain is the most complex organ in our body conversely it is the least understood. But what is it that makes our brain so complicated?

The human brain contains a large number of cells – with an estimated of 10^{11} neurons and $3x10^{12}$ glial cells – almost 10 times greater than the number of hepatocytes and similar to the number of dermal cells but in comparison only $1/10^{th}$ of the number of erythrocytes that we have in our blood (Bianconi et al., 2013). We have a good understanding of how red blood cells or most organs of our body work. In contrast, neuroscience cannot, to date, give a clear answer to the question of how many cell types comprises the brain. For example it has been shown in the last years that glial cells are not a single group of cells but in fact arise from different origins and are classified at least into three broad groups: microglia, macroglia (like astrocytes) and others. These groups should probably be further subdivided (Cahoy et al., 2008), based on additional properties, such as gene expression patterns. On the other hand, neurons have a single common feature, they are all electrically excitable, but at the same time they are also highly diverse. The criteria for classifying neurons in subgroups are still highly debated but good candidates could be gene profiles, neurotransmitters expression or the pattern of their processes (Fishell and Heintz, 2013). The cell types problem is tightly linked to a large diversity of cell connections and interactions happening in the brain. Both neurons and glial cells can possess numerous processes, which can either be extremely ramified and fine (Bushong et al., 2002), e.g. astrocytes for removing neurotransmitters from the synaptic cleft, or in the case of neurons develop over several millimeters to connect one to another. The extreme complexity of the anatomical properties of brain cells is one of the main reasons why the brain is difficult to study. In addition, although not discussed further, the multitude of plasticity mechanisms that can also alter communication between neurons, without changing the anatomy. The anatomy however provides a frame of possibilities and limitations, showing us which brain areas and cells are directly interacting.

Camillo Golgi (1844-1926) and Santiago Ramón y Cajal (1852–1906) were pioneers in the field of labeling and 'reconstructing' the neuron morphology and presented us the first impressive portraits of brain cells (**Figure 1.1**; (Sotelo, 2003)).

Both researchers worked with a silver-chrome staining method that Golgi had developed, leading to a black staining of random cells ('la reazione nera'; see **Figure 1.1**) and permitting the visualization of neural networks (Golgi, 1873). Since these early days of neuroanatomy our knowledge of the neuronal wiring has increased drastically and numerous diagrams of isolated brain circuits within, or between brain areas have been developed (e.g. **Figure 1.2**).

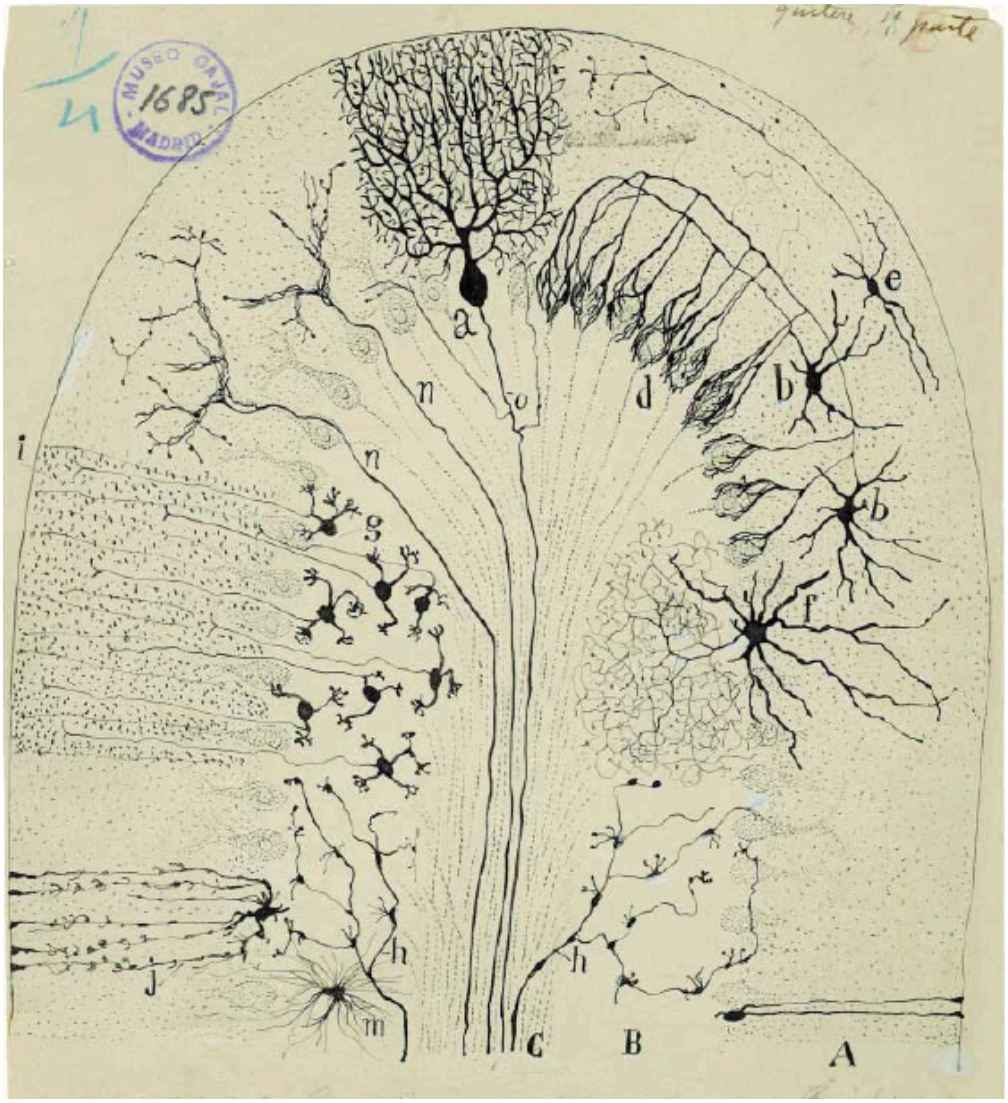

Figure 1.1 The organization of a follum of the cerebellar cortex.

This drawing, made by Ramón y Cajal in 1894 for a conference at the Medical Sciences Academy of Catalonia, places all neural cells and afferent fibres in a three-dimensional perspective. In this parasagittal section, dots represent the parallel fibres. Figure from (Sotelo, 2003)

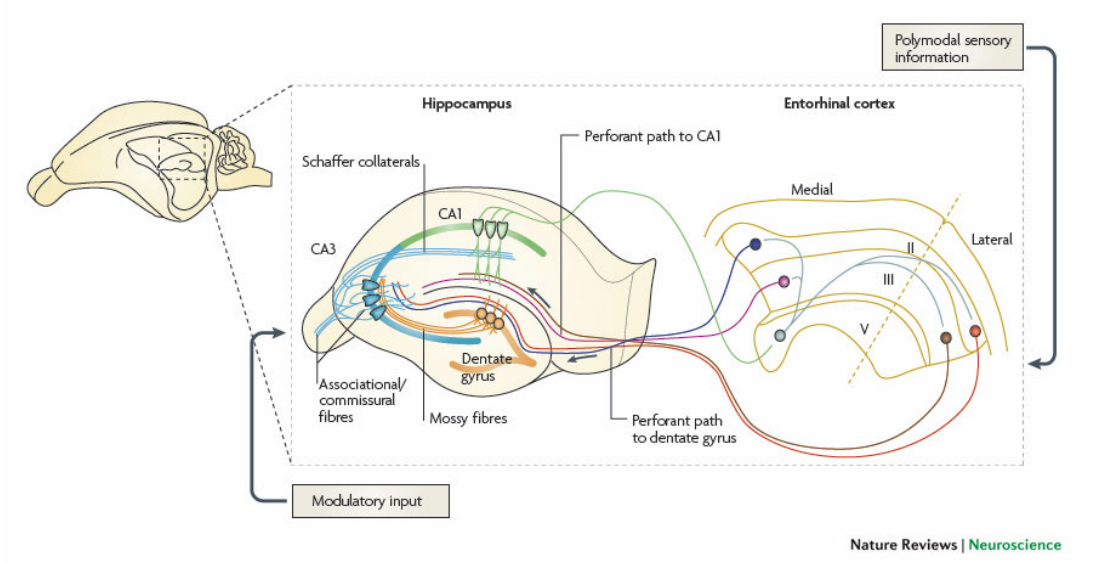

Figure 1.2 Simplified wiring diagram of the hippocampus

The entorhinal cortex (EC) receives sensory information that is afterwards sent to the hippocampus trough several pathways. The EC projects directly to the dentate gyrus via the perforant path. Other layers of the EC project to the distal regions of CA1 cells. Granule cells of the DG region send their axons to the proximal regions of CA3 pyramidal cells. CA3 pyramidal cells form a densely interconnected, associative network. CA3 pyramidal cells also project to the proximal regions of CA1 cells. Finally CA1 works as the main output region of the hippocampus, sending fibers to the deeper layers of EC. Further modulatory input to hippocampal neurons is received by fibers from other brain areas such as the septum. Figure modified from (Neves et al., 2008)

Before we just storm out looking for a full description of all circuits in the brain, which we (unfortunately?) do not possess and also will not have in any time soon, it would be important to define what is it that we are looking for? For one, drawing maps of the neuronal network is a cartographic endeavor, describing in a way similar to what is being done with electrical circuits, a sequence of (electrical) units, arranged in series or parallel. Having circuit maps of the brain bears the advantage that we can compare them, find patterns, common schemes and/or alterations in disease. However, when looking at single cell resolution we will either have to reduce the maps to the important parts, otherwise it will become too complicated (see the simplified diagram of the hippocampus **Figure 1.2**), or even better annotate a factor of relevance to each link (see **Figure 1.3**). Such an annotation could reflect how commonly the connection occurs, how strong it typically is or even if it is functionally

relevant. Important features beyond the connection/non-connection of the circuit are which cell types are involved, and information about the synapse types and locations.

Among the distinct brain areas in the human brain the one that sticks out as the most puzzling is the neocortex. This layered structure that has *colonized* around 85% in the human brain and is crucial for all our higher cognitive function. Structurally, it is tremendously intertwined in a complex fashion and many of its neurons seem to not respect their layer boundaries, with input and output from/to countless areas. In fact, regarding neuronal contacts in the neocortex, only a few general rules are applicable, which help us to understand the information flow through the cortex. Those common cortical denominators, called canonical circuits (**Figure 1.3**), have been discussed recently together with the course that has been taken for finding those paths of the neocortex (Douglas and Martin, 2007).

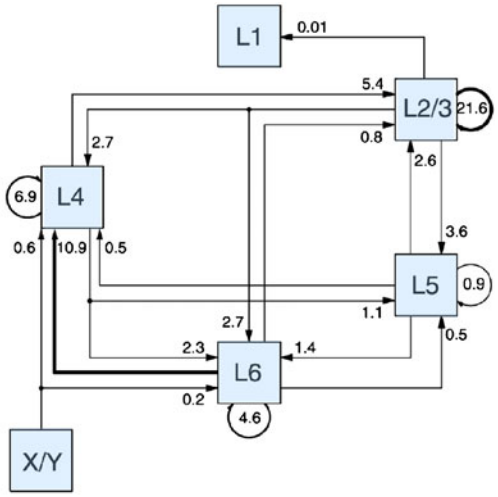

Figure 1.3 Canonical neocortical circuits
Quantitative map of anatomical connections between the major excitatory and inhibitory neuron types in area 17 of the cat, including the X-type and Y-type afferents to area 17 from the dorsal LGN. Each arrow is labeled with a number indicating the proportion of all the synapses that are formed between excitatory neurons. Figure from (Binzegger et al., 2004)

The development of new methods for studying brain wiring has always been a substantial part of neurosciences, allowing us to address numerous different aspects of anatomical and functional connectivity (e.g. frequency, density or type of connection). Such methods are all indispensable to improve our understanding of the brain. In line with this notion, the first goal of my Ph.D. project was to implement and develop new techniques that would allow a new perspective on the brain wiring. Each of the methods has merits and drawbacks and in **Chapter 2.1** both will be discussed for a cutting-edge technique that has been introduced in the last years, the mono-trans-synaptic tracing, a method that allows the identification of the input of a defined set of neurons.

Chapter 2.2. describes the development and application of a new viral vector which we developed during this PhD project to facilitate the tracing and reconstruction of morphological features of neurons. We demonstrate the capacity and potential of this anterograde variant of the recombinant glycoprotein-deleted rabies virus for sparse labeling and computational reconstruction of all key morphological features of neurons: dendrites, spines, long-ranging axons throughout the brain and bouton terminals (Haberl et al., 2014).

In the last years new tools have been introduced and used to study the brain wiring in healthy brains and cognitive disorders and it has become evident that several brain diseases exhibit alterations in the neuronal wiring. Most prominent among those are neurodegenerative diseases (Greicius and Kimmel, 2012) but also schizophrenia (Uhlhaas, 2013) and developmental disorders like autism spectrum disorders (ASD) (Geschwind and Levitt, 2006). Fragile X Syndrome (FXS) is the most frequent genetic cause of ASD and most common inherited mental retardation, leading to learning and memory deficits, repetitive behavior, seizures and hypersensitivity to sensory stimuli (O'Donnell and Warren, 2002). ASDs and FXS are both thought to have a wiring component as a feature of their deficits (Geschwind and Levitt, 2006; He and Portera-Cailliau, 2013). As described in **Chapter 2.3** we applied a combination of neuroanatomical tools to define the how the circuits are changed in FXS on the large- and small-scale. We used magnetic resonance imaging, to scan the entire brain and measure the anatomical and functional connectivity. This allowed us to identify connectivity alterations in several areas, which we further explored using viral tracers. Using retrograde rabies virus to visualize and quantify the number of neurons projecting to such an area we confirmed an altered input connectivity to the primary visual cortex, which could contribute to the altered visual information processing found in FXS.

1.1. Novel Tools for Studying Brain Wiring

Brains are unique in the complexity with which individual cells are connected to one another. Untangling these interconnections is a tremendous challenge given that e.g. the human brain consists of ~85 billion neurons most of which form over 1000 contacts with other neurons. Large efforts in neuroscience are devoted to delineate these connections for the purpose of creating maps of the brain structure, with the hope it will be helpful to understand the function of the brain. The extraordinary thing about the structure of neurons is their shape, usually having many extensions, which we know now serve as wires for the physical transmission of their communication signals. With this in mind we can also describe the questions about the neuronal anatomy differently - in terms of communication - and it becomes more evident why structure is an important feature. It contains the knowledge about where the neurons receive signals from and where they transmit to. The list of techniques used for these questions is long. Such techniques can reveal connections between brain-areas (Goñi et al., 2014) or even of between single-cell (Vélez-Fort et al., 2014), some methods are able to proof functional connections of defined cells (Debanne et al., 2008), others are able to provide quantitative measures of synaptic connectivity and synapse location (Binzegger et al., 2004). None of the techniques currently available is sufficient alone, to provide us a complete description of all connections and the connection strength in a complex brain, but most of the techniques can be used in a complementary fashion and will advance our knowledge when well combined. Neural circuits consist of local connections - where pre- and postsynaptic partners reside within the same brain area - and long-distance connections, which link different areas. Connectivity studies can therefore address short- and/or long-ranging connections. In this chapter I will introduce the concepts of two powerful techniques, which were used in this work: (i) the tracing of neuronal networks with viral vectors, which is invasive, but provides cellular resolution about the structure; and (ii) the non-invasive magnetic resonance imaging, limited to the macroscale, but which allows us to glean a structural and functional overview of connections of the whole brain.

1.1.1 Viral Tracing Tools to Unravel Neuronal Circuits

Due to several important features, viral vectors are widely used for studying the structure and function of neuronal circuits and more recently to achieve cellular precision. One major advantage of viral vectors is that they are ideal for expressing transgenes, allowing us to label circuits and monitor or manipulate the activity within these circuits (Osakada and Callaway, 2013). In transneuronal viruses, this feature is further combined with their ability to cross multisynaptic pathways and still achieve sufficient protein expression after several steps, making them ideal for the study of neuronal circuits (reviewed (Callaway, 2008)).

A number of different viruses are commonly used to study neuronal circuits and for each question at hand the best vector should be identified beforehand. Those vectors differ in a number of properties the most important among those are ease of handling, ease of production, packaging size, diffusion in the tissue, cellular uptake point, cell tropism, expression levels, expression speed and cytotoxicity.

Gold standards for the type of viral tracer that infects cells at the cell body/dendrite and fills their axonal projections anterogradely - which are called anterograde tracers (**Figure 1.4 A**) - are lentivirus (LV) and adeno-associated virus (AAV). LVs provide the advantages of a relatively strong and fast protein expression (e.g. fluorescence labeling) and large packaging size (Jakobsson and Lundberg, 2006), whereas AAVs exhibit basically no cytotoxicity, can infect large brain areas and provide a different tropism, targeting preferentially inhibitory and excitatory cells (Nathanson et al., 2009) but suffering from a lower packaging capacity (Aschauer et al., 2013; Wu et al., 2010). AAVs can be thoroughly purified and concentrated to extremely high titers, further reducing side effects that are often introduced to the injected brain tissue by impurities coming from the production process (McClure et al., 2011).

Anterograde tracers are commonly used to label the projections and thereby target regions of a particular brain area or to reconstruct features of neuronal morphology. Retrograde tracers, on the other hand, are mainly used to identify the, classify and study neurons projecting to a certain target area. Anterograde and retrograde tracers alone or together have been used over decades to identify brain pathways. Recently three different large-scale mapping projects injected such tracers

into hundreds of target areas in the mouse brain (Hunnicutt et al., 2014; Oh et al., 2014; Zingg et al., 2014) providing us now with a large online repository about the neuronal circuits.

Retrograde tracers get taken up by axon terminals of neuronal projections and label also the cell bodies of those projecting neurons (**Figure 1.4 B**). Commonly used retrograde tracers are chemical tracers like horseradish peroxidase, cholera-toxin subunit B, or fluoro-gold. Neurotropic viruses like rabies virus or pseudorabies virus (mainly the Bartha strain) are often used to trace multiple steps trans-synaptically as described below. In our hands the use of viral tracers in general has the advantage that it can provide an intense, complete labeling of the cells, which facilitates the subsequent counting and localization of projecting cells, which might not always be achieved by chemical tracers. Chemical retrograde tracers also do not reveal whether axons branching in the region of interest make synaptic contacts onto particular cells. Such information can be gathered using transsynaptic viruses, which label chains of synaptically connected neurons. They cross from one neuron to another and replicate at each step, therefore amplifying their signal, which chemical tracers will not do. Commonly used transneuronal tracers (reviewed in (Callaway, 2008)) are herpes viruses and different types of rabies strains (reviewed in (Kelly and Strick, 2000)). Recently, a genetically modified rabies virus variant has been engineered that allows monosynaptic trans-synaptic tracing in a retrograde manner, defining the presynaptic 'input map' into neurons (**Figure 1.4 C**).

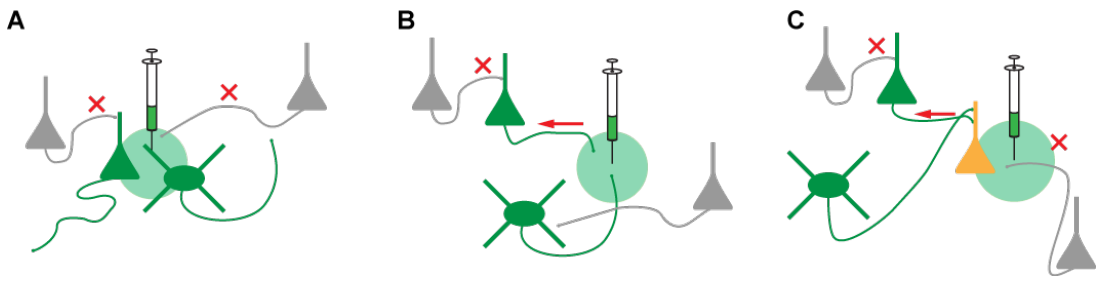

Figure 1.4 Scheme of different tracer types. A) Anterograde tracers label cells and projections from the cell body. B) Retrograde tracer enter the cells at the axons and label those projecting cells. C) Mono-trans-synaptic retrograde tracer, label specifically the pre-synaptic connections of a defined subset of cells, thereby labeling the input of the starter cells. Modified from (Ginger et al., 2013)

The next section provides a description/discussion of how a new recombinant glycoprotein-deleted variant of the SAD-strain of rabies virus has been created and

further how the new vector is now being widely used for two experimental settings (i) as retrograde tracer (not trans-synaptic) and (ii) as retrograde mono-trans-synaptic tracer for mapping the input of specific brain regions or neurons.

1.1.2 Rabies Virus Based Mono-Trans Synaptic Input Mapping

Unfortunately trans-neuronal viral tracers cross multiple synapses and it is suspected that they cross some (e.g. stronger) synapses faster than others making the distinction between first and higher-order connections close to impossible. Therefore, the development of a trans-synaptic tracer that is restricted to mono-synaptic connected cells was a ground-breaking development in the field of circuit neuroscience. The method is based on a pseudotyped rabies virus derived from the vaccine strain of rabies virus, Street Alabama Dufferin (SAD) B19. Rabies virus is a single-stranded enveloped RNA-virus and a member of the Rhabdoviridae family. The negative stranded RNA contains only five genes, encoding for the nucleoprotein (N), the phosphoprotein (P), the matrixprotein (M), the glycoprotein (G) and the polymerase (L). It was possible to reconstitute the SAD B19 strain from the individual cDNAs and an antisense genome construct. As a result the function of all gene products can be examined and modifications can be engineered in the virus genome (Conzelmann and Schnell, 1994). Furthermore, it permitted the introduction of foreign genes, rendering rabies virus useful as vector for transgene expression. The next important step was the development of a recombinant rabies virus strain, SADΔG, in which the endogenous gene encoding the G protein was deleted (Mebatsion et al., 1999). This renders the virus incapable of crossing synapses (Etessami et al., 2000). The retrograde variant of this virus is generated by pseudotyping this recombinant virus with its own glycoprotein, thereby generating the single-step retrograde tracer SADΔG -(SAD-G) (Wickersham et al., 2007a).

To generate the mono-trans-synaptic tracer, the virus was instead pseudotyped with an envelope protein (EnvA) derived from the subgroup A avian sarcoma and leukosis virus -(ASLV-A) (Wickersham et al., 2007b). This pseudotyping makes the virus infectious exclusively to cells expressing the TVA viral receptor, a protein found in birds but not in mammals. The resulting pseudotyped virus is hereafter referred to as SADΔG-eGFP(EnvA). Therefore, mammalian neurons can only be

infected by SADΔG-eGFP(EnvA) if they express the TVA receptor. In these infected neurons trans-complementation with rabies G protein is necessary to enable trans-synaptic spreading. With its own glycoprotein rabies virus spreads in a retrograde manner and therefore labels the pre-synaptically connected cells by eGFP expression. This spreading is restricted to a single synaptic step, because the presynaptic cells do not express the rabies virus glycoprotein (RG). By tracing cells infected with this modified rabies virus, one can visualize neurons that are directly pre-synaptic to a given target neuron. This approach provides an interesting tool for tracing circuits for studying connectivity within the brain. Our review in **Chapter 2.1** summarizes recent developments of the RABV based mono-trans-synaptic tracing technology showing the wide toolbox it opens to dissect neuronal circuit structure and function. We described further details about rhabdoviridae in general and their use as viral tracers in a recent book chapter, which is attached as **Appendix**, Manuscript N. 4 Use of Rhabdoviruses to Study Neural Circuitry. Melanie Ginger*, Guillaume Bony*, Matthias Haberl and Andreas Frick (Appearing in Biology and Pathogenesis of Rhabdo- and Filoviruses by World Scientific Publishing Co.).

1.1.3 Using Magnetic Resonance Imaging to Study Brain Networks

Magnetic resonance imaging (MRI) is a widely employed non-invasive technology for taking images of tissue using a strong magnetic field. MRI is being used for a range of different types of applications and can be used repeatedly on a patient since it does not involve a harmful procedure like the ionizing radiation used for X-ray computer tomography. While the underlying mechanisms of MRI are complex as their physical, biophysical mechanisms can just be correctly described using quantum mechanics, the overview here will cover mainly the practical aspects, which are required to understand and interpret the results.

Diffusion Tensor Imaging

Diffusion tensor MR imaging (DT-MRI) is an advanced non-invasive imaging technique to measure the large-scale structural connectivity of brains. DT-MRI is based on the diffusion of water in the brain tissue in multiple orientations. At every voxel the combination of several vectors, each corresponding to the diffusion in a

different direction, is reconstructed into a diffusion ellipsoid. The directionality and anisotropy of the ellipsoid gives information about how structured the brain tissue is. Cellular membranes, axonal bundles and organelles, all restrict the diffusion of the water in the tissue. Therefore the shape and the size of the diffusion ellipsoid reflects whether and how cells and fibers have a preferential orientation. This technique is therefore frequently used to look at tissue that has a parallel orientation like the axonal bundles of the white matter (WM) and in some cases for grey matter (Basser et al., 1994). The diffusion tensor can be analyzed with respect to its mean diffusivity (MD) revealing how restricted the overall diffusion is due to cells in the tissue. The MD is calculated per voxel as the average of the vectors into three perpendicular directions. Another commonly used parameter is the diffusion anisotropy (or fractional anisotropy, FA), which reveals the directionality or in other words, how pointy (the maximal FA value is 1) or round the ellipse (the minimal FA value is 0) is shaped. The FA value of cerebro-spinal fluid is 0 since it can diffuse equally in all directions, whereas the values in parallel fiber bundles or the white matter (WM) are high. It is important to note that DT-MRI however deals inadequately with crossing fibers and therefore the FA is rarely used in the grey matter. For example, the FA value could approach 0 in a scenario where three fibers cross perpendicular to each other in one voxel, since now the ellipsoid would have no preferred orientation. Images of single slices are usually acquired in 100 ms or less to eliminate the chance of a head motion, since even a tiny shift can lead to significant artifacts in the acquisition and reconstructed image (Alexander et al., 2007).

DT-MRI has often been used in to study the structural integrity in cognitive diseases, e.g. for Alzheimer's Disease where a reduced FA in the WM and an increased MD in the grey matter was found. This data has to be interpreted carefully, but usually additional methods can help to define the origin of changes in DT-MRI values. In Alzheimer's Disease patients it was found that the altered FA and MD values correspond to a degradation of myelin and axons in the WM and a neuronal loss in the grey matter, respectively (Clerx et al., 2012).

Resting-state functional MRI

Activity in a brain region causes a locally and temporary increased blood flow (Roy and Sherrington, 1890). A change in the blood flow causes a shift in the blood

oxygenation level or in the ratio of oxyhemoglobin and deoxyhemoglobin. Since oxygenated and deoxygenated blood are different in their magnetic susceptibility this change can be detected with an MRI scanner as a signal variation. This Blood Oxygen Level Dependent Signal (BOLD) is measured for the use of functional Magnetic Resonance Imaging (fMRI). Since brain areas are active even in the absence of external stimuli, fluctuation in the BOLD signal can be measured during resting state (rs-fMRI). Rs-fMRI provides indications about the functional connectivity of different brain areas by correlating their activity states over repeated measurements. A commonly used method for analyzing the signals is based on seed-points or regions of interest (ROIs). In this analysis, the signal of defined ROIs is used to calculate their correlation to the signal at other ROIs in the brain. The correlation coefficient is used to infer whether, and how strong, the respective ROIs are functionally connected. Among the non-invasive techniques for measuring brain connectivity rs-fMRI provides a high spatial resolution (typically 500μm - 1 mm) over the entire brain, even though only a limited temporal resolution (few seconds). Although, rs-fMRI cannot prove whether the brain areas are directly connected, it can demonstrate interactions. An extensive review about the merits and drawbacks of fMRI can be found in Logothetis (2008) (Logothetis, 2008). To address shortcomings of this technique it is often complemented with other techniques, for example electroencephalography (EEG), which provides a high temporal resolution (less than a ms) but lacks the spatial resolution, or with methods that can provide conclusive evidence for a structural connection.

1.2 Fragile X Syndrome and Brain Wiring Defects

Fragile X Syndrome (FXS) is the most common form of inherited mental retardation passed along by the X-Chromosome affecting approximately 1/4000 males and 1/8000 females (Bassell and Warren, 2008; Garber et al., 2008). FXS is caused by a mutation silencing a single gene, *Fmr1,* encoding the Fragile X mental retardation protein (FMRP). FMRP is a regulatory protein controlling the expression and function of a large number of other proteins, which causes the myriad of effects found in its absence in FXS. In order to understand how the cellular defects lead to the behavioural symptoms that patients with FXS develop we also need a better understanding about changes on the intermediate level, the neuronal networks.

1.2.1 Cause of the Fragile X Syndrome

The primary cause of FXS is the absence of the gene product of the *Fmr1* gene, the Fragile X mental retardation protein (FMRP) (Pieretti et al., 1991). The cause of the silencing of the *Fmr1* gene is an excessive expansion of the CGG trinucleotide repeat in the 5' untranslated region (UTR) of the gene (O'Donnell and Warren, 2002). The number of CGG repeats is normally ~6-54, 55-200 in premutation carriers and >200 in FXS patients (Willemsen et al., 2011). In the case that more than 200 CGG repeats are accumulated, the CpG island in the 5'-untranslated region (UTR) becomes hypermethylated, which causes a suppressed transcription and therefore a lack of the FMRP protein (Sutcliffe et al., 1992). Trinoclueotide repeats can expand from one to the next generation and cause that the offspring of a premutation carrier develops FXS (Loesch and Hagerman, 2012; O'Donnell and Warren, 2002). A recent study estimated that 1/151 females (or ~1 million women in the United States) and 1/468 males, (or ~320,000 men in the United States) are carrier of a FXS premutation (Seltzer et al., 2012).

1.2.2 Fragile X Phenotype

The most striking deficit observed in FXS patients is a mild to severe mental retardation. Their intelligence quotient (IQ) is typically in the range of 40-70 (Merenstein et al., 1996). In addition, FXS patients usually suffer from a number of neurological and behavioral alterations. The most frequent symptom, found in almost

all male and around 30% of the female patients, is a pronounced attention deficit hyperactivity disorder (ADHD)(McLennan et al., 2011). Another common feature is hypersensitivity to sensory stimuli, in particularly of tactile, auditory and visual modalities (Hagerman and Hagerman, 2002; Miller et al., 1999). Indeed, hypersensitivity to visual stimuli and visual avoidance is present in more than 90% of male patients (Merenstein et al., 1996). FXS patients often exhibit autistic features, with autism occurring in ~30% of the males with FXS and autism spectrum disorder (ASD) in an additional ~30% of males that did not meet the criteria for autism. In fact social anxiety is one of the most common problems of FXS patients (Harris et al., 2008; Kaufmann et al., 2004). Many patients also suffer from epilepsy, more specifically ~15% of FXS patients experience seizures (Berry-Kravis, 2002; Berry-Kravis et al., 2010) and ~70% of FXS patients have irregular EEGs spiking patterns (Berry-Kravis, 2002; Sabaratnam et al., 2001). Difficulties with their vision are also common in FXS patients (in ~25%), often caused by strabismus and refractive errors (Hatton et al., 1998). Besides these pronounced neurological, cognitive and sensory problems, FXS often also leads to visible alterations in the peripheral tissues causing prolonged faces, macroorchidism, and hyperextensible joints (Hagerman and Hagerman, 2002).

1.2.3 Fragile X Mental Retardation Protein (FMRP) Function

FMRP occurs in a number of different tissues but it is foremost expressed in neurons of the central nervous system (CNS) and in testes. FMRP operates as RNA-binding protein (Darnell et al., 2001; Siomi et al., 1994). It targets a large variety of mRNA molecules, with up to as many as 800 mRNAs as binding partners (Brown et al., 2001). This equals ~ 4% percent of all mRNA transcripts that occur in the mammalian brain (Bassell and Warren, 2008). A recent study identified that hundreds of targets of FMRP are mRNAs encoding part of the pre- and postsynaptic proteome (**Figure 1.5**; (Darnell et al., 2011)). This large number of interactions explains why a single-gene deficit leads to such a complex sequence of events and makes it difficult to assess the full extent of the consequences of this cognitive disorder. It could further explain why FXS is one of the few single gene mental retardation disorders, since the loss FMRP might affect so many other genes that compensatory mechanisms are insufficient to avoid strong cognitive defects. FMRP has a number of RNA binding

motifs (Darnell et al., 2001; Siomi et al., 1994) (metadata recently reviewed in (Suhl et al., 2014)) through which it mainly represses the translation of mRNAs (Li et al., 2001) and only in the case of a few proteins increased translation levels where found in the absence of FMRP (Zalfa et al., 2003). It is thought that phosphorylated FMRP suppresses translation of target mRNAs and conversely dephosphorylated FMRP enhances translation (Ceman et al., 2003). It has further been shown that FMRP can also reversibly stall polyribosomes, hindering the translation of the associated mRNAs (Darnell et al., 2011).

In addition to its strong effects on the translational level, FMRP is also thought to have a role in the transport of mRNAs to the synapse. For example, it was shown that blocking the FMRP mediated transport to the synapse lead to altered spine morphology, resembling the changes found in the absence of FMRP (Dictenberg et al., 2008).

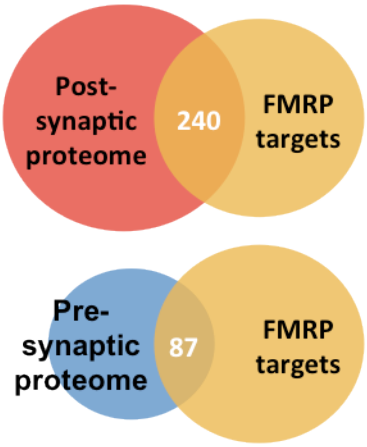

Figure 1.5 Comparison of FMRP target mRNAs with the curated dataset of mouse brain synaptic proteins (from the Genes to Cognition database, G2Cdb).
This identified a strong overlap with the postsynaptic proteome (>30% of FMRP targets) and also, to a lesser extend, with the presynaptic proteom (13% of FMRP targets)
Adapted from (Darnell et al., 2011)

1.2.4 Fragile X Mouse Model

A number of different approaches have been taken to get a better understanding of FXS and the role of FMRP in health and disease. The help of different genetically modified organisms, most importantly Drosophila (Zhang et al., 2001) and knock-out mice (1994) have brought a wealth of findings that are important for human patients. In fact much of what we know today about the function of FMRP *in vivo* was originally discovered in studies using those two animal models.

Fmr1, which is the homologue gene in the mouse of the human *FMR1* is 97% identical to the human gene at the amino acid level and to 95% identical at the

nucleotide level in the coding region (Ashley et al., 1993). Also the expression patterns of *FMR1* and *Fmr1* are similar in human and mouse tissues (Verheij et al., 1995). The first *Fmr1* knockout (*Fmr1*KO) mouse was generated by introducing a neomycin gene into exon 5 of the murine *Fmr1* gene through homologous recombination in embryonic stem cells (1994). Many parallels to human FXS patients have been found in the *Fmr1*KO mouse model with biochemical and behavioral tests (Bakker and Oostra, 2003; Kooy, 2003). For example, *Fmr1*KO mice also suffer from cognitive impairments, even though they are less severe than those described in FXS patients (D'Hooge et al., 1997; Dobkin et al., 2000; Kooy et al., 1996; Van Dam et al., 2000; 1994). The knockout mice also display macroorchidism (1994), which is common in male FXS patients and various other important aspects of the disease, including sensory hypersensitivity and thin, immature dendritic spines. Craniofacial abnormalities have been reported in zebrafish (Tucker et al., 2006) they were not found in an MRI study of *Fmr1*KO mice (Ellegood et al., 2010). Although *Fmr1* KO mice do not express FMRP, the *Fmr1* promoter in those mice is intact and residual *Fmr1* transcription was found in these mice. To resolve the uncertainty whether the residual transcript functions in some way the *Fmr1* KO2 mouse line, a complete null knockout mouse, has been created by excision of the *Fmr1* promoter and first exon (Mientjes et al., 2006). These animal models have become vital not only for studying the cellular basis of deficits in FXS but also for testing promising drugs that can rescue individual or several of the cellular, behavioral or cognitive deficits.

1.2.5 Mechanisms of Fragile X Syndrome

Concurrent Theories

The currently dominant mechanistic hypothesis about FXS is known as ‘mGluR theory’ (Bear, 2005; Bear et al., 2004) (reviewed in (Bhakar et al., 2012)). This theory proposes (a) that the core symptoms in FXS are caused by an over-activation of the metabotrobic glutamate receptor 5 (mGluR5) because (b) the principal role of FMRP for the synaptic function is to control the mGluR-dependent forms of long-term plasticity. A number of indications support this theory: (i) FMRP is increasingly synthesized in response to mGluR activation (Weiler et al., 1997) (ii) mGluR-dependent long-term depression (LTD) is elevated in *Fmr1*KO mice in the hippocampus and cerebellum (Hou et al., 2006; Huber et al., 2002; Koekkoek et al.,

2005) (iii) mGluR5 blockers, like MPEP showed correction of several symptoms in the KO mouse model (reviewed in (Berry-Kravis et al., 2011; D'Hulst and Kooy, 2009)) and even reversal of already established FXS phenotypes (Michalon et al., 2012).

Today the theory is widely accepted, but despite all hopes the drug tests in humans showed much less effect than expected and the disease might be more complex than initially thought. Novartis stopped in April 2014 the drug trials done with the mGluR5 antagonist mavoglurant (AFQ056) as a consequence of negative results in the large international clinical trial in adult FXS patients (http://www.fraxa.org/novartis-discontinues-development-mavoglurant-afq056-fragile-x-syndrome/). Drug trials of two large pharmaceutical companies are ongoing with GRN-529 (Pfizer) and RG7090 (Roche), which both also target mGluR5 receptors.

Besides the mGluR theory a second prominent theory has been developed to describe the disease status in Fragile X, the 'GABA theory of Fragile X Syndrome'. GABA is the principal inhibitory neurotransmitter in adults. The GABA theory is based on the observation that expression levels of GABA receptor type A is reduced (D'Hulst et al., 2006) in animal models of FXS and a decreased GABAergic inhibition was found in the hippocampus (Curia et al., 2009) and amygdala (Olmos-Serrano et al., 2010). An impaired inhibition could contribute to epilepsy and other symptoms of Fragile X. To this end several groups proposed rescue approaches targeting GABA receptors to restore the excitation/inhibition balance with the hope to cure the ADHD and hyperexcitability phenotypes (Braat and Kooy, 2014; Heulens et al., 2010; 2012). Again transforming the results from animal research into a successful human application have been difficult. Seaside Therapeutics announced in May 2013 the end of any clinical trials with their GABA-B agonist Arbaclofen (STX209) for FXS patients, although positive results were reported in a number of patients.

Apart from those two prominent receptor alterations in the absence of *Fmr1* an increasing number of differences have been found with potential implications for the cellular and network function and which might contribute to certain behavioral phenotypes. Several groups reported a circuit hyperexcitability, or extended upstates in the activity of networks (Gibson et al., 2008; Gonçalves et al., 2013). Most likely

there are several factors that contribute to this hyperexcitability, ranging from receptor and cellular mechanisms to changes in the network.

On the cellular level, besides the mGluR5 and GABA receptors, also a number of other alterations have been described that may contribute to the phenotype of the disease. Cellular excitability was shown to be altered and a broadening of action potentials was found (Deng et al., 2013). In the hippocampal CA3-CA1 synapse a recent study found an elevated release probability during repetitive activity (Wang et al., 2014). Synaptic plasticity was shown to be altered in a number of studies using different stimulating protocols, animal ages, brain areas. A reduced long-term potentiation was found in the anterior somatosensory cortex (at 8-10 weeks) (Li et al., 2002) in the primary olfactory cortex (only from 6 months on) (Larson et al., 2005), in the anterior cingulated cortex and the lateral amygdala (at 6-8weeks) (Zhao et al., 2005), the visual cortex layer (L)5 (Wilson and Cox, 2007), and the temporal cortex (2-3 months) (Hayashi et al., 2007). Apart from the deficits on the synaptic and cellular level it is also important to understand whether the circuitry is intact or altered in FXS to get a better understanding about the cause of the cognitive defects in FXS.

1.2.6 Neuroanatomy in Fragile X Syndrome

Defective brain wiring can have devastating neurological and psychiatric consequences and those defects are suspected to underlie several brain disorders including autism (Geschwind and Levitt, 2006; Müller et al., 2011). FXS is the leading single gene mutation causing ASD and several ASDs have already been associated with structural changes in the synaptic contacts and connectivity alterations (reviewed in (Peça and Feng, 2012)). Yet, the data about circuit alterations in FXS is sparse when we compare it to the numerous studies addressing basic functions of FMRP (recently reviewed in (Darnell and Klann, 2013)). However, among the list of putative targets of FMRP there are a number of mRNAs known to regulate cytoskeletal structure (reviewed in (Bagni and Greenough, 2005)). Moreover, several studies already suggested that changes occur in the circuitry of FXS patients and animal models, which will be summarized in the subsequent sections.

Studies addressing the wiring of the brain in FXS have been conducted mainly on two levels, first top-down approaches - mostly implicating human patients - that

looked at large scale structural (reviewed in (Lightbody and Reiss, 2009)) and functional network connectivity (Hall et al., 2013; van der Molen et al., 2014), and second using bottom-up approaches that examined local networks or single cells in the different animal models (Patel et al., 2014).

To date we have not found studies combining those different approaches or providing the link of small- to large-scale network alterations in FXS. Even though it would be of major importance to improve our understanding of this complex syndrome given that sensory information is processed on different scales in parallel. Each individual brain area may act as a computational unit with a very defined function, but the real functionality required to process sensory information will only emerge, by arranging these individual processing units in the very specific manner our brains do. Therefore the wiring on the small scale is inseparably linked to the wiring on the large scale, both are equally relevant and just in conjunction they allow that the sensory information is faithfully processed in the brain network. Affected networks could be involved in visual, auditory, somatosensory sensation and motor control or more elusive functions as perception, learning and memory or motivation. Therefore in any neurologic disorder it is possible that altered networks may play a role either being the cause or consequence and depending on the type and number of networks affected this may be reflected in specific or global deficits. While it will become very difficult to untangle if network changes are the cause or a consequence it would be a good first step to identify which networks are mainly affected. Studies of behavior and performance are an excellent starting point to identify the candidate brain areas/pathways that should be further inspected. Also large-scale studies, performed on the whole brain, may provide good indications. Fragile X Syndrome is an intellectual disability and the range of neurological changes and behavioral effects in human patients and mouse models is wide, as described above. In the subsequent paragraphs large- and fine-scale studies of brain network alterations in Fragile X Syndrome in humans and model organisms will be discussed in more detail. Since those studies did not establish direct links between findings in the large and fine scale networks they will be treated in separate sections.

1.2.6.1 Large-Scale Neuroanatomy in Fragile X Syndrome

From studies in human FXS patients we know about a number of changes in the size of several brain structures (caudate nucleus, hippocampus, superior temporal gyrus, cerebellar vermis, amygdala). Furthermore, also changes in the activation of certain brain areas where found (insula, the caudate, hippocampus) when individuals with FXS perform cognitive tasks e.g. involving eye gaze processing (reviewed in (Lightbody and Reiss, 2009)).

Initial neuroanatomical studies in FXS patients focused on gross-scale volume measurements of the brain structures. The first brain abnormality found in human FXS patients was a reduced size of the cerebellar vermis (the structure that connects the right and left hemisphere of the cerebellum) by using magnetic resonance imaging (MRI) (Reiss et al., 1988). The same deficit was confirmed in later studies, looking during development and adulthood to the cerebellar vermis (Hoeft et al., 2008). It is thought that this bears relevance for the behavioural deficits in FXS patients since the cerebellum is important for visual-spatial processing, learning, executive function and language (Stoodley and Schmahmann, 2009) and the vermis is linked to the amygdala and hippocampus (Hessl et al., 2004). In fact it was possible to use the posterior vermis size to predict the visual-spatial performance and executive function in FXS patients (Gothelf et al., 2007).

The second unusual change that is consistently found in FXS patients is an enlarged caudate nucleus (Hallahan et al., 2011). The caudate nucleus is part of (the striatum and) the basal ganglia, a system which is responsible not only for voluntary movement but also several other non-motor functions like learning, memory, sleep, and social behavior and plays a major role in planning (Grahn et al., 2008). Several studies found an inverse correlation between the IQ and the caudate size in FXS patients (Gothelf et al., 2007; Reiss et al., 1995) but the link remains to be understood.

A few studies also noticed a reduced volume of the amygdala in FXS patients at young and adolescent age (Gothelf et al., 2007; Hazlett et al., 2009; Kates et al., 1997). The amygdala is major player in emotions and has therefore it also been carefully examined on the cellular level, which also found alterations in FXS models (Zhao et al., 2005). It is thought that changes in the amygdala and insula are related to the anxiety and emotional troubles found in FXS patients. It is unclear what the reasons are for regional changes of brain volume in FXS but it has been suggested

that it could be linked to changes in the synaptic pruning and dendritic maturation during development with deficient or absent FMRP (Lightbody and Reiss, 2009).

The brain areas are not only affected individually but also the connections between them are changed in FXS. Changes were found in the white matter of FXS patients by using DT-MRI. A loss of axonal order or structure was found in fronto-striatal pathways and in parietal sensory-motor tracts indicated by lower Fractional Anisotropy (FA) values in the DT-MRI (Goraly et al., 2003; Haas et al., 2009). In a later study Hall, et al., (2013) looked at large-scale resting-state networks in children and adolescent (aged 10-23 years) FXS patients and identified region-specific alterations in brain structures (Hall et al., 2013). The FXS patients showed a widespread reduction in their functional connectivity across multiple cognitive and affective brain networks. Five large-scale networks were identified that were significantly decreased in their functional connectivity: the salience, precuneus, left executive control, language, and visuospatial networks. The salience network is thought to play a role in recruiting brain regions for sensory information processing; the precuneus is involved in self-referential processing, imagery, and memory and is suggested to be a core node or hub of the default mode network. Both, structural and functional abnormalities were found in the left insular cortex. The insula has also been implicated in autism spectrum disorders and is thought to be important for a variety of functions, including interoceptive awareness and emotions. The authors further suggested that their method of combining structural and functional in this study could also be used to establish an imaging biomarker for FXS (Hall et al., 2013).

A recent study used resting-state EEG to characterize functional brain connectivity and brain network organization in male FXS patients and healthy controls. A decrease in global functional connectivity was found for upper alpha (8-15 Hz) and beta frequency bands (16-31 Hz). For theta oscillations (4-7 Hz), the authors saw an increased connectivity in long-range (fronto-posterior) and short-range (frontal-frontal and posterior-posterior) clusters (van der Molen et al., 2014).

Over the last years the resolution of MRI studies has been constantly improving and it became therefore possible to also use this technique to study the KO

mouse model. While earlier studies did not see large differences (Kooy et al., 1999) a more recent study using a 7.0 Tesla MRI scanner in developing mice (postnatal age P30) found that cerebellum and striatum both decreased in size. Significant volume decreases were also discovered in two regions in two deep cerebellar nuclei (nucleus interpositus and the fastigial nucleus). The authors saw a decrease in NeuN positive signal (and conversely a increase in GFAP positive cells) and concluded that the decreased size is due to a loss of neurons in the deep cerebellar nuclei. Here DT-MRI measurements did not reveal any significant changes in the white matter structures of the *Fmr1*KO mice compared to the WT mice (Ellegood et al., 2010).

1.2.6.2 Fine-Scale Neuroanatomy in Fragile X Syndrome

When considering the structural deficits on the fine scale the literature can be grouped in the (i) cellular defects, mainly addressing the dendritic spine morphology and density and (ii) short range networks within the immediate proximity.

Neuronal Structure in Fragile X Syndrome

An altered spine phenotype – with increased density and a shift towards long, thin immature appearing spines - is often proclaimed as a major hallmark in FXS and in fact it is probably the most commonly described structural change, which has been described in both human patients (Hinton et al., 1991) and animal models (reviewed in (Bagni and Greenough, 2005; He and Portera-Cailliau, 2013)). Over time however the picture has become increasingly complex and the initially thought striking phenotype is not found in all brain areas and actually, for unclear reasons, several studies could not confirm the previous findings. **Figure 1.6** summarizes the complicating findings concerning the spine phenotype in mouse models of FXS. The prevalent opinion today is that *Fmr1*KO mice have an increased number of spines due to defects in dendritic pruning (Galvez et al., 2003; Pfeiffer and Huber, 2007) but several studies reported the deficits occur just transiently (Nimchinsky et al., 2001). Even though we know now that the spine phenotype is more complex than initially thought (e.g. see (Wijetunge et al., 2014)) it has been and still is often being used as a parameter to evaluate for example the efficacy of a rescue approach (Dolan et al., 2013; Henderson et al., 2012) and it is speculated to provide a possible link between several causes of ASDs (Tang et al., 2014).

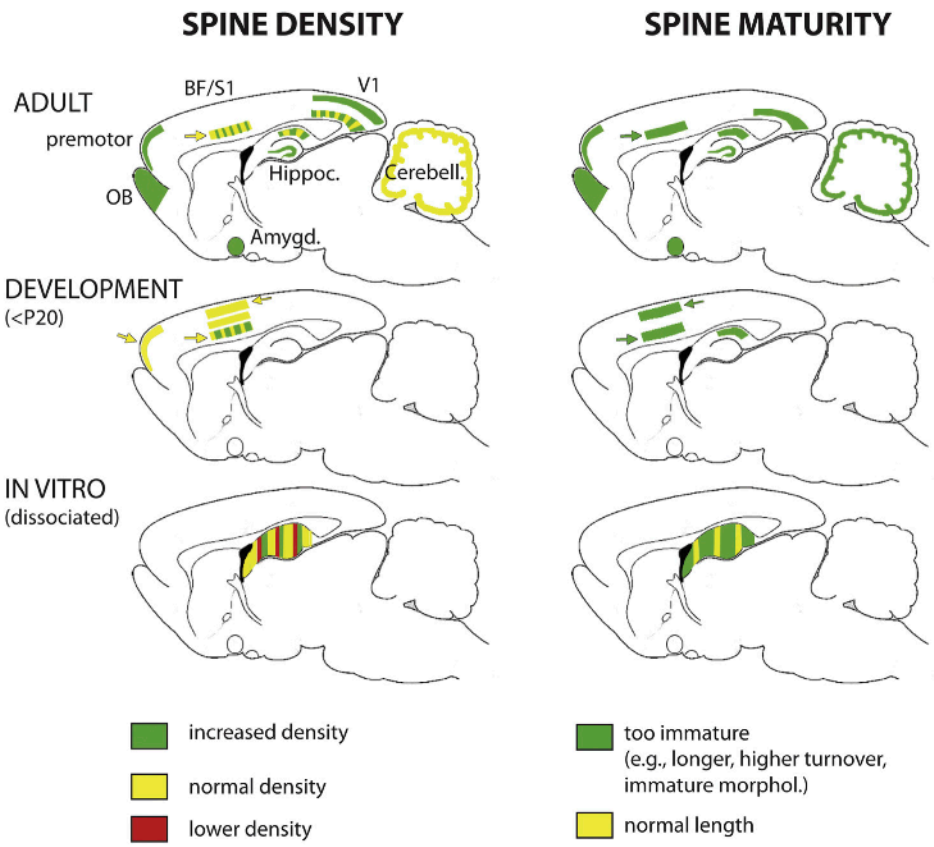

Figure 1.6 The spine phenotype in the Fragile X knock-out mouse model

Regional distributions of reported spine defects in the brain of Fmr1 KO mice. Data on dendritic spines in *Fmr1* KO mice are displayed on a sagittal view of the mouse brain. Data from the adult brain, developing brain (P20), and in vitro results from dissociated neurons in culture (hippocampus only) are shown in the top, middle and bottom rows, respectively. Colored stripes indicate the existence of published studies reporting different results on either spine density or maturity. The relative thickness of the colored stripes reflects approximately the relative number of studies supporting one finding or another. Studies that used imaging in living neurons (in vivo or in acute/organotypic brain slices) are indicated by arrowheads next to the stripes. Note that results of studies are much more consistent for the spine immaturity phenotype than for the spine density phenotype. Abbreviations used in the figures: BF: barrel field; OB: olfactory bulb; S1: somatosensory cortex; V1: visual cortex. Figure adapted from (He and Portera-Cailliau, 2013).

Curiously much less is known about the counterpart of the spines, the presynaptic boutons in FXS. This is remarkable given that a study using a mosaic model of *Fmr1* KO mouse, found a reduced connectivity in the CA3-CA3 network, which was independent of the FMRP in the postsynaptic cell, but instead determined by the pre- or absence of FMRP in the presynaptic cell (Hanson and Madison, 2007).

A later study, also using the mosaic model, showed that FMRP in the presynaptic cell was responsible for the loss of connection strength onto inhibitory neurons (Patel et al., 2013). Even though the pre-dominant opinion is that FMRP acts mostly on the postsynapse by regulating translation and pruning of spines there are indications that FMRP plays a role in the initial axonal guidance. FMRP expression has been observed in axons and axon growth cones (Antar et al., 2006), and growth cones from developing neurons of *Fmr1*KO mice exhibit a hyper-abundance of filopodia and a reduction in dynamicity in hippocampal cultures (Antar et al., 2006). In the zebrafish, a knockdown of *Fmr1* was associated with abnormal axon branching (Tucker et al., 2006); although it was later contested as an artifact by using a newly generated zebrafish null knock-out (Broeder et al., 2009). In drosophila, FMRP is required for efficient activity-dependent pruning of axon branches in the Mushroom Body (Tessier and Broadie, 2008). Immunoelectron microscopy revealed FMRP in axons and presynaptic terminals (Akins et al., 2012; Christie et al., 2009). In the analysis of mRNA translational profiles of *Fmr1*KO mice a large number of different presynaptic FMRP targets appeared were revealed (Brown et al., 2001; Darnell and Richter, 2012) and proteomic studies found that the levels of various presynaptic proteins was affected due to the loss of FMRP (Klemmer et al., 2011; Liao et al., 2008). In the drosophila a neuronal overexpression of the *Fmr1* homologue, *dfxr*, resulted in fewer and larger synaptic boutons, while knocking the gene out caused enlarged synaptic terminals, which was mediated through a regulatory role in the microtubule-dependent growth of synapses (Zhang et al., 2001).

Small-Scale Networks in Fragile X Syndrome

Our knowledge about the short-range connectivity in FXS is limited, derived from individual studies and restricted to a few brain areas at a defined age or during a narrow time window. Most of those studies examined the connectivity in the neocortex of *Fmr1* KO mice.

Gibson et al. examined the within-layer excitation in L4 of the somatosensory cortex in *Fmr1* KO mice and found that it is extensively reduced (~50%) to fast spiking (FS) inhibitory neurons and to a lesser extend also decreased to excitatory spiny stellate neurons as well as the between neighboring excitatory neurons (Gibson et al., 2008). This loss of connection to FS neurons was later attributed to the lack of

FMRP in the presynaptic neuron, resulting in a reduced neurotransmitter release (Patel et al., 2013). Bureau et al. also found a reduction in intralayer connectivity within the same barrel column in the *Fmr1*KO mice. Photostimulation of L4 neurons lead to a less intense response in L3 neurons but when examining the strength of individual connections from L4 to L3 the authors found them to be unaltered. This suggests that a reduced number of connections is the reason for the changes seen in the *Fmr1* KO. Interestingly, filling of individual L4 cells and axon reconstruction showed similar axonal arborization in L2/3, speaking against a problem in axon growth. Furthermore the authors noted that the connectivity, which they found altered at 2 weeks of age was normal again at 4 weeks of age (Bureau et al., 2008). Opposed to the decrease in local connectivity in the previous studies, Teste-Silva et al. found an increased mid-range connectivity in *Fmr1* KO mice. Here L5 pyramidal cells in the medial prefrontal cortex were examined in 25 – 100 μm distance and an increased connectivity was found in between them in *Fmr1*KO mice (Testa-Silva et al., 2012). Interestingly the connectivity changes found in all of those studies were only transient and disappeared at a later point during development even though the synaptic strength changes remained (Bureau et al., 2008; Gibson et al., 2008; Testa-Silva et al., 2012). A more recent study looking at the interconnectivity of L5A pyramidal cells, specifically the intratelencephalic type, using paired recordings surprisingly found a different effect due to an impairement in synaptic pruning. The L5A-L5A connectivity decreased between the third and fifth postnatal weeks in WT animals, which indicates a period of connection pruning, while it did not decrease in the *Fmr1*KO mice, leaving these neurons in a hyperconnected state at postnatal day P30. The use of the mosaic mouse model showed that the pruning was dependent on the postsynaptic neuron (Patel et al., 2014).

Besides the neocortex it has also been inferred that the wiring in the amygdala is affected in *Fmr1* KO mice. Recordings from principle neurons in the basolateral amygdala (BLA) showed a decreased number of spontaneous and miniature inhibitory postsynaptic currents (sIPSCs and mIPSCs), which is likely the result of a reduced input from surrounding inhibitory neurons (Olmos-Serrano et al., 2010).

Taken together these data suggest that FMRP plays a role in the formation or maintenance of connections in cortical and subcortical areas, which could be exhibited by the axon guidance or the spine pruning, but most likely it has an

important role regulating both.

Network States

The wiring and the excitation/inhibition balance as well as the synaptic strength and intrinsic properties of neurons, all contribute to the response a network exhibits to a given stimulus. Since so many of these parameters were found to be altered it is not surprising that also the response and the dynamics of the network are changed in FXS. And a number of studies (Gibson et al., 2008; Gonçalves et al., 2013; Hays et al., 2011; Ronesi et al., 2012) found a hyperexcitable cortical network in the Fmr1KO mice that reacted with a prolonged activated state upon stimulation, which could explain the epileptic features often found in FXS .

1.3 Aims of this Study

The aim of this work was to study the anatomical and functional connectivity of neuronal networks and develop novel tools for this purpose. At the beginning of this study rabies virus was available as a retrograde polysynaptic, as a retrograde mono-transsynaptic and as a single-cycle retrograde vector. For several research questions it would be beneficial, to use the same viral vector to infect neurons at the injection site - and hence mark those neurons and their projections anterogradely - together with one of the retrograde variants to label the input. We therefore first set out to develop an anterograde variant of the rabies virus, which would allow us to also study the morphological features of the cells in the injection site together with the input after a single stereotactic injection.

We applied this technique in combination with other approaches to probe neuronal connectivity defects in Fragile X Syndrome (FXS). One of the morphological hallmarks of FXS is an alteration in the shape/number of spines, the major sites for synaptic input. In addition, FMRP regulates the RNAs of molecules that regulate the anatomical connectivity (cytoskeleton, axon and dendrite branching, spines) within cortical circuits. In fact an altered anatomical and functional connectivity has been proposed to play a role in both FXS and ASDs (Geschwind and Levitt, 2007), yet our understanding of the nature of these defects is limited due to the complex nature of these syndromes.

Profound knowledge of deficits in the neuronal circuits will be necessary to bridge the gap, between alterations on the molecular level/local circuitry, and the global changes in behavior and cognition. Correct wiring is critical for maintaining normal brain function and for the processing of sensory information. In particular, the long-range connections between different brain areas are crucial for a successful sequential processing and transmission of sensory information from lower to higher hierarchical areas. Since hypersensitivity to visual, auditory, tactile, and olfactory stimulation is a prominent feature of human FXS patients and *Fmr1*KO mice, we were interested in studying connectivity changes both to- and in between- the neocortical sensory areas. We hypothesized that long-range connections between brain areas might be altered in FXS given the deficits previously found in axonal outgrowth and spine morphologies. Yet, long-range wiring deficits underlying FXS have been largely unexplored as a potential mechanism underlying cognitive deficits.

Therefore we set out to quantify brain-wide connectivity features in the *Fmr1*KO mouse model and to correlate them with functional connectivity features. We have probed changes in neuronal connectivity, and the functional consequences of these changes on information processing in the neocortical circuits in *Fmr1*KO mouse model of Fragile X Syndrome. For this, we used a combination of cutting-edge approaches ranging from viral tracing, magnetic-resonance-imaging and optical imaging to novel anatomical quantification methods.

2. Results

2.1. Novel Tools to Unravel the Neuronal Wiring

2.1.1 Mono-trans-synaptic input mapping

Newly developed methods need a phase of thorough evaluation and often improvement to aim for the highest standards and ensure that the results are reproducible, can be fully trusted and biases are avoided by all means possible.
Mono-trans-synaptic tracing with a glycoprotein deleted variant of rabies virus has been a method offering unprecedented possibilities of mapping the input of a group of or individual cells. In the next section we described in a review article the results that have been gained with this method by several groups over the last couple of years until the date of publication as well as possibilities and limitations the method bears. A more recent update on this matter can be found in our recent book chapter, in the Appendix.

Publication N. 1

Revealing the secrets of neuronal circuits
with recombinant rabies virus technology

Melanie Ginger*, **Matthias Haberl***,
Karl-Klaus Conzelmann, Martin K. Schwarz and Andreas Frick

*Equal contributions

Frontiers in Neural Circuits, Published online January 24, 2013

frontiers in
NEURAL CIRCUITS

REVIEW ARTICLE
published: 24 January 2013
doi: 10.3389/fncir.2013.00002

Revealing the secrets of neuronal circuits with recombinant rabies virus technology

***Melanie Ginger*[1,2†], *Matthias Haberl*[1,2,3†], *Karl-Klaus Conzelmann*[4], *Martin K. Schwarz*[5] and *Andreas Frick*[1,2*]**

[1] *Neurocentre Magendie, INSERM U862, Bordeaux, France*
[2] *University of Bordeaux, Bordeaux, France*
[3] *Institute of Neuroinformatics, University of Zürich, Zürich, Switzerland*
[4] *Max-von-Pettenkofer Institute and Gene Center of the Ludwig-Maximilians University Munich, Munich, Germany*
[5] *Department of Molecular Neurobiology, Max Planck Institute for Medical Research Heidelberg, Heidelberg, Germany*

Edited by:
Charles F. Stevens, The Salk Institute for Biological Studies, USA

Reviewed by:
Edward M. Callaway, The Salk Institute for Biological Studies, USA
Charles F. Stevens, The Salk Institute for Biological Studies, USA

****Correspondence:***
Andreas Frick, Neurocentre Magendie, INSERM U862, 146 Rue Léo Saignat, 33077 Bordeaux, France.
e-mail: andreas.frick@inserm.fr

† These authors equally contributed to this work.

An understanding of how the brain processes information requires knowledge of the architecture of its underlying neuronal circuits, as well as insights into the relationship between architecture and physiological function. A range of sophisticated tools is needed to acquire this knowledge, and recombinant rabies virus (RABV) is becoming an increasingly important part of this essential toolbox. RABV has been recognized for years for its properties as a synapse-specific trans-neuronal tracer. A novel genetically modified variant now enables the investigation of specific monosynaptic connections. This technology, in combination with other genetic, physiological, optical, and computational tools, has enormous potential for the visualization of neuronal circuits, and for monitoring and manipulating their activity. Here we will summarize the latest developments in this fast moving field and provide a perspective for the use of this technology for the dissection of neuronal circuit structure and function in the normal and diseased brain.

Keywords: connectivity, wiring diagram, neuronal tracer, synapses, monosynaptic

INTRODUCTION

How does the brain process information, encode perception, and generate behavior? An answer to these questions requires a mechanistic understanding of the operation of the brain's neural circuits. The operation of these neural circuits is determined by their structure, the physiological properties of the neuronal connections, and the integrative properties of the neurons. Thus, an understanding of the brain's computations is inevitably linked to knowledge of the relationship between the structure of its neuronal circuits and their function (Lichtman and Denk, 2011; Rancz et al., 2011). Rabies virus (RABV) has outstanding properties as a retrograde tracer of synaptically connected neuronal populations (Kelly and Strick, 2000; Wickersham et al., 2007a; Ugolini, 2011). Recently, the development of a glycoprotein gene-deleted (ΔG) RABV based method has enabled the tracing and functional investigation of monosynaptic connections of defined neurons (Wickersham et al., 2007b; Callaway, 2008; Marshel et al., 2010). This methodology can be readily combined with the expression of a variety of genes, optical/electrophysiology methods, and behavioral assays to drive integrative studies of neural circuits (Callaway, 2008; Arenkiel and Ehlers, 2009; Osakada et al., 2011; Wickersham and Feinberg, 2012).

In this review we present an update on recent developments in the field of RABV ΔG based trans-synaptic tracing technology. We explain the basic principles of this technology, and show how, in recent studies, it has been adapted to reveal specific aspects of neuronal circuit structure/function. We also discuss what we believe to be the major potential and shortcomings of recombinant RABV technology. Lastly, we provide an overview of how this approach complements other recent technological developments in the field of neural circuit analysis and the kind of questions that can be addressed using a combination of these approaches.

TRANS-SYNAPTIC TRACERS FOR THE STUDY OF NEURAL CIRCUIT CONNECTIVITY

POLYSYNAPTIC TRACERS

Conventional anterograde and retrograde tracers have significantly advanced our knowledge of connectivity between different brain areas (Cowan, 1998; Luo et al., 2008; Lichtman and Denk, 2011). These tracers reveal which brain areas are connected to one another and the location and identity of the projections neurons. However, since these tracers do not cross synapses, they are unable to establish direct synaptic connectivity between neurons.

Polysynaptic tracers, on the other hand, have the ability to spread from one neuron to another, permitting the identification of networks of synaptically connected neurons. These polysynaptic tracers can be divided into two types: non-viral and viral tracers. Non-viral polysynaptic tracers are, for the most part, limited to certain types of plant lectin and bacterial toxins (Cowan, 1998; Carter and Shieh, 2010). These tracers have a number of advantages including their safety, ease of use and ability to be genetically encoded. However, they also suffer from one or more shortcomings (reviewed in references Callaway, 2008; Luo et al., 2008; Lichtman and Denk, 2011; Wickersham and Feinberg,

2012), importantly severe dilution of signal with each synaptic step.

These limitations can be overcome by the use of certain polysynaptic viral tracers, in particular those belonging to the classes of α-herpes viruses (herpes simplex virus type 1 and pseudorabies virus) and RABV (reviewed in Callaway, 2008; Ekstrand et al., 2008). In contrast to non-viral tracers, trans-synaptic viral labeling is amplified rather than diluted due to the replicative nature of viruses. This labeling can be revealed by the expression of suitable morphological markers such as native viral proteins or reporter molecules in the case of recombinant virus strains (reviewed in Ekstrand et al., 2008). Not all of the polysynaptic viral tracers spread exclusively at synaptic sites, thereby labeling neurons that are not necessarily connected by synapses. The CVS derived strains of RABV and the Bartha strain of pseudorabies virus (PRV), however, have been shown to spread in a synapse-specific manner (reviewed in references Callaway, 2008; Ekstrand et al., 2008; Luo et al., 2008; Ugolini, 2011). Furthermore, these two viruses spread in a defined (retrograde) direction, enhancing their value for neural circuit analysis. RABV has two main advantages over PRV, namely a significantly reduced cytotoxicity and the ability to be used in primates (Callaway, 2008). The relative merits of these polysynaptic viruses for neural circuit analysis have been discussed in detail elsewhere (Callaway, 2008; Ekstrand et al., 2008; Ugolini, 2011).

Altogether, these features make RABV a very useful virus for the study of neural circuit connectivity (Ugolini, 1995; Kelly and Strick, 2000; Callaway, 2008; Ugolini, 2011). However, the fact that native RABV (like other trans-synaptic viruses) is a polysynaptic tracer causes potential ambiguity in the interpretation of how many synaptic steps have been crossed at any given time. For instance, such ambiguity would occur if RABV crosses synapses at different rates depending on their strength or simply because of differences in the RABV transport time along presynaptic axons that span several orders of magnitude in length (for discussion of synapse strength see references Ugolini, 1995, 2011; Callaway, 2008; Wickersham and Feinberg, 2012). Furthermore, it is not possible to concomitantly use this method for both circuit tracing and the manipulation of first-order connections (see below), since higher-order connections will also be affected.

RABV AS A MONOSYNAPTIC TRACER

Revealing first-order connections

An elegant solution to this problem led to a technique, which has come to be known as monosynaptic trans-synaptic tracing (Wickersham et al., 2007b) or mono-trans-synaptic tracing for short (Miyamichi et al., 2011). Mono-trans-synaptic tracing uses a pseudotyped, recombinant RABV to identify direct presynaptic inputs to a defined target cell population. These connections are "mono-synaptic" because trans-synaptic traversal is limited to one synaptic step between initial infected cells (i.e., the source cells) and their immediate presynaptic partners. The exquisite specificity of the RABV ensures that only synaptically connected neurons are labeled.

To implement this highly specific tracing system, Wickersham et al. (2007b) employed a deletion mutant RABV (RABV ΔG) (Mebatsion et al., 1996a), deficient in the expression of the RABV envelope glycoprotein (RG) (**Figures 1A,B**). RG is essential for the assembly of infectious virus particles during the natural life cycle of RABV (Mebatsion et al., 1996a), as well as for mediating trans-synaptic crossing of the virus (Mebatsion et al., 1996a; Etessami et al., 2000) (**Figure 1B**). Infectious properties can be rescued by cultivating the virus in a trans-complementing cell line (pseudotyping; **Figures 1C,D**). The resulting virus, however, behaves as a single-cycle tracer and is trapped in the source cells. Exogenous expression of RG in the same source cell population is sufficient to rescue the trans-synaptic capabilities of the virus—but in a highly restricted manner, which is limited to first order connections (Wickersham et al., 2007b) (**Figure 1E**).

In the original description of the method, pseudotyping was employed as a means of limiting the initial infection to a defined source cell population. To achieve this, Wickersham et al. (2007b) exploited the envelope glycoprotein (EnvA) of the avian sarcoma and leukosis virus, whose cognate receptor (TVA) has no homologue in mammalian cells (Bates et al., 1993; Young et al., 1993; Federspiel et al., 1994). Ectopic TVA expression is required to permit infection by RABV ΔG(EnvA) and needs to occur in the same cells expressing RG, to correctly demarcate the source cell population (**Figure 1E**). In order to visualize the resulting trans-synaptically labeled neurons, RABV was modified to express a fluorescent protein (eGFP) and source cells are distinguished by the addition of a second fluorescent marker (Wickersham et al., 2007b) (**Figure 1B**). Pseudotyping can also be achieved with a variety of viral glycoproteins provided that the glycoprotein is suitably engineered to contain the cytoplasmic domain of the native RABV glycoprotein (Mebatsion et al., 1995; Conzelmann, 1998; Choi et al., 2010; Choi and Callaway, 2011). In such cases, the source cell population is defined by the resulting tropism of the pseudotyped virus.

Features of RABV vectors

RABV is, in many ways, the prototypic neurotropic virus since its life cycle is entirely adapted to survival and spread in the nervous system. RABV derived vectors thus possess a number of features, which endow them with excellent properties for a viral tracer. These include efficient long-range transport in neurons, low cytotoxicity, and high-level gene expression (Mebatsion et al., 1996b; Wickersham et al., 2007a; Dietzschold et al., 2008). Wild-type RABV has a broad host species range that includes almost all terrestrial mammals, bats, and birds (Gough and Jorgenson, 1976; Nel and Markotter, 2007), and this likely extends to all RABV derived vectors making them suitable for use in a range of animal model systems. The RABV genome (Conzelmann et al., 1990) is small, modular, and readily accepts foreign genes without the issues of instability inherent to other RNA viruses (Mebatsion et al., 1996b; Conzelmann, 1998). Moreover, RABV is confined to the cytoplasm throughout its life cycle (Albertini et al., 2011). This precludes integration into the host genome and the subsequent disruption or inappropriate transcriptional activation of host genes, which is reported to occur for other vectors such as lentivirus (Sakuma et al., 2012). The highly stable and tightly bound ribonucleoprotein core (Albertini et al., 2011) also

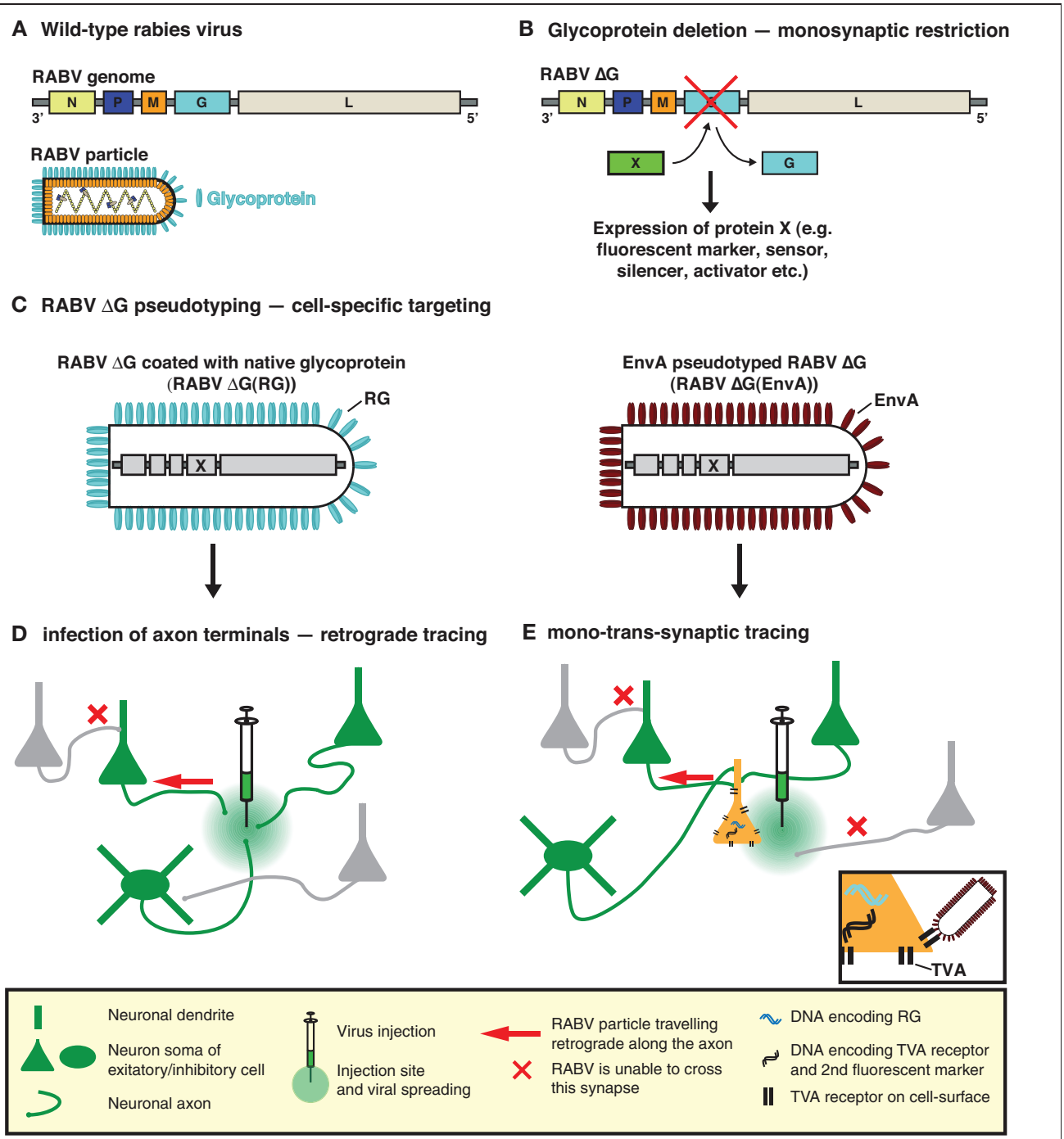

FIGURE 1 | RABV—the trans-synaptic tracing toolbox. (A) The RABV genome encodes five proteins including the envelope glycoprotein (G). **(B)** Deletion of G (ΔG) is sufficient to prevent trans-synaptic spreading and results in a single-cycle vector. A gene of interest can then be inserted in the place of the deleted G. This gene of interest can encode a fluorescent protein such as GFP, permitting the visualization of virally traced neurons. It can also permit the expression of an almost unlimited choice of genetically encoded tools for the manipulation/visualization of neuronal circuits, e.g., biosensors, synapse markers, activators/repressors of neuronal activity. **(C)** RABV ΔG can be pseudotyped, either with its native glycoprotein or an engineered surface protein (e.g., EnvA). Pseudotyping restores the normal infection capabilities or enables cell-type selective infection, respectively. **(D)** RABV ΔG coated with its native glycoprotein is taken up by axon terminals and can be used to trace neurons in a retrograde manner. **(E)** EnvA pseudotyped RABV ΔG [RABV ΔG(EnvA)] only infects neurons expressing the TVA receptor. Trans-complementation with RG enables RABV ΔG to cross one synaptic step to infect the presynaptic partners of a defined neuron or neuronal population. The virus is then trapped in these presynaptic partner cells and cannot spread further due to the deficiency of RG in these presynaptic cells, hence limiting the strategy to a mono-trans-synaptic event. Initially infected source cells are identified by the expression of an additional fluorescent marker.

prevents recombination between the RNA genome and cellular RNAs.

Transgene expression from a RABV vector is integrally tied to viral genome expression and is thus constitutively ON. RABV transcription starts at the 3′ end (upstream of the N gene; **Figure 1A**) and proceeds sequentially throughout the genome. Attenuation at gene boundaries generates a gradient of transcripts with respect to gene order (reviewed in references Conzelmann et al., 1990; Albertini et al., 2011), resulting in a finely tuned ratio of gene products in the native virus (reviewed in references Conzelmann, 1998; Albertini et al., 2011). This feature can be manipulated to some extent to influence the level of expression of a transgene. In addition, "engineered" gene border transcription signals (Finke et al., 2000) or regulatory elements from other RNA viruses can also be deployed to modify transgene expression levels (Marschalek et al., 2009). RABV ΔG vectors expressing a single transgene have typically made use of the endogenous transcription signals, which normally flank the glycoprotein gene (Wickersham et al., 2007b; Osakada et al., 2011). In addition, it is possible to insert additional cistrons as long as each is flanked by suitable transcription start/stop signals (Conzelmann, 1998; Osakada et al., 2011). This principle was used to express two-independent genes from a RABV ΔG vector (Osakada et al., 2011). In this case 3.6 kb of exogenous sequence was effectively integrated into the RABV ΔG viral genome and subsequently packaged into infectious particles. Unlike other vectors, the most important factor limiting "cloning capacity" is probably not the total insert size, but instead the number of additional transcription initiation start sites introduced with the exogenous genes.

The RABV genome never encompasses a DNA form and this poses particular constraints on RABV derived vectors. Certain genetic tools such as lox P sites, tet-regulatory sequences or cell-specific promoters simply do not function with a negative-sense single-stranded RNA [(−)ssRNA] virus since a double stranded DNA binding site or substrate is required. Unfortunately, this precludes the use of a number of genetic tools that are normally employed for cell-specific or inducible expression of the viral-driven transgene (see **Figure 4**). The (−)ssRNA RABV genome also presents practical difficulties for the production of recombinant viral particles. Although improved methods for RABV ΔG rescue have recently been described (Wickersham et al., 2010; Osakada et al., 2011; Ghanem et al., 2012), reverse genetics approaches, required for the recovery of infectious RABV ΔG from cloned DNA, remain several orders of magnitude less efficient than for positive strand RNA or DNA viruses (Schnell et al., 1994; Ghanem et al., 2012). This being said, it is worth noting that once a new recombinant form of RABV ΔG has been recovered from DNA, it is straightforward to amplify the virus using an RG-expressing cell line (Osakada et al., 2011).

STRATEGIES FOR TRACING MONOSYNAPTIC CONNECTIONS TO SPECIFIC BRAIN REGIONS, NEURON TYPES, OR INDIVIDUAL NEURONS

TARGETING SPECIFIC BRAIN REGIONS

A specific brain region can simply be targeted via stereotaxic injection of CNS competent viral vectors expressing TVA/RG, followed several days later by injection into the same region of the RABV ΔG(EnvA). For example, mono-trans-synaptic tracing was crucial for determining synaptic connections between oxytocin-expressing neurons of the hypothalamic accessory magnocellular nucleus and neurons of the central amygdala (Knobloch et al., 2012).

TARGETING A DEFINED NEURONAL CELL POPULATION

While the aforementioned approach maps the connectivity of multiple neuron types within the respective brain structure, it may be desirable to target a defined neuronal cell population. In the next paragraphs we will highlight the variety of approaches that have been developed to achieve neuron type specific mono-trans-synaptic tracing.

One way to achieve this is by taking advantage of an ever-increasing list of mice expressing cre-recombinase in specific neuronal cell types (e.g., reference Gong et al., 2003). TVA/RG is then selectively expressed in these cell types using a cre-dependent viral vector (Wall et al., 2010; Watabe-Uchida et al., 2012) (**Figure 2A**). This strategy was applied to map reciprocal synaptic connections between PKC-δ^- and PKC-δ^+ interneurons in the central amygdala (Haubensak et al., 2010), and to perform brain-wide labeling of neurons providing direct input to dopaminergic neurons of the midbrain (Watabe-Uchida et al., 2012).

Alternatively, neuron types can be targeted based on their expression of cell surface receptors that recognize specific ligands. For example, a specific class of interneurons in the neocortex expresses the receptor ErbB4 that binds the soluble ligand neuregulin β1. A recent study took advantage of this interaction to target ErbB4-positive neurons by pseudotyping RABV ΔG with an avian virus envelope protein (EnvB) that binds to a neuregulin β1-EnvB receptor (TVB) bridge protein (Choi and Callaway, 2011). A lentivirus was pseudotyped in the same way to permit RG expression in the same source cell population (Choi and Callaway, 2011). Such approaches may also be of interest for studies of schizophrenia, which have been linked to a dysfunction in neuregulin signaling (Mei and Xiong, 2008). This approach could also provide a means for targeting RABV ΔG infection to particular cell populations in situations where genetic-based targeting approaches are not available, for example in primate systems (Choi and Callaway, 2011).

An alternative way to target a very specific source cell population is the use of a helper virus capable of propagating exclusively in dividing cells. Certain retroviruses, such as the Moloney murine leukemia virus (MMLV), are restricted in this manner and have classically been used to mark newly born neurons in the dentate gyrus of the hippocampus (reviewed in van Praag et al., 2002; Ming and Song, 2005). Stereotaxic injection of the MMLV expressing TVA/RG/fluorescent marker, followed by subsequent injection of RABV ΔG(EnvA) was thus used as a means of following the functional integration of newly born granule cells into existing neuronal circuits (Vivar et al., 2012).

All of the aforementioned examples necessitate two sequential stereotaxic injections into the same brain region [e.g., virus expressing TVA/RG, followed by RABV ΔG(EnvA)]. One can bypass the first step of this procedure by using RABV ΔG(EnvA)

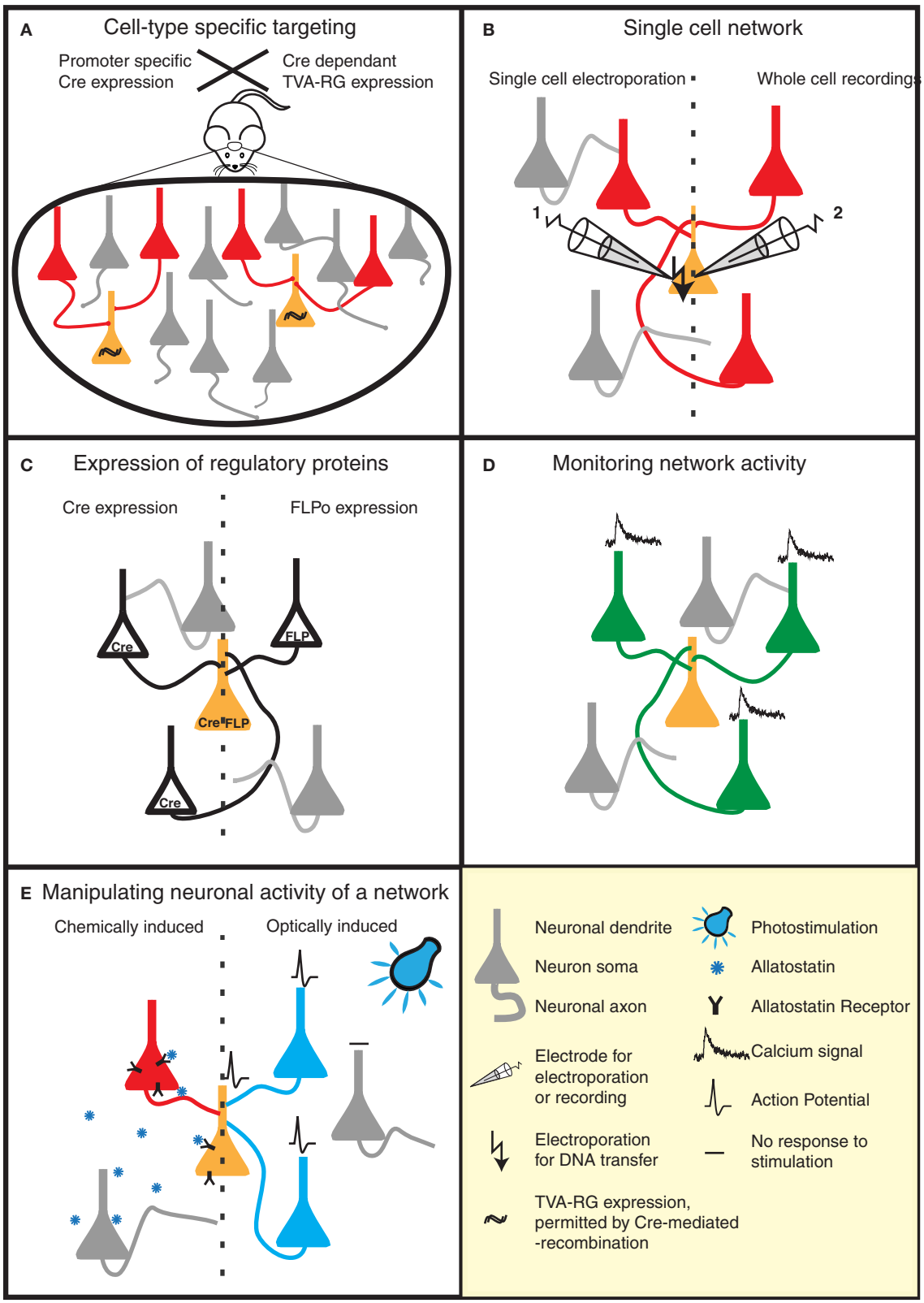

FIGURE 2 | Strategies to reveal the secrets of defined neural circuits. **(A,B)** There are several strategies to target the rabies infection to individual neurons or specific cell types. **(A)** Genetic strategies such as the Cre-lox system take advantage of cell-specific promoters to restrict Cre expression to a defined cell-type. Injection of a Cre-dependent helper virus expressing

(Continued)

FIGURE 2 | Continued
RG and TVA permits RABV ΔG(EnvA) infection, and subsequent mono-trans-synaptic tracing, to be limited to a specific source cell population. **(B)** Patch pipettes can be used to infect individual neurons with the plasmids encoding RG and specific surface proteins (e.g., TVA). These neurons are subsequently infected with pseudotyped (e.g., EnvA) RABV ΔG. This allows the tracing of the presynaptic partners of specific neurons. **(C–E)** RABV ΔG mediated expression of a number of genetic tools permit the dissection of structure/function of specific networks in a temporally and spatially controlled manner. **(C)** RABV ΔG mediated expression of recombinases (Cre/FLP) permits loss- or gain-of-function studies through conditional expression of specific genes in the infected network. **(D)** Population activity of specific neuronal networks can be monitored, for instance, by RABV ΔG directed expression of calcium indicators. **(E)** The activity of the starter cells, and their presynaptic network can be very specifically controlled by the expression of either allatostatin receptor or light-activated ion channels. Binding of allatostatin to its cognate receptor or activation of these channels by light of a specific wavelength leads to specific inhibition/activation of RABV ΔG infected neurons.

together with a bi-transgenic mouse line, in which TVA/RG is induced in a brain region- or cell-type specific manner under the control of a tet-regulatable promoter (Weible et al., 2010). This approach is suited to tracing long-range connections between nuclei that can be discretely targeted by cell-specific tetracycline transactivator expression. However, carefully designed controls are required to ensure that RG expression only occurs in the targeted source cell population and not in directly presynaptic neurons, as this would confound the interpretation of the tracing results (first-order vs. higher-order connectivity).

Mono-trans-synaptic tracing from defined source cell populations can also be achieved using a simpler targeting strategy which eliminates the need for the EnvA-TVA system, and instead takes advantage of the inherent qualities of certain retrogradely-transported viruses. Recent studies utilized this approach, by co-injecting RABV ΔG pseudotyped with its native G together with an RG-expressing retrogradely transported helper virus (Stepien et al., 2010; Yonehara et al., 2011). The source cell population was thus defined by their specific projection characteristics, rather than by their molecular identity. Injections were made into known target regions for the axons of certain neurons, thereby permitting the infection of axon terminals. With this approach, mono-trans-synaptic tracing enabled the identification of direct synaptic inputs to motor neurons targeting discrete muscle groups (Stepien et al., 2010), and to ON direction-selective retinal ganglion cells (Yonehara et al., 2011).

STRATEGIES TO TARGET INDIVIDUAL NEURONS

The aforementioned strategies (sections "Targeting specific brain regions" and "Targeting a defined neuronal cell population") may not permit the unambiguous identification of the presynaptic partners of a given neuron, because more than one source cell is typically targeted. Furthermore, in situations where a presynaptic partner of a source cell also expresses RG, an additional trans-synaptic crossing step may occur, resulting in the labeling of higher-order connections. One strategy to reduce this ambiguity is exemplified by Arenkiel et al. (2011). In this study the authors developed an elegant strategy to allow mono-trans-synaptic tracing of a very sparse and defined neuronal population. They transfected neuronal progenitor cells in the subventricular zone of the lateral ventricles in early postnatal mice with a targeting construct expressing TVA/RG. Adult-born granule cells derived from these progenitors migrate to the olfactory bulb and establish functional connections (Panzanelli et al., 2009). However, only a small number of migrated, functionally integrated daughter cells retained the ability to express TVA/RG, by virtue of rare integration events leading to stable expression of this targeting construct (Arenkiel et al., 2011). These source cells were then infected with RABV ΔG(EnvA) by stereotaxic injection into the olfactory bulb. The authors were thus able to trace microcircuits derived from sparsely distributed individual source granule cells.

The ability to target sparsely-distributed source cells may also be important for studies of long-range connections, where the topography or convergence of inputs needs to be examined and therefore the source cell number needs to be strictly limited. To achieve this, a complex strategy involving a conditional bi-transgenic mouse line and an AAV vector expressing TVA/RG under the control of a tetracycline-dependent promoter was employed (Miyamichi et al., 2011). RABV ΔG(EnvA) was subsequently injected into the same region as the AAV helper virus 14 days later. These tools not only permit tracing in a very sparse neuronal population, but also precise temporal control over TVA/RG expression.

Although mono-trans-synaptic tracing has most frequently been applied to populations of source cells, it also has great power for determining inputs into a single neuron *in vitro* and *in vivo* (**Figure 2B**). To target a single neuron, the plasmids encoding the tracing components (TVA/RG) and a fluorescent marker are first introduced together into this neuron. Two approaches have thus far been employed to achieve this *in vivo*—two-photon-guided electroporation and whole cell recording (Marshel et al., 2010; Rancz et al., 2011). Such *in vivo* approaches are painstaking, but permit the unambiguous identification of neurons presynaptic to a defined individual neuron. Furthermore, when combined with for instance whole-cell recordings and sensory stimulation, information regarding the anatomical receptive field of this neuron can be linked with its synaptic receptive field (Rancz et al., 2011).

RECENT ADVANCES IN NEURONAL CIRCUIT ANALYSIS EMPLOYING THE RABV ΔG APPROACH

MAPPING OF LONG-RANGE CONNECTIONS

One of the great advantages of RABV ΔG mediated mono-trans-synaptic tracing over other assays for synaptic connections [e.g., electron microscopy (EM) and paired electrophysiological recordings] is the ability to identify long-range synaptic connections. For example, RABV ΔG has been used to map direct long-range connections between mitral cells in the olfactory bulb and their postsynaptic targets in basal forebrain regions (Miyamichi et al., 2011). Such connections had previously been

inferred from the presence of axons (e.g., reference Scott et al., 1980), but direct synaptic connectivity had not been proven. Similarly, Knobloch et al. (2012) employed the RABV ΔG technology as part of a complex toolkit to elucidate novel connections between oxytocin expressing neurons in the hypothalamus and neurons of the central amygdala. In this case, synaptic connections were strongly suggested by a variety of supporting evidence, obtained from optogenetic-based mapping and electron microscopy data. However, mono-trans-synaptic tracing was essential for confirming the presence of a functional synapse.

RABV ΔG based tracing approaches have also been exploited to map inputs into specific dopaminergic populations of the midbrain—in this case, on the scale of the whole brain (Watabe-Uchida et al., 2012). The authors were able to correct or refine previous findings obtained with conventional tracing or optogenetic approaches. By targeting genetically defined source cell populations they identified more specific subsets of presynaptically connected neurons. In addition, the authors showed that striatal neurons do in fact provide direct input to dopaminergic neurons of the ventral tegmental area or substantia nigra (Watabe-Uchida et al., 2012). Lastly, the exquisite labeling of the neuronal morphology afforded by RABV-driven eGFP expression aided the identification of the type of presynaptic neurons.

FUNCTIONAL INTEGRATION OF POSTNATAL-BORN NEURONS INTO A NEURAL CIRCUIT

In addition to the validation of known connections, or the discovery of novel connections, a recent study examined the plasticity-induced remodeling of neural circuits (Arenkiel et al., 2011). In this study, the authors traced the connections formed by postnatal-born, newly migrated, differentiated granule cells following their integration into established circuits of the olfactory bulb. The authors further showed that odor stimulation resulted in increased input onto these neurons, as well as remodeling of their dendritic morphology. This study demonstrates the immense power of RABV ΔG based monosynaptic tracing for both screening of neural circuit changes as well as for fine morphological analysis.

A different study (Vivar et al., 2012) describes the time-dependent incorporation of adult-born granule cells of the dentate gyrus into existing neuronal circuits. To do this, the authors performed mono-trans-synaptic tracing at various time points after the initial labeling of adult-born daughter cells. They were then able to demonstrate quantitative changes in the type and number of the presynaptic neurons over time. In particular, they showed a transient period of input coming from mature granule cells, and that intra-hippocampal and cortical inputs increased with time. They also identified a novel "back-projection" from CA3 pyramidal cells. This study demonstrates the utility of RABV ΔG based mono-trans-synaptic tracing for the identification of novel connections, as well as for studying the remodeling of circuits.

THREE-DIMENSIONAL TOPOGRAPHY OF PRESYNAPTIC NEURONS

With the use of RABV ΔG based trans-synaptic tracing, Stepien et al. (2010) were able to demonstrate that distinct populations of premotor neurons project to functionally-defined motor neuron pools, and that these populations extend over a large three-dimensional space along the spinal cord. In a related study the authors showed that premotor interneurons controlling antagonistic extensor-flexor muscles are segregated from one another along the medial lateral axis of the dorsal spinal cord (Tripodi et al., 2011). In an unrelated study Miyamichi et al. (2011) examined the topography of inputs from olfactory bulb into different olfactory cortex regions. In doing so, the authors were able to correlate topography of post/presynaptic neurons and divergence/convergence of connections with the presumed functionality of each type of olfactory processing center. These studies demonstrate that the topography of connections can yield additional information about the functionality of circuits.

NOVEL RABV ΔG VARIANTS AND THEIR UTILITY FOR NEURONAL CIRCUIT ANALYSIS

A range of RABV ΔG variants have recently been described. These variants include vectors expressing the *trans*-acting factors required for conditional expression of other transgenes (e.g., Cre, FLP recombinase; **Figure 2C**), a genetically encoded calcium sensor (Osakada et al., 2011; Kiritani et al., 2012) (**Figure 2D**) and molecules for the activation[51] or silencing of circuits (Osakada et al., 2011) [e.g., allatostatin receptor, channelrhodopsin-2 (ChR2); **Figure 2E**]. Variants expressing additional fluorescent markers to permit a greater array of tracing possibilities are also described (Wickersham et al., 2007b; Osakada et al., 2011). These aforementioned tools can be combined with a variety of mouse models, for example those expressing Cre-or FLP-dependent reporters or conditional mutations permitting loss- or gain-of-function studies in defined neuronal circuits. A RABV ΔG vector expressing the light-activatable ChR2 has recently been used for the analysis of defined spino-cortical and cortico-striatal circuits (Apicella et al., 2012; Kiritani et al., 2012).

PERSPECTIVES FOR THE ANALYSIS OF NEURAL CIRCUIT STRUCTURE/FUNCTION

To date, our understanding of the wiring diagrams of neuronal circuits and the spatiotemporal dynamics of their electrical signals is rather limited. Critical steps toward this goal are the identification of the inputs of the circuit's diverse neuron types, and an understanding of their interaction within the circuit. The last years have seen numerous innovations in methods that rapidly advance the analysis of neural circuits. These include improvements in optical methods for stimulation and imaging, genetics, and computational methods. In the next paragraphs we will discuss how the RABV ΔG technology in concert with these methods can help shed light on some of the outstanding questions in this field.

TRACING STRUCTURE—FROM THE NANOSCALE TO THE MESOSCOPIC SCALE

RABV ΔG has outstanding properties for the labeling of the fine-scale neuronal morphology, due to its high-level expression of fluorescent proteins (Wickersham et al., 2007b). This feature

is advantageous for visualization approaches where further signal amplification is not feasible. Such approaches include fluorescence imaging of entire mouse brains following a chemical clearing procedure (Dodt et al., 2007; Hama et al., 2011) or using serial two-photon tomography (STP tomography) (Ragan et al., 2012). Similarly, the high-intensity expression of morphological markers permits the dynamic observation of processes such as spine stability/turnover in living animals (for a recent review see Holtmaat and Svoboda, 2009), and likely satisfies the requirements for super-resolution imaging at nanoscale resolution (for review, see references Huang et al., 2009; Sigrist and Sabatini, 2012). Furthermore, RABV mediated expression of horseradish peroxidase may be a way to enhance the intensity of labeling required for ultrastructural techniques such as serial block-face scanning electron microscopy (Denk and Horstmann, 2004; Briggman et al., 2011; Li et al., 2011).

RABV ΔG pseudotyped with RG can be used as a retrograde tracer (**Figure 1D**) to infer connectivity between brain regions by labeling cells projecting to a specific target region (Wickersham et al., 2007a; Apicella et al., 2012; Kiritani et al., 2012). In combination with large-scale fluorescence imaging techniques (Dodt et al., 2007; Hama et al., 2011; Ragan et al., 2012) this approach allows systematic brain-wide mapping of neuronal circuits at the mesoscopic scale (Bohland et al., 2009) (see also Mouse Brain Architecture Project).

Thus, the RABV ΔG technology has the potential to aid visualization of neuronal morphology over spatial dimensions ranging from the nanoscale (electron microscopy/super-resolution light microscopy) to the entire mouse brain (light-sheet microscopy/STP tomography).

CLASSIFYING NEURONAL CELL TYPES

One of the intractable problems with neuronal circuit analysis is the ability to define the neuronal cell types present within such a circuit. Cellular identity is based on an ever-more refined list of criteria such as electrical properties, patterns of gene expression and morphological features (Petilla Interneuron Nomenclature Group et al., 2008; Arenkiel and Ehlers, 2009). Ideally one would also link cell identity to the expression of a fluorescent marker to facilitate analysis of the properties of these cells within a circuit (Arenkiel and Ehlers, 2009; Lichtman and Denk, 2011; Steinmeyer and Yanik, 2012). For certain cell types this has been achieved with high specificity in transgenic mice (Gong et al., 2003) (reviewed in reference Lichtman and Denk, 2011). Pseudotyping of RABV ΔG permits the targeting of specific cellular populations, for example projection neurons or those expressing a certain surface protein (Mebatsion et al., 1997; Choi and Callaway, 2011). This enables the identification/classification of a neuron based on its morphology, projections, and in the case of mono-trans-synaptic tracing their connectivity properties. In the latter case, the morphological labeling of the presynaptic neurons aids their identification as well. RABV ΔG technology has been used, for example, to characterize neurons in the primate visual cortex (Nassi and Callaway, 2007; Nhan and Callaway, 2012) rodent neocortex (Larsen, 2008; Marshel et al., 2010; Rancz et al., 2011; Apicella et al., 2012; Kiritani et al., 2012) and rodent midbrain together with their presynaptic partners (Watabe-Uchida et al., 2012).

REVEALING SYNAPTIC CONNECTIVITY

The construction of neural circuit connectomes requires comprehensive knowledge of the underlying synaptic connectivity. We are still lacking quantitative measurements regarding the numbers and sub-cellular organization of the different inputs received by a neuron. EM, paired electrophysiological recording, and optical simulation approaches have done much to advance our knowledge of synaptic connections between neurons. However, these approaches are either time-intensive (EM, paired recordings), currently limited to microcircuits (EM), or can only demonstrate the existence of synaptic connections, but not their precise sub-cellular location (paired recordings, optical stimulation methods).

The elegance and power of the RABV ΔG mono-trans-synaptic tracing has now been amply demonstrated (as discussed above). Specifically, this technology provides information about the type, localization, and number of presynaptic neurons forming synaptic connections with particular target cell types. As such, it can be used for the validation of known neuronal synaptic connections (e.g., Stepien et al., 2010), but may also reveal hitherto unknown connections or a re-organization of wiring diagrams under physiological and pathophysiological conditions (**Figure 3A**). For example, the question of whether memories are stored in the connections formed by neurons (Seung, 2009) could be tested using this approach. Similarly, the integration of adult-born neurons (Arenkiel and Ehlers, 2009) into functional neuronal circuits can be examined (**Figure 3B**). A range of targeting approaches is now available (see above) to permit experimental design to be tailored to meet the requirements of a particular study. Lastly, in combination with techniques labeling synaptic contacts (GRASP/BLINC), mono-trans-synaptic tracing may be used to identify the sub-cellular location of synaptic inputs (Kim et al., 2012; Wickersham and Feinberg, 2012).

PROBING SYNAPTIC PROPERTIES AND SYNAPTIC INTEGRATION

One important parameter defining neuronal circuits is the physiological properties of specific anatomical connections (i.e., release probability, strength, short-term dynamics etc.). So far, the most precise method to achieve this is the use of simultaneous electrophysiological recordings between synaptically connected neurons (e.g., reference Frick et al., 2008). Specific labeling of pre- and post-synaptic neurons with mono-trans-synaptic tracing greatly enhances the sampling efficiency of synaptic connections for a given postsynaptic neuron (Wickersham et al., 2007b) (**Figure 3C**). In addition, the integration of synaptic inputs from a number of presynaptic neurons within an individual neuron can be studied. As an alternative approach to simultaneous electrophysiological recordings, presynaptic partners could be stimulated optically following RABV ΔG driven expression of light-activated ion channels or heterologous receptor systems (Osakada et al., 2011) (**Figures 2E** and **3C**).

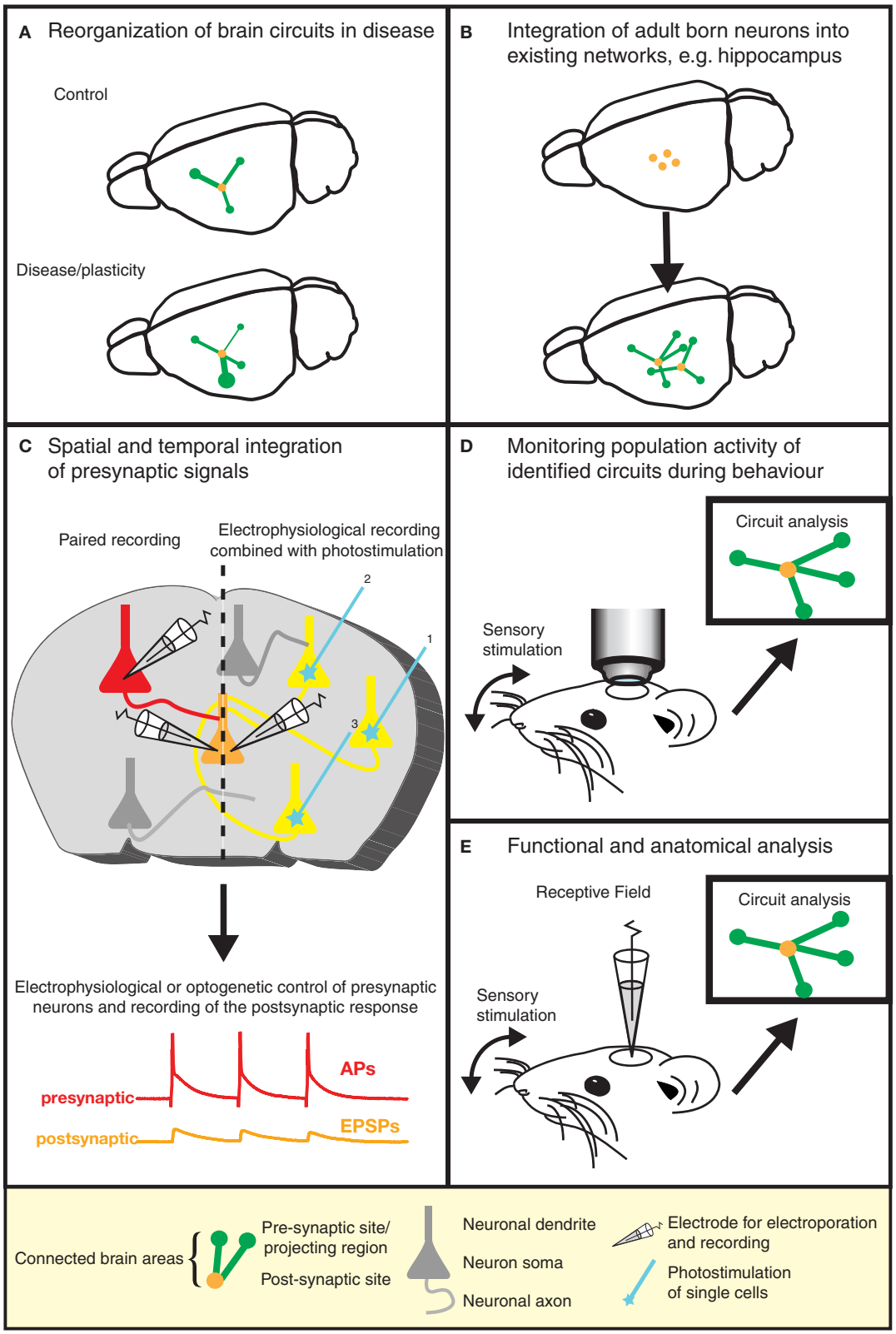

FIGURE 3 | Gaining insight into brain function by the dissection of neuronal circuits. Recent advances in RABV ΔG technology provide invaluable tools for gaining a better understanding of the function and structure of neuronal circuits. **(A)** For instance, the re-organization of neuronal circuits resulting from plasticity or disease can be revealed by comparing the

(Continued)

FIGURE 3 | Continued
wiring diagram of experimental and control brains. **(B)** We can learn more about plasticity in the adult brain by studying the integration of adult-born neurons into existing neuronal networks. Similar approaches might be used to study circuit integration following stem cell therapy. **(C)** The analysis of the physiological properties of synaptic connections between defined neuron types (in addition to the anatomical wiring diagram) is greatly aided by this technique. Furthermore, the spatial and temporal integration of signals from a larger number of presynaptic neurons can be examined in postsynaptic neurons. **(D)** The population activity of a defined neuronal circuit can also be measured during active sensory stimulation or behavior and subsequently correlated with the anatomical input network of a defined starter population. **(E)** The receptive field properties of individual neurons can be combined with the analysis of the anatomical wiring diagram of their presynaptic network.

COMBINING PHYSIOLOGY WITH ARCHITECTURE

Information processing in neural circuits depends on the spatiotemporal dynamics of the electrical signals within its neurons. It is therefore desirable to measure or manipulate the activity of these neurons during a particular behavioral task and to link the cellular activity with the circuit's structure (**Figures 2D,E**, and **3D**). Electrophysiology is the most direct method to measure electrical activity, and provides a very high signal-to-noise ratio. Recently, it has become feasible to combine direct electrophysiological measurements of individual neurons *in vivo* with RABV ΔG mono-trans-synaptic tracing (Rancz et al., 2011) (**Figures 2B** and **3E**).

In other instances it is advantageous to use imaging approaches to monitor the cellular activity of identified populations of neurons during a specific task (**Figure 3D**). The advent of genetically-encoded indicators for calcium ions, membrane potential, and neurotransmitters (for a recent review, see reference Looger and Griesbeck, 2012) makes it possible to express such sensors of cellular activity using RABV ΔG technology (Osakada et al., 2011) (**Figure 2D**). For instance, the cellular resolution afforded by two-photon microscopy imaging of changes in calcium ions provide a proxy for action potentials in neuronal populations *in vivo* (recently reviewed in reference Grewe et al., 2010). Although measurements of changes in membrane potential provide a more direct readout of electrical activity, the lack of suitable genetically encoded voltage sensors has, so far, hampered *in vivo* measurements of neuronal activity with cellular resolution. A new class of voltage sensors may permit this notion to become a reality (Kralj et al., 2012; Looger and Griesbeck, 2012). These sensors can be readily incorporated into the RABV ΔG expression system for combined functional neural circuit studies. Further developments in the form of new variants (see **Figure 4**) are likely to increase the range of applications for which the unique properties of RABV ΔG vectors can be exploited for imaging of neuronal circuits in the intact animal.

Finally, gain- or loss-of-function experiments can also be implemented employing the RABV ΔG technology (Osakada et al., 2011). There is now a large selection of available light-activated ion channels and heterologous receptors to control neuronal excitability (for reviews see references Arenkiel and Ehlers, 2009; Fortin et al., 2011; Yizhar et al., 2011). For example, specific firing patterns can be triggered or neurons be silenced in targeted neuronal circuits (as defined by the RABV ΔG transfection strategy) within freely moving mice. This optical control of neuronal activity can then be integrated with measurements of the compatible readout, such as behavior, fluorescence measurements, electrical recordings, or fMRI signals (reviewed in reference Yizhar et al., 2011), and finally linked to the structural circuit information.

SHORTCOMINGS OF THIS APPROACH AND ALTERNATIVE MONOSYNAPTIC VIRAL TRACERS

UNDERSAMPLING OF PRESYNAPTIC NEURONS

Although immensely powerful, RABV ΔG based tracing is, like any technology, affected by particular shortcomings. Certainly the most perplexing issue is the undersampling of labeled presynaptic neurons. This has been most clearly demonstrated by targeting single pyramidal neurons in the primary visual cortex *in vivo* (Marshel et al., 2010; Rancz et al., 2011). Mono-trans-synaptic tracing from individual layer 2/3 pyramidal neurons resulted in the labeling of fewer than 100 presynaptic neurons (Marshel et al., 2010), while up to ∼700 presynaptic neurons were labeled by targeting individual layer 5 pyramidal neurons (Rancz et al., 2011). Furthermore, mono-trans-synaptic tracing from a single starter cell in layer 5 of the S2 somatosensory cortex resulted in the tracing of 249 presynaptic cells (Miyamichi et al., 2011). These differences may be partially due to cell type and/or other factors such as plasmid delivery or regulation of transgene expression. Nonetheless, the number of labeled presynaptic neurons was substantially lower than that expected from calculations based on dendritic spine numbers and the average number of synapses formed between connected pairs of neocortical pyramidal neurons (e.g., references Larkman, 1991; Defelipe and Farinas, 1992; Markram et al., 1997; Feldmeyer et al., 2002). One possible explanation for this undersampling is the level of expression of RG which may fail to meet the stoichiometry required for the efficient assembly and trans-synaptic crossing of RABV particles *in vivo* (Marshel et al., 2010). It remains to be shown whether certain properties of the synaptic contacts (strength, activity, or molecular signature of presynaptic neuron) could influence the efficacy of synaptic crossing. A recently developed single-cell targeting technique using a recombinant polysynaptic RABV (Nguyen et al., 2012) should help shed some light on this issue, as should a more detailed analysis of the molecular characteristics of the synapses that are efficiently crossed.

NEUROINVASIVENESS

At least one study has pointed to a limited time window for experimental infection by RABV ΔG following intramuscular injection. Stepien et al. (2010) reported that motor neurons are refractory to infection by the peripheral route after approximately postnatal day 10. This limitation most likely stems from the fact that the RABV ΔG mono-trans-synaptic tracing approach employs a recombinant virus derived from the Street Alabama

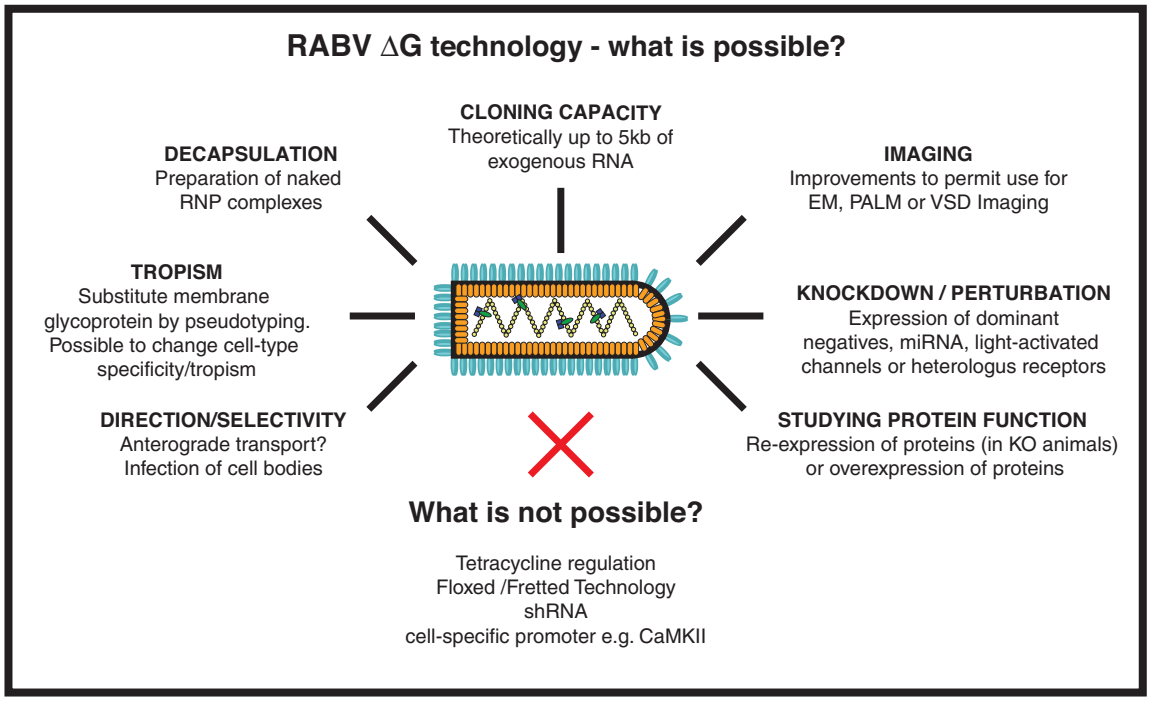

FIGURE 4 | RABV ΔG virus technology—what is possible? Here we provide an overview of the numerous tools that could, in the future, be developed using RABV ΔG vectors. Such possibilities include the expression of genetically encoded tools to aid imaging/microscopy approaches and tools to examine loss-of-function (knockdown) or gain-of-function of a gene/protein of interest. Other possibilities involve retargeting using engineered envelope proteins or the possibility of transfection using naked ribonucleoprotein (RNP) complexes. Some approaches are not possible with RABV ΔG vectors including the integration of lox P sites, cell specific promoters or tet-regulatory sequences, or expression of shRNA. RNP, Ribonucleoprotein, core of the RABV; EM, Electron microscopy; PALM, Photo-activated localization microscopy; VSD, Voltage-sensitive dye; miRNA, micro RNA; shRNA, short hairpin RNA.

Dufferin (SAD) B19 strain of RABV. This strain is highly attenuated for infection by the peripheral route and is only neuroinvasive following peripheral injection in young mice (Finke and Conzelmann, 2005; Rasalingam et al., 2005; Dietzschold et al., 2008). This may perhaps lead to the misconception that RABV ΔG technology can only be applied over a limited postnatal time window. For direct injections into the CNS, however, there is no such impediment. Efficient tracing has been observed in a variety of brain areas in both rats and mice of 1–6 months of age (Haubensak et al., 2010; Arenkiel et al., 2011; Rancz et al., 2011; Knobloch et al., 2012; Watabe-Uchida et al., 2012).

TIME WINDOW FOR TRACING

Features that make RABV extremely efficient both as pathogen and as viral tracer are also associated with its reduced cytotoxicity (Dietzschold et al., 2008; Lafon, 2011; Rieder and Conzelmann, 2011; Ugolini, 2011). Deleting RG is suggested to further decrease its cytotoxicity (Wickersham et al., 2010). Nevertheless, there is a finite time window for RABV ΔG mediated tracing experiments. RABV ΔG infected cortico-thalamic neurons maintain normal electrophysiological parameters up to 12 days following infection (Wickersham et al., 2007b). However, morphological defects or cell death were observed from 14–16 days post-infection (Wickersham et al., 2007b; Arenkiel et al., 2011). Osakada et al. (2011) suggest a 5–11 days (post-infection) time window for viable physiological experiments, which would also take into account any increased toxicity related to the nature of the virally expressed protein. Altogether, these data suggest a sufficiently broad time-window for RABV ΔG based tracing experiments. These findings may be contrasted with the significant perturbations in neuronal physiology that were reported to occur as early as 72 h post-infection with a GCaMP2-expressing PRV strain derived from the highly attenuated PRV-Bartha (Granstedt et al., 2009).

ALTERNATIVE VIRUS-BASED MONO-TRANS-SYNAPTIC TRACING TECHNIQUES

In spite of the many advantages of RABV ΔG, this technology is currently restricted to mapping *input* to a neuronal population. An alternative approach, permitting anterograde trans-synaptic tracing from a defined source cell population was recently described (Lo and Anderson, 2011). This approach employs a modified, thymidine kinase-deleted herpes simplex virus 1 (HSV-1) derived from strain 129 and capable of propagating in a selective manner in cre-expressing starter cells. This virus was tested in a variety of cre-expressing transgenic mouse lines and resulted in reliable anterograde trans-synaptic mapping of defined neuronal circuits. Notably, this system can be

readily combined with the large number of existing cre-/BAC-cre transgenic mouse lines and appears to be specific with respect to trans-synaptic transmission. Unfortunately, this approach is limited to the extent that it is not monosynaptic. In addition, it suffers from the cytotoxicity inherent to HSV-1 viruses and may also have the disadvantage of infecting axon terminals at the site of injection (Lo and Anderson, 2011). A cell-targetable, anterograde monosynaptic tracer derived from a glycoprotein-deleted vesicular stomatitis virus has recently been described (Beier et al., 2011). However, it is uncertain whether these findings can be reproduced *in vivo* (see Beier et al., 2012).

CONCLUDING REMARKS

Recent developments in the field of RABV ΔG technology convincingly establish the importance and power of this tool for neural circuit mapping. Combined with other imaging, physiological, and behavioral approaches, it promises to open new avenues of research permitting a greater understanding of the mammalian connectome and its function. RABV ΔG is applicable to a range of experimental paradigms and permits not only the study of circuit structure, but also the ability to manipulate or monitor its function.

RABV ΔG is invaluable as a viral tracer. In addition, it has considerable potential as a neuronal expression vector. In contrast to classical polysynaptic viral tracers, the current technology permits a greater degree of control over initially infected source cells, by virtue of pseudotyping technology and other genetic targeting approaches. RABV ΔG technology allows a comprehensive reconstruction of the input map of defined neurons as well as physiological monitoring of defined neuronal populations. This tool shows great promise for improving our understanding of neuronal circuit structure/function and its plastic modification during physiological processes or in disease. Future strategies for neuronal circuit analysis will involve a close alliance of genetics, circuit tracing, light- or heterologous receptor-mediated control, high-resolution imaging, and electrophysiology, and RABV ΔG will be an essential part of this tool box.

ACKNOWLEDGMENTS

We are grateful to N. Rebola, M. Helmstaedter, S. Silva, and members of our teams for their helpful comments. The following funding sources are acknowledged: INSERM, Max-Planck-Society, Region of Aquitaine, Erasmus-Mundus/ENC Network and DFG SFB 870.

REFERENCES

Albertini, A. A. V., Ruigrok, R. W. H., and Blondel, D. (2011). "Chapter 1 – Rabies virus transcription and replication," in *Advances in Virus Research*. Vol. 79. ed A. C. Jackson (Academic Press), 1–22.

Apicella, A. J., Wickersham, I. R., Seung, H. S., and Shepherd, G. M. (2012). Laminarly orthogonal excitation of fast-spiking and low-threshold-spiking interneurons in mouse motor cortex. *J. Neurosci.* 32, 7021–7033.

Arenkiel, B. R., and Ehlers, M. D. (2009). Molecular genetics and imaging technologies for circuit-based neuroanatomy. *Nature* 461, 900–907.

Arenkiel, B. R., Hasegawa, H., Yi, J. J., Larsen, R. S., Wallace, M. L., Philpot, B. D., et al. (2011). Activity-induced remodeling of olfactory bulb microcircuits revealed by monosynaptic tracing. *PLoS ONE* 6:e29423. doi: 10.1371/journal.pone.0029423

Bates, P., Young, J. A., and Varmus, H. E. (1993). A receptor for subgroup A *Rous sarcoma* virus is related to the low density lipoprotein receptor. *Cell* 74, 1043–1051.

Beier, K. T., Saunders, A., Oldenburg, I. A., Miyamichi, K., Akhtar, N., Luo, L., et al. (2011). Anterograde or retrograde transsynaptic labeling of CNS neurons with vesicular stomatitis virus vectors. *Proc. Natl. Acad. Sci. U.S.A.* 108, 15414–15419.

Beier, K. T., Saunders, A., Oldenburg, I. A., Miyamichi, K., Akhtar, N., Luo, L., et al. (2012). Correction for Beier et al. Anterograde or retrograde transsynaptic labeling of CNS neurons with vesicular stomatitis virus vectors. *Proc. Natl. Acad. Sci. U.S.A.* 109, 9219–9220.

Bohland, J. W., Wu, C., Barbas, H., Bokil, H., Bota, M., Breiter, H. C., et al. (2009). A proposal for a coordinated effort for the determination of brainwide neuroanatomical connectivity in model organisms at a mesoscopic scale. *PLoS Comput. Biol.* 5:e1000334. doi: 10.1371/journal.pcbi.1000334

Briggman, K. L., Helmstaedter, M., and Denk, W. (2011). Wiring specificity in the direction-selectivity circuit of the retina. *Nature* 471, 183–188.

Callaway, E. M. (2008). Transneuronal circuit tracing with neurotropic viruses. *Curr. Opin. Neurobiol.* 18, 617–623.

Carter, M., and Shieh, J. C. (2010). *Guide to Research Techniques in Neuroscience*. Amsterdam; Boston, MA: Elsevier/Academic Press.

Choi, J., and Callaway, E. M. (2011). Monosynaptic inputs to ErbB4-expressing inhibitory neurons in mouse primary somatosensory cortex. *J. Comp. Neurol.* 519, 3402–3414.

Choi, J., Young, J. A. T., and Callaway, E. M. (2010). Selective viral vector transduction of ErbB4 expressing cortical interneurons *in vivo* with a viral receptor–ligand bridge protein. *Proc. Natl. Acad. Sci. U.S.A.* 107, 16703–16708.

Conzelmann, K. K. (1998). Nonsegmented negative-strand RNA viruses: genetics and manipulation of viral genomes. *Annu. Rev. Genet.* 32, 123–162.

Conzelmann, K. K., Cox, J. H., Schneider, L. G., and Thiel, H. J. (1990). Molecular cloning and complete nucleotide sequence of the attenuated rabies virus SAD B19. *Virology* 175, 485–499.

Cowan, W. M. (1998). The emergence of modern neuroanatomy and developmental neurobiology. *Neuron* 20, 413–426.

Defelipe, J., and Farinas, I. (1992). The pyramidal neuron of the cerebral cortex: morphological and chemical characteristics of the synaptic inputs. *Prog. Neurobiol.* 39, 563–607.

Denk, W., and Horstmann, H. (2004). Serial block-face scanning electron microscopy to reconstruct three-dimensional tissue nanostructure. *PLoS Biol.* 2:e329. doi: 10.1371/journal.pbio.0020329

Dietzschold, B., Li, J., Faber, M., and Schnell, M. (2008). Concepts in the pathogenesis of rabies. *Future Virol.* 3, 481–490.

Dodt, H.-U., Leischner, U., Schierloh, A., Jährling, N., Mauch, C. P., Deininger, K., et al. (2007). Ultramicroscopy: three-dimensional visualization of neuronal networks in the whole mouse brain. *Nat. Methods* 4, 331–336.

Ekstrand, M. I., Enquist, L. W., and Pomeranz, L. E. (2008). The alpha-herpesviruses: molecular pathfinders in nervous system circuits. *Trends Mol. Med.* 14, 134–140.

Etessami, R., Conzelmann, K. K., Fadai-Ghotbi, B., Natelson, B., Tsiang, H., and Ceccaldi, P. E. (2000). Spread and pathogenic characteristics of a G-deficient rabies virus recombinant: an *in vitro* and *in vivo* study. *J. Gen. Virol.* 81, 2147–2153.

Federspiel, M. J., Bates, P., Young, J. A., Varmus, H. E., and Hughes, S. H. (1994). A system for tissue-specific gene targeting: transgenic mice susceptible to subgroup A avian leukosis virus-based retroviral vectors. *Proc. Natl. Acad. Sci. U.S.A.* 91, 11241–11245.

Feldmeyer, D., Lubke, J., Silver, R. A., and Sakmann, B. (2002). Synaptic connections between layer 4 spiny neurone-layer 2/3 pyramidal cell pairs in juvenile rat barrel cortex: physiology and anatomy of interlaminar signalling within a cortical column. *J. Physiol.* 538, 803–822.

Finke, S., and Conzelmann, K. K. (2005). Replication strategies of rabies virus. *Virus Res.* 111, 120–131.

Finke, S., Cox, J. H., and Conzelmann, K. K. (2000). Differential transcription attenuation of rabies virus genes by intergenic regions: generation of recombinant viruses overexpressing the polymerase gene. *J. Virol.* 74, 7261–7269.

Fortin, D. L., Dunn, T. W., Fedorchak, A., Allen, D., Montpetit, R.,

Banghart, M. R., et al. (2011). Optogenetic photochemical control of designer K+ channels in mammalian neurons. *J. Neurophysiol.* 106, 488–496.

Frick, A., Feldmeyer, D., Helmstaedter, M., and Sakmann, B. (2008). Monosynaptic connections between pairs of L5A pyramidal neurons in columns of juvenile rat somatosensory cortex. *Cereb. Cortex* 18, 397–406.

Ghanem, A., Kern, A., and Conzelmann, K.-K. (2012). Significantly improved rescue of rabies virus from cDNA plasmids. *Eur. J. Cell Biol.* 91, 10–16.

Gong, S., Zheng, C., Doughty, M. L., Losos, K., Didkovsky, N., Schambra, U. B., et al. (2003). A gene expression atlas of the central nervous system based on bacterial artificial chromosomes. *Nature* 425, 917–925.

Gough, P. M., and Jorgenson, R. D. (1976). Rabies antibodies in sera of wild birds. *J. Wildl. Dis.* 12, 392–395.

Granstedt, A. E., Szpara, M. L., Kuhn, B., Wang, S. S., and Enquist, L. W. (2009). Fluorescence-based monitoring of *in vivo* neural activity using a circuit-tracing pseudorabies virus. *PLoS ONE* 4:e6923. doi: 10.1371/journal.pone.0006923

Grewe, B. F., Langer, D., Kasper, H., Kampa, B. M., and Helmchen, F. (2010). High-speed *in vivo* calcium imaging reveals neuronal network activity with near-millisecond precision. *Nat. Methods* 7, 399–405.

Hama, H., Kurokawa, H., Kawano, H., Ando, R., Shimogori, T., Noda, H., et al. (2011). Scale: a chemical approach for fluorescence imaging and reconstruction of transparent mouse brain. *Nat. Neurosci.* 14, 1481–1488.

Haubensak, W., Kunwar, P. S., Cai, H., Ciocchi, S., Wall, N. R., Ponnusamy, R., et al. (2010). Genetic dissection of an amygdala microcircuit that gates conditioned fear. *Nature* 468, 270–276.

Holtmaat, A., and Svoboda, K. (2009). Experience-dependent structural synaptic plasticity in the mammalian brain. *Nat. Rev. Neurosci.* 10, 647–658.

Huang, B., Bates, M., and Zhuang, X. (2009). Super-resolution fluorescence microscopy. *Annu. Rev. Biochem.* 78, 993–1016.

Kelly, R. M., and Strick, P. L. (2000). Rabies as a transneuronal tracer of circuits in the central nervous system. *J. Neurosci. Methods* 103, 63–71.

Kim, J., Zhao, T., Petralia, R. S., Yu, Y., Peng, H., Myers, E., et al. (2012). mGRASP enables mapping mammalian synaptic connectivity with light microscopy. *Nat. Methods* 9, 96–102.

Kiritani, T., Wickersham, I. R., Seung, H. S., and Shepherd, G. M. (2012). Hierarchical connectivity and connection-specific dynamics in the corticospinal-corticostriatal microcircuit in mouse motor cortex. *J. Neurosci.* 32, 4992–5001.

Knobloch, H. S., Charlet, A., Hoffmann, L. C., Eliava, M., Khrulev, S., Cetin, A. H., et al. (2012). Evoked axonal oxytocin release in the central amygdala attenuates fear response. *Neuron* 73, 553–566.

Kralj, J. M., Douglass, A. D., Hochbaum, D. R., Maclaurin, D., and Cohen, A. E. (2012). Optical recording of action potentials in mammalian neurons using a microbial rhodopsin. *Nat. Methods* 9, 90–95.

Lafon, M. (2011). Evasive strategies in rabies virus infection. *Adv. Virus Res.* 79, 33–53.

Larkman, A. U. (1991). Dendritic morphology of pyramidal neurones of the visual cortex of the rat: III. Spine distributions. *J. Comp. Neurol.* 306, 332–343.

Larsen, D. D. (2008). Retrograde tracing with recombinant rabies virus reveals correlations between projection targets and dendritic architecture in layer 5 of mouse barrel cortex. *Front. Neural Circuits* 1:5. doi: 10.3389/neuro.04.005.2007

Li, J., Erisir, A., and Cline, H. (2011). *In vivo* time-lapse imaging and serial section electron microscopy reveal developmental synaptic rearrangements. *Neuron* 69, 273–286.

Lichtman, J. W., and Denk, W. (2011). The big and the small: challenges of imaging the brain's circuits. *Science* 334, 618–623.

Lo, L., and Anderson, D. J. (2011). A Cre-dependent, anterograde transsynaptic viral tracer for mapping output pathways of genetically marked neurons. *Neuron* 72, 938–950.

Looger, L. L., and Griesbeck, O. (2012). Genetically encoded neural activity indicators. *Curr. Opin. Neurobiol.* 22, 18–23.

Luo, L., Callaway, E. M., and Svoboda, K. (2008). Genetic dissection of neural circuits. *Neuron* 57, 634–660.

Markram, H., Lubke, J., Frotscher, M., Roth, A., and Sakmann, B. (1997). Physiology and anatomy of synaptic connections between thick tufted pyramidal neurones in the developing rat neocortex. *J. Physiol.* 500(Pt 2), 409–440.

Marschalek, A., Finke, S., Schwemmle, M., Mayer, D., Heimrich, B., Stitz, L., et al. (2009). Attenuation of rabies virus replication and virulence by picornavirus internal ribosome entry site elements. *J. Virol.* 83, 1911–1919.

Marshel, J. H., Mori, T., Nielsen, K. J., and Callaway, E. M. (2010). Targeting single neuronal networks for gene expression and cell labeling *in vivo*. *Neuron* 67, 562–574.

Mebatsion, T., Finke, S., Weiland, F., and Conzelmann, K. K. (1997). A CXCR4/CD4 pseudotype rhabdovirus that selectively infects HIV-1 envelope protein-expressing cells. *Cell* 90, 841–847.

Mebatsion, T., Konig, M., and Conzelmann, K. K. (1996a). Budding of rabies virus particles in the absence of the spike glycoprotein. *Cell* 84, 941–951.

Mebatsion, T., Schnell, M. J., Cox, J. H., Finke, S., and Conzelmann, K. K. (1996b). Highly stable expression of a foreign gene from rabies virus vectors. *Proc. Natl. Acad. Sci. U.S.A.* 93, 7310–7314.

Mebatsion, T., Schnell, M. J., and Conzelmann, K. K. (1995). Mokola virus glycoprotein and chimeric proteins can replace rabies virus glycoprotein in the rescue of infectious defective rabies virus particles. *J. Virol.* 69, 1444–1451.

Mei, L., and Xiong, W.-C. (2008). Neuregulin 1 in neural development, synaptic plasticity and schizophrenia. *Nat. Rev. Neurosci.* 9, 437–452.

Ming, G.-L., and Song, H. (2005). Adult neurogenesis in the mammalian central nervous system. *Annu. Rev. Neurosci.* 28, 223–250.

Miyamichi, K., Amat, F., Moussavi, F., Wang, C., Wickersham, I., Wall, N. R., et al. (2011). Cortical representations of olfactory input by trans-synaptic tracing. *Nature* 472, 191–196.

Nassi, J. J., and Callaway, E. M. (2007). Specialized circuits from primary visual cortex to V2 and area MT. *Neuron* 55, 799–808.

Nel, L. H., and Markotter, W. (2007). Lyssaviruses. *Crit. Rev. Microbiol.* 33, 301–324.

Nguyen, T. D., Wirblich, C., Aizenman, E., Schnell, M. J., Strick, P. L., and Kandler, K. (2012). Targeted single-neuron infection with rabies virus for transneuronal multisynaptic tracing. *J. Neurosci. Methods* 209, 367–370.

Nhan, H. L., and Callaway, E. M. (2012). Morphology of superior colliculus- and middle temporal area-projecting neurons in primate primary visual cortex. *J. Comp. Neurol.* 520, 52–80.

Osakada, F., Mori, T., Cetin, A. H., Marshel, J. H., Virgen, B., and Callaway, E. M. (2011). New rabies virus variants for monitoring and manipulating activity and gene expression in defined neural circuits. *Neuron* 71, 617–631.

Panzanelli, P., Bardy, C., Nissant, A., Pallotto, M., Sassoe-Pognetto, M., Lledo, P. M., et al. (2009). Early synapse formation in developing interneurons of the adult olfactory bulb. *J. Neurosci.* 29, 15039–15052.

Petilla Interneuron Nomenclature Group (PING), Ascoli, G. A., Alonso-Nanclares, L., Anderson, S. A., Barrionuevo, G., Benavides-Piccione, R., Burkhalter, A., et al. (2008). Petilla terminology: nomenclature of features of GABAergic interneurons of the cerebral cortex. *Nat. Rev. Neurosci.* 9, 557–568.

Ragan, T., Kadiri, L. R., Venkataraju, K. U., Bahlmann, K., Sutin, J., Taranda, J., et al. (2012). Serial two-photon tomography for automated *ex vivo* mouse brain imaging. *Nat. Methods* 9, 255–258.

Rancz, E. A., Franks, K. M., Schwarz, M. K., Pichler, B., Schaefer, A. T., and Margrie, T. W. (2011). Transfection via whole-cell recording *in vivo*: bridging single-cell physiology, genetics and connectomics. *Nat. Neurosci.* 14, 527–532.

Rasalingam, P., Rossiter, J. P., Mebatsion, T., and Jackson, A. C. (2005). Comparative pathogenesis of the SAD-L16 strain of rabies virus and a mutant modifying the dynein light chain binding site of the rabies virus phosphoprotein in young mice. *Virus Res.* 111, 55–60.

Rieder, M., and Conzelmann, K.-K. (2011). Interferon in rabies virus infection. *Adv. Virus Res.* 79, 91–114.

Sakuma, T., Barry, M. A., and Ikeda, Y. (2012). Lentiviral vectors: basic to translational. *Biochem. J.* 443, 603–618.

Schnell, M. J., Mebatsion, T., and Conzelmann, K. K. (1994). Infectious rabies viruses from cloned cDNA. *EMBO J.* 13, 4195–4203.

Scott, J. W., McBride, R. L., and Schneider, S. P. (1980). The organization of projections from the olfactory bulb to the piriform cortex and olfactory tubercle in the rat. *J. Comp. Neurol.* 194, 519–534.

Seung, H. S. (2009). Reading the book of memory: sparse sampling versus dense mapping of connectomes. *Neuron* 62, 17–29.

Sigrist, S. J., and Sabatini, B. L. (2012). Optical super-resolution microscopy in neurobiology. *Curr. Opin. Neurobiol.* 22, 86–93.

Steinmeyer, J. D., and Yanik, M. F. (2012). High-throughput single-cell manipulation in brain tissue. *PLoS ONE* 7:e35603. doi: 10.1371/journal.pone.0035603

Stepien, A. E., Tripodi, M., and Arber, S. (2010). Monosynaptic rabies virus reveals premotor network organization and synaptic specificity of cholinergic partition cells. *Neuron* 68, 456–472.

Tripodi, M., Stepien, A. E., and Arber, S. (2011). Motor antagonism exposed by spatial segregation and timing of neurogenesis. *Nature* 479, 61–66.

Ugolini, G. (1995). Specificity of rabies virus as a transneuronal tracer of motor networks: transfer from hypoglossal motoneurons to connected second-order and higher order central nervous system cell groups. *J. Comp. Neurol.* 356, 457–480.

Ugolini, G. (2011). Rabies virus as a transneuronal tracer of neuronal connections. *Adv. Virus Res.* 79, 165–202.

van Praag, H., Schinder, A. F., Christie, B. R., Toni, N., Palmer, T. D., and Gage, F. H. (2002). Functional neurogenesis in the adult hippocampus. *Nature* 415, 1030–1034.

Vivar, C., Potter, M. C., Choi, J., Lee, J.-Y., Stringer, T. P., Callaway, E. M., et al. (2012). Monosynaptic inputs to new neurons in the dentate gyrus. *Nat. Commun.* 3:1107. doi: 10.1038/ncomms2101

Wall, N. R., Wickersham, I. R., Cetin, A., De La Parra, M., and Callaway, E. M. (2010). Monosynaptic circuit tracing *in vivo* through Cre-dependent targeting and complementation of modified rabies virus. *Proc. Natl. Acad. Sci. U.S.A.* 107, 21848–21853.

Watabe-Uchida, M., Zhu, L., Ogawa, S. K., Vamanrao, A., and Uchida, N. (2012). Whole-brain mapping of direct inputs to midbrain dopamine neurons. *Neuron* 74, 858–873.

Weible, A. P., Schwarcz, L., Wickersham, I. R., Deblander, L., Wu, H., Callaway, E. M., et al. (2010). Transgenic targeting of recombinant rabies virus reveals monosynaptic connectivity of specific neurons. *J. Neurosci.* 30, 16509–16513.

Wickersham, I. R., and Feinberg, E. H. (2012). New technologies for imaging synaptic partners. *Curr. Opin. Neurobiol.* 22, 1–7.

Wickersham, I. R., Finke, S., Conzelmann, K.-K., and Callaway, E. M. (2007a). Retrograde neuronal tracing with a deletion-mutant rabies virus. *Nat. Methods* 4, 47–49.

Wickersham, I. R., Lyon, D. C., Barnard, R. J. O., Mori, T., Finke, S., Conzelmann, K.-K., et al. (2007b). Monosynaptic restriction of transsynaptic tracing from single, genetically targeted neurons. *Neuron* 53, 639–647.

Wickersham, I. R., Sullivan, H. A., and Seung, H. S. (2010). Production of glycoprotein-deleted rabies viruses for monosynaptic tracing and high-level gene expression in neurons. *Nat. Protoc.* 5, 595–606.

Yizhar, O., Fenno, L. E., Davidson, T. J., Mogri, M., and Deisseroth, K. (2011). Optogenetics in neural systems. *Neuron* 71, 9–34.

Yonehara, K., Balint, K., Noda, M., Nagel, G., Bamberg, E., and Roska, B. (2011). Spatially asymmetric reorganization of inhibition establishes a motion-sensitive circuit. *Nature* 469, 407–410.

Young, J. A., Bates, P., and Varmus, H. E. (1993). Isolation of a chicken gene that confers susceptibility to infection by subgroup A avian leukosis and sarcoma viruses. *J. Virol.* 67, 1811–1816.

Conflict of Interest Statement: The authors declare that the research was conducted in the absence of any commercial or financial relationships that could be construed as a potential conflict of interest.

Received: 09 October 2012; paper pending published: 29 October 2012; accepted: 05 January 2013; published online: 24 January 2013.

Citation: Ginger M, Haberl M, Conzelmann K-K, Schwarz MK and Frick A (2013) Revealing the secrets of neuronal circuits with recombinant rabies virus technology. Front. Neural Circuits 7:2. doi: 10.3389/fncir.2013.00002

GLOSSARY

Anterograde tracing: Tracing of projection neurons by transport from the cell bodies to the axon terminals.

Connectome: Here referred to as a complete map of all synaptic connections of the brain or a neural circuit.

Mono-trans-synaptic tracing or monosynaptic trans-synaptic tracing: The process of tracing connections between source cells and first-order synaptically connected partners.

Neurotropic virus: Virus preferentially infecting neurons.

Polysynaptic tracer: This term is often used quite loosely to describe tracers that spread from one neuron to another (trans-neuronal tracer), but not always exclusively between synaptically connected cells. In contrast to mono-trans-synaptic tracers, tracing can occur between chains of connected neurons.

Pseudotyping: The process of replacing the native surface glycoprotein of a virus with that of another virus to alter viral tropism.

Retrograde tracing: Tracing of projection neurons by transport from the axon terminals to the cell bodies.

Reverse genetics: In the context of virology the term reverse genetics implies the reconstitution of live infectious virus particles using cDNAs, transfected into heterologous cells, as starting material.

Source cells: Initially infected postsynaptic neuron/s that allows retrograde RABV ΔG spread upon RG transcomplementation, thereby revealing directly presynaptic partners.

Trans-neuronal tracer: A tracer that passes from one neuron to another, for which synapse specificity has not been adequately identified.

Trans-synaptic tracer: A tracer that spreads exclusively between neurons that are connected by synaptic contacts.

Tropism: Preferential or specific infection of, and replication within, a certain cell-type.

2.1.2 Anterograde Rabies Virus for 3D Reconstruction of Neuronal Morphology

Much of our current knowledge about the circuits of the brain comes from studies labeling the output of a brain region, anterogradely, either in bulk or sparsely followed by a projection-quantification or a precise reconstruction of individual axons, respectively. In particular sparse labeling has always been difficult to achieve and cumbersome, which could be facilitated by genetic strategies. The next section describes the generation of a new viral vector that facilitates the reconstruction of the neuronal structure. The experimental methods and materials used as well as the results are thoroughly described in the publication included in the subsequent section.
The computational reconstruction and figure preparation shown in Figure 2 has been performed by Jason Guest and Marcel Oberlaender. The author of the thesis was involved in the design, the performing and analysis of all experiments, partially or fully, and produced the here presented novel viral vectors.

Publication N. 2

An anterograde rabies virus vector for high-resolution large-scale reconstruction of 3D neuron morphology

Matthias Georg Haberl*, Silvia Viana da Silva*,
Jason M. Guest, Melanie Ginger, Alexander Ghanem,
Christophe Mulle, Marcel Oberlaender,
Karl-Klaus Conzelmann and Andreas Frick

Brain Structure and Function, Published online April 11, 2014

Brain Struct Funct
DOI 10.1007/s00429-014-0730-z

ORIGINAL ARTICLE

An anterograde rabies virus vector for high-resolution large-scale reconstruction of 3D neuron morphology

Matthias Georg Haberl · Silvia Viana da Silva · Jason M. Guest · Melanie Ginger · Alexander Ghanem · Christophe Mulle · Marcel Oberlaender · Karl-Klaus Conzelmann · Andreas Frick

Received: 24 September 2013 / Accepted: 7 February 2014

Abstract Glycoprotein-deleted rabies virus (RABV ΔG) is a powerful tool for the analysis of neural circuits. Here, we demonstrate the utility of an anterograde RABV ΔG variant for novel neuroanatomical approaches involving either bulk or sparse neuronal populations. This technology exploits the unique features of RABV ΔG vectors, namely autonomous, rapid high-level expression of transgenes, and limited cytotoxicity. Our vector permits the unambiguous long-range and fine-scale tracing of the entire axonal arbor of individual neurons throughout the brain. Notably, this level of labeling can be achieved following infection with a single viral particle. The vector is effective over a range of ages (>14 months) aiding the studies of neurodegenerative disorders or aging, and infects numerous cell types in all brain regions tested. Lastly, it can also be readily combined with retrograde RABV ΔG variants. Together with other modern technologies, this tool provides new possibilities for the investigation of the anatomy and physiology of neural circuits.

Keywords Neuronal morphology · Connectivity · Sparse labeling · Circuit reconstruction · Neuron-type classification · Alzheimer's disease

Introduction

The reconstruction of neuronal circuits is central to many questions in neuroscience. Indeed, knowledge of the fine-scale morphology of neurons provides not only insight into the identity and function of individual neurons, but also into the function of neural circuits (Douglas and Martin 2004; Lichtman and Denk 2011; Oberlaender et al. 2012a;

M. G. Haberl and S. Viana da Silva contributed equally to this work.

M. G. Haberl · M. Ginger · A. Frick (✉)
Physiopathologie de la plasticité neuronale, INSERM, Neurocentre Magendie, U862, Bordeaux, France
e-mail: andreas.frick@inserm.fr

M. G. Haberl · M. Ginger · A. Frick
Physiopathologie de la plasticité neuronale, Univ. Bordeaux, Neurocentre Magendie, U862, Bordeaux, France

M. G. Haberl
Institute of NeuroInformatics, University of Zurich, Zurich, Switzerland

S. Viana da Silva · M. Ginger · C. Mulle
Interdisciplinary Institute for Neuroscience, CNRS, UMR 5297, Bordeaux, France

S. Viana da Silva · M. Ginger · C. Mulle
Interdisciplinary Institute for Neuroscience, Univ. Bordeaux, UMR 5297, Bordeaux, France

S. Viana da Silva
PDBEB CNC, University of Coimbra, Coimbra, Portugal

J. M. Guest · M. Oberlaender
Digital Neuroanatomy, Max Planck Florida Institute for Neuroscience, Jupiter, FL, USA

A. Ghanem · K.-K. Conzelmann
Max-von-Pettenkofer Institute and Gene Center of the Ludwig-Maximilians-University Munich, Munich, Germany

M. Oberlaender
Computational Neuroanatomy Group, Max Planck Institute for Biological Cybernetics, Tuebingen, Germany

M. Oberlaender
Bernstein Center for Computational Neuroscience, Tuebingen, Germany

Published online: 11 April 2014

Parekh and Ascoli 2013; Svoboda 2011). Successful neuronal reconstruction depends on a number of key parameters: (1) Neurons must be labeled in a way that permits visualization of all neuronal structures (dendrites, spines, axons, boutons). (2) The full extent of neuronal processes should be efficiently labeled. In particular, this applies to the axons, which extend over large brain volumes (Oberlaender et al. 2011). (3) Labeling would ideally permit visualization by high-resolution light microscopy approaches (such as confocal, two-photon, or super-resolution microscopy). In effect, this means efficient expression of a volume-filling fluorescent marker and a high signal-to-noise ratio for the labeled structure. (4) The ideal labeling method would not only be suited to bulk labeling of populations of neurons, but importantly also provide intense labeling of sparse populations of neurons, or even single neurons. This is, because to date the most successful reconstructions of complete neuronal morphology require sparse or single-cell labeling since the axons of bulk labeled neurons become indistinguishable in the densely packed neuropil unless resolved with electron microscopy (da Costa and Martin 2013; Helmstaedter 2013).

Viral vectors fulfill many of these criteria due to their self-amplifying properties (ensuring a high-level expression of volume-filling markers) (Callaway 2008; van den Pol et al. 2009). In particular, genetically modified rabies virus (RABV) is well suited to this approach due to its highly neurotropic nature, rapid, high-level expression of encoded proteins and relatively low cytotoxicity (Wickersham et al. 2007a; Ginger et al. 2013b). The glycoprotein gene-deleted RABV variant, (RABV ΔG) is an especially useful tool that permits the manipulation of the tropism of the virus through pseudotyping approaches (Mebatsion et al. 1997; Ginger et al. 2013b). This principle has previously been exploited for both retrograde labeling of neurons (Wickersham et al. 2007a; Larsen et al. 2007; Nhan and Callaway 2012) and for labeling inputs into a specific cell population (i.e., mono-trans-synaptic tracing) (Wickersham et al. 2007b; Choi et al. 2010).

Here, we employ a RABV ΔG-based method that allows direct transduction of cell bodies, permitting the tracing and complete 3D reconstruction of dendritic and axonal arbors of sparsely labeled neurons. This method combines the advantages of an anterograde tracer with the brilliant morphological labeling previously described for recombinant RABV ΔG (Wickersham et al. 2007a). This vector fulfills all of the aforementioned criteria for neuronal labeling. Low cytotoxicity, fast and strong expression and intense labeling of even the most distant processes set it apart from 'classical' viral and non-viral anterograde neuroanatomical tracing approaches. Moreover, the ability to infect a range of cell types over a large age window makes this vector a versatile tool for a large number of experimental situations.

Results

To render RABV ΔG capable of cell body infection, we pseudotyped it with a chimeric envelope protein containing the N-terminal domain of the vesicular stomatitis virus glycoprotein (VSV-G). VSV-G binds to highly ubiquitous receptors (Finkelshtein et al. 2013), thus conferring the ability to transduce a wide range of cell types, a property that has previously been exploited for the production of VSV-G pseudotyped viral vectors such as retro- and lentiviruses (Burns et al. 1993). We replaced the membrane anchor and C-terminal cytoplasmic sequence of the authentic VSV-G with that of the RABV-G protein (^{RtmC}) to support selective incorporation of the protein into the RABV ΔG envelope (Fig. 1a). We have generated vectors expressing either a membrane-targeted form of tdTomato labeling the neuronal membrane for subsequent surface reconstruction (Fig. 1c, lower panels; Fig. 3c), or cytoplasmic fluorescent proteins (eGFP and mCherry) (all other figures). The resulting vector [RABV ΔG (VSV G^{RtmC})] consistently transduced cells at the site of injection (Figs. 1, 2, 3, 4, 5, 6).

Important criteria determining the suitability of a viral vector for neuronal tracing are the time course for expression, the intensity of expression, and the morphological detail provided by the labeling. Thus, we compared RABV ΔG (VSV G^{RtmC}) with two commonly used anterograde viral tracers, namely lentivirus, and adeno-associated virus (AAV). We quantified fluorescence intensity and the signal-to-noise ratio for eGFP expressing neurons following injection of these vectors into the hippocampal dentate gyrus (DG) region (Fig. 1b). Fluorescence intensity and signal-to-noise ratio measured at the cell bodies of transduced neurons were significantly higher for RABV ΔG compared to both other vectors (one-way Anova followed by Tukey multiple-comparison; $p < 0.001$). Importantly, these superior labeling qualities were achieved (with no sign of cytotoxicity) at much shorter time scales of infection (6 days post infection for RABV ΔG (VSV G^{RtmC}) versus 12 and 22 days for lentivirus and AAV, respectively). Moreover, dendrites, spines, axons, boutons, as well as filopodia were readily distinguished within RABV ΔG (VSV G^{RtmC}) infected neurons, aiding their visualization and reconstruction (Fig. 1c). Notably, the labeled neurons presented here are DG granule cells, neurons that are difficult to infect using the native RABV (reviewed in Ohara et al. 2009).

We noted that the transduction with RABV ΔG (VSV-G^{RtmC}) occurred in a purely anterograde manner (i.e., infection of cell bodies and subsequent labeling of axons and dendrites). To exclude the possibility that RABV ΔG (VSV-G^{RtmC}) is transported in a retrograde or trans-synaptic manner, we performed injections into the whisker-

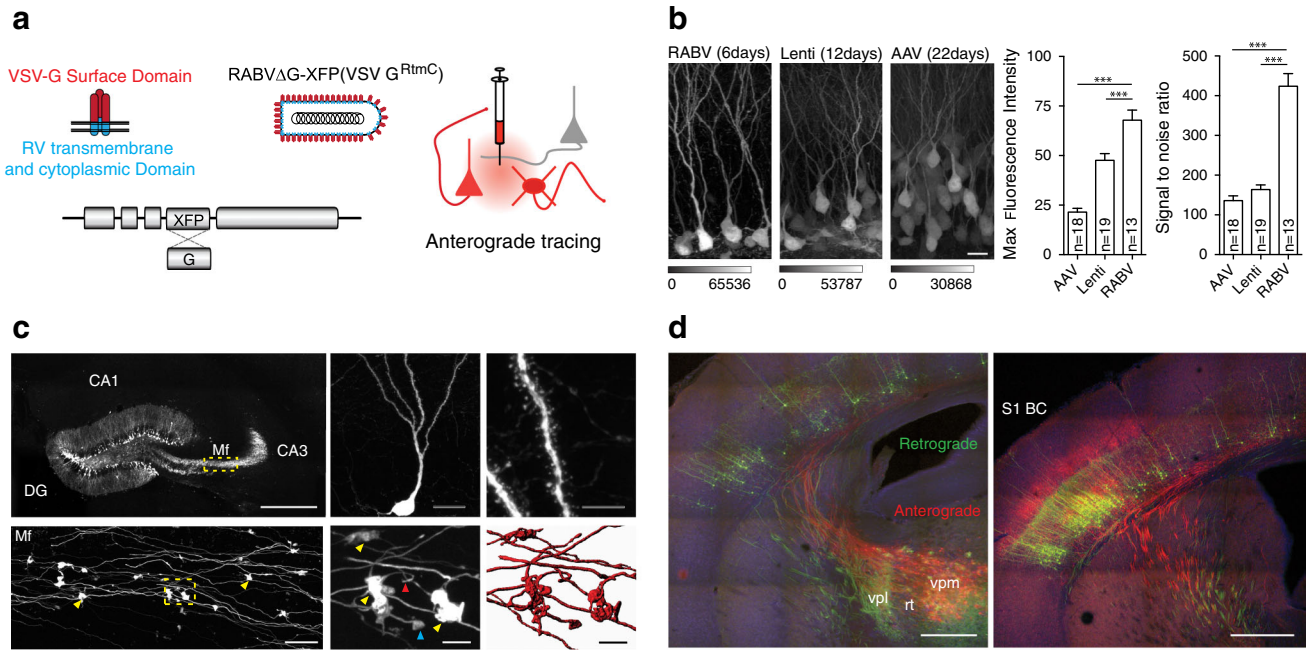

Fig. 1 Novel rabies virus variant for anterograde tracing of neuronal morphology. **a** RABV ΔG expressing a fluorescent protein (XFP: eGFP, mCherry or myr-TdTom) was pseudotyped with a chimeric surface protein containing the transmembrane and cytoplasmic domain of the native RABV glycoprotein (RtmC) and surface domain of the G protein of VSV Indiana virus. **b** Comparison of fluorescence intensity and signal-to-noise ratio of cells infected with RABV ΔG (VSV $G^{RtmC)}$ (RABV), VSV G-pseudotyped lentivirus (LV) and adeno-associated virus (AAV). Data are mean ± SEM $^{***}p < 0.001$ (one-way ANOVA test). **c** RABV ΔG(VSV G^{RtmC}) infection of the hippocampal dentate gyrus (DG) region resulted in intense labeling of granule cells revealing their fine morphological details including the dendritic tree (*upper middle*), spines (*upper right*), mossy fibers (Mf), and mossy fiber boutons (MfBs, *yellow arrowheads*). This permits semi-automated volume reconstruction (*lower middle* and *lower right panel*) of MfBs with their adjacent filopodia (e.g., *red arrowhead*) and satellites (e.g., *blue arrowhead*). *Scale bars* 500 µm, *upper left* 25 µm, *lower left* 15 µm, *upper middle* 5 µm, *upper right*, *lower middle* and *right*. **d** Reciprocal thalamo-cortical and cortico-thalamical projections in S1 BC and VPm following co-injection of retrograde (*green*) and anterograde (red) RABV ΔG. *Scale bars* 500 µm

related barrel cortex (BC) and visually inspected regions known to connect to this structure. While neurons were infected locally at the site of injection, no labeled cell bodies were found in any of the following regions: thalamic ventral posterior medial (VPm) division and posterior medial (POm) division, other areas of the primary somatosensory cortex (S1), secondary somatosensory cortex (S2), primary motor cortex (M1), and contralateral S1 (not shown). In fact, we saw no infected cell outside the local injection site in S1. This property of RABV ΔG (VSV-G^{RtmC}) permits its combined use with a retrogradely transducing RABV ΔG variant (Wickersham et al. 2007a) to unambiguously trace projections both to-, and from-, a given region. An example for this type of experiment is shown for the labeling of reciprocal projections between the VPm division of mouse thalamus and the primary somatosensory barrel cortex (S1-BC; Fig. 1d). Importantly, we found a complete absence of retrograde infection in all injections using RABV ΔG (VSV-G^{RtmC}).

In the aforementioned examples, we demonstrate the utility of this vector for the transduction of populations of neurons. However, as stated previously, reconstruction of the complete structure of a neuron, including its complex and wide-reaching axonal arbors, requires methods for sparse- or single-neuron labeling. This is often achieved by intracellular filling with biocytin (or its analogs), as most viral-based tracers are completely unsuited to this task. RABV, however, is somewhat unique due to its ability to amplify sufficiently from a single infectious particle (reviewed in Callaway 2008) to confer robust, high intensity labeling to all morphological aspects of an infected cell. Although this property is known from the wild-type CVS strain of RABV (Callaway 2008), it has not been demonstrated for glycoprotein-deleted pseudotyped variants of the SAD B19 strain. To examine the ability of our anterograde RABV ΔG vector to confer the sparse labeling necessary for single neuron reconstruction, we injected 5–10 viral particles into the thalamic POm division of a 16-week-old mouse. Within the investigated thalamic volume of ~400 µm × 400 µm × 400 µm, only seven cells were labeled (Fig. 2a), including three excitatory projecting neurons, one inhibitory interneuron and three astrocytes (Fig. 2a, b). However, all cells were intensely labeled throughout the extent of their processes.

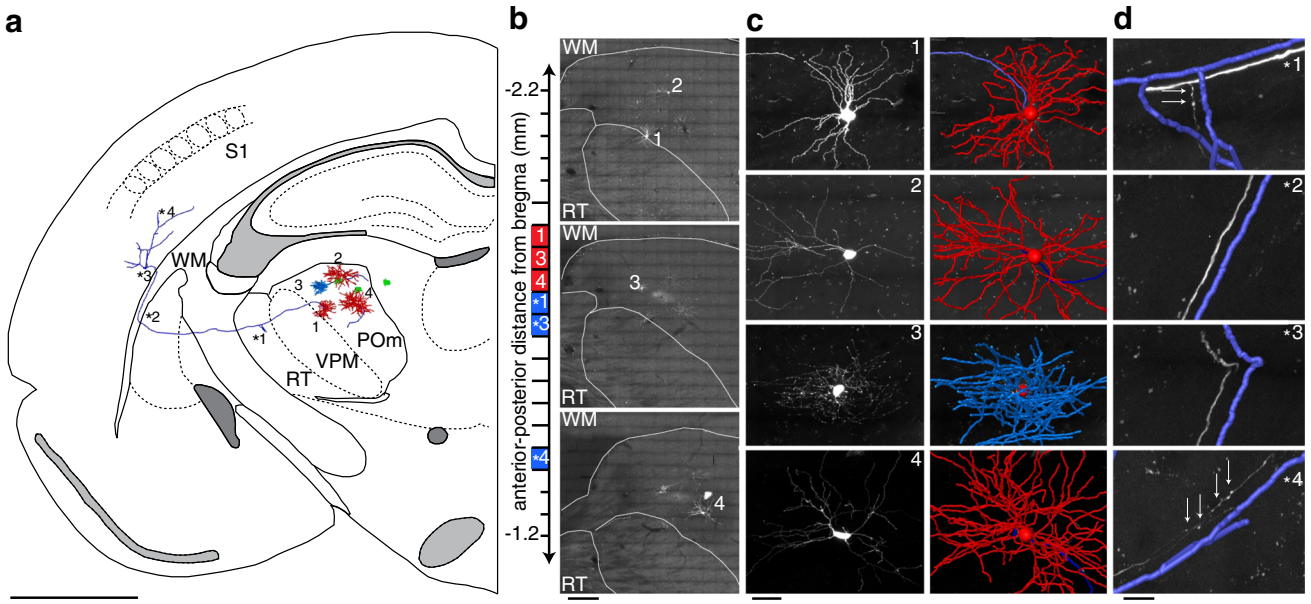

Fig. 2 3D reconstruction of thalamic neurons sparsely labeled with RABV ΔG (VSV-G^{RtmC}). **a** Three excitatory neurons, one inhibitory interneuron (soma/dendrites: *red*, axon: *blue*) and three astrocytes (*green*) were reconstructed within the imaged volume in thalamus and cortex. **b** Cells were reconstructed from 12 consecutive 50-µm-thick brain sections (*long dashes* of the anterior–posterior axis). Maximum projection images of three sections containing the neuronal somata are shown (*red* within the anterior–posterior axis). **c** *Left* zoom of panel **b**. *Right* Semi-automated reconstructions of the neuronal skeletons are superimposed. In case of the interneuron in *panel 3*, only the soma and axonal arbor are shown. Please note: Reconstructed branches that are not visible in the projection image, such as the gap in the axon in *panel 1*, were traced in adjacent brain sections. **d** One axon was traced into cortex. Maximum projections superimposed with semi-automated reconstructions are shown from exemplary parts of the axon (*blue* within the anterior–posterior axis, *panel* **b**). It branched first within RT (**1*), where individual boutons (at *arrow locations*, not reconstructed) indicated potential synapse locations; traversed through the WM (**2*, **3*), where the axon was perfectly visible; and entered the vibrissal cortex, where labeling quality did not decrease with distance from the soma (i.e., individual boutons were still clearly visible). *Scale bars* 1 mm (**a**) 50 µm (**b**, **c**) and 10 µm (**d**)

Using high-resolution, large-scale confocal microscopy and automated image processing routines (Oberlaender et al. 2007), we reconstructed the somata, dendrites and axons of the four RABV-infected neurons within 12 consecutive 50-µm-thick brain sections (Fig. 2). The high labeling quality in terms of fluorescent intensity, signal-to-noise ratio, and homogeneity across cells (Fig. 2c) including their entire axonal arbor (Fig. 2d) enabled the automated tracing of all morphological fine-structures within the imaged volume. To demonstrate this, we reconstructed the complete 3D morphology of all dendrites, the complete axon of the interneuron, and the initial parts of the axons from the three projecting neurons. Furthermore, we traced and reconstructed one long-range axon. In this case, the neuron projected to the nucleus reticularis (RT) and continued to traverse the white matter tract before entering the vibrissal cortex (S1). This type of axon trajectory has been reported previously for POm neurons (Deschenes et al. 1998). The axon showed no obvious decrease in labeling quality with distance from the soma, allowing identification of individual boutons within thalamus and cortex (Fig. 2d). These results clearly demonstrate the ability of our anterograde RABV ΔG tracer to amplify its genome sufficiently, following infection of a cell by a single particle, to enable tracing of long-ranging axons. As a result of this analysis, we found that the initial axonal segments of the traced neurons were less unidirectional than those described using other methods (Deschenes et al. 1998), possibly indicating that POm projects more diversely to regions other than S1.

To better characterize the efficacy/versatility of our vector, we performed injections into a variety of brain areas and over a range of ages. RABV ΔG (VSV G^{RtmC}) transduced cells in all mouse brain areas tested, i.e., somatosensory cortex, thalamus, hippocampal dentate gyrus, substantia nigra and cerebellum (Figs. 1c, d, 2b, 3, 4). RABV ΔG (VSV-G^{RtmC}) was capable of transducing excitatory and inhibitory neurons, as well as glial cells, as illustrated in Figs. 2, 4 and 6. For example, in the cerebellum, we found that the virus efficiently transduced inhibitory stellate cells, basket cells and Purkinje cells, as well as the excitatory granule cells. Notably, this vector mediated efficient and intense cell labeling in mice of all ages tested (1–15 months), permitting its use for the neuroanatomical study of neurodegenerative disorders (AD) or aging, as demonstrated in Fig. 5.

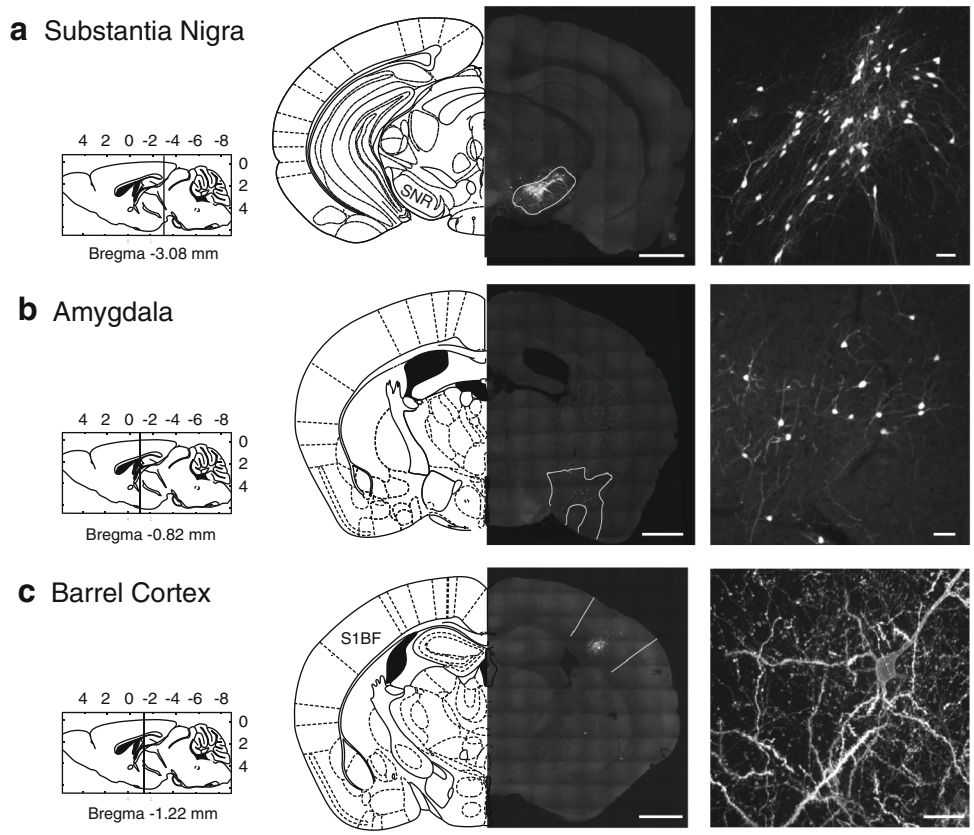

Fig. 3 Efficiency of transduction of targeted brain areas. RABV ΔG XFP (VSV-G^{RtmC}) transduced cells in all brain structures examined. Confocal microscope images of fluorescently labeled neurons following stereotaxic injection into **a** substantia nigra, **b** anterior amygdaloid, dorsal region, and **c** layers 5 and 6 of the somatosensory cortex. *Scale bars left panels* 1 mm, *right panels* 50 μm

To investigate its tropism in the neocortex in greater detail, we performed injections into layer 5 of S1-BC (Fig. 6), where the composition of cell types has been previously well characterized (i.e., ~70 % neurons vs. ~30 % glial cells (Tsai et al. 2009; Meyer et al. 2011)). We found that ~71 % of the labeled cells in layer 5 were neurons (and thus 29 % were glial cells). Interestingly, only 0.4 % of infected neurons were inhibitory interneurons in contrast to the ~80 % excitatory versus ~20 % inhibitory neurons previously reported for layer 5 of the barrel cortex (Meyer et al. 2011). This suggests a strong bias for the transduction of excitatory neurons, as previously reported for VSV-G pseudotyped lentiviral vectors (Nathanson et al. 2009). To further characterize the types of infected glial cells, we used markers for astrocytes [S100β, (Zuo et al. 2004)] and microglia [Iba1, (Schafer et al. 2012)]. We found that ~15 % of infected cells fell into the former category (Fig. 6g–i), while virtually no microglia were labeled (data not shown). We would like to point out, however, that glial cells form a non-homogeneous group of differing origins and several markers coexist in the various types (Cahoy et al. 2008). Our finding is therefore only the first step in characterizing the infection of various glial cell types by RABV ΔG (VSV G^{RtmC}). Nonetheless, our data provide evidence for the ability of pseudotyped RABV ΔG variants to infect glial cells and thus extends the range of cell types that may be amenable to manipulation with RABV ΔG.

Discussion

Here, we demonstrate the utility of RABV ΔG (VSV-G^{RtmC}) for neuroanatomical studies involving not only bulk populations of neurons, but also sparse or individual neurons. Our vector is exclusively anterograde, permits rapid high intensity labeling, without cytotoxic side effects and can be used over a sufficiently extended time window to permit physiological experiments. In addition, it can transduce a range of cell types/brain areas in both young and aged animals. These qualities are unequaled by any other type of viral tracer, and in addition render it useful for the study of aging or neurodegenerative disorders (Fig. 5) where age/toxicity might be a factor limiting labeling success.

We show that RABV ΔG (VSV-G^{RtmC}) is able to amplify sufficiently from single-particle infection of a host cell to confer the high intensity labeling necessary for automated detection of morphological features (without prior amplification of the signal) (Fig. 2). Most other viral vectors such as lentivirus and AAV do not provide sufficient labeling intensity for reconstruction upon sparse

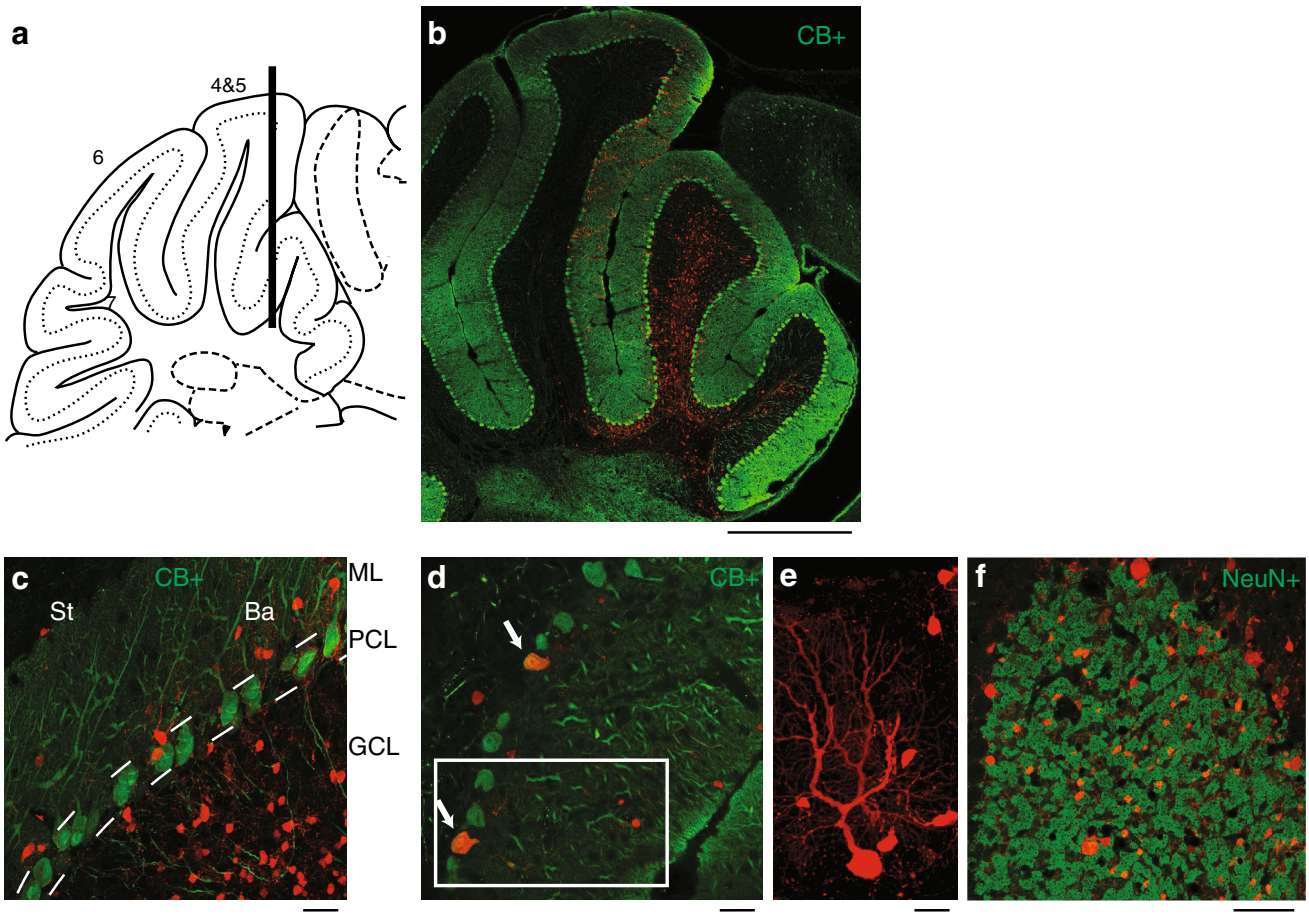

Fig. 4 Transduction in the cerebellum. A multiple-step injection at different depths was applied to investigate the transduction efficacy of RABV ΔG (VSV-G^{RtmC}) in the cerebellar cortex. **a** Injection scheme, black bar illustrates the virus injections into different depths along the needle track. **b** Injection overview of RABV ΔG (VSV-G^{RtmC}) infected cells (*red*) overlaid with calbindin- (CB+) positive cells (*green*). **b**, **c** Transduced cells were found in the molecular layer (ML), the Purkinje cell layer (PCL) and at high abundance in the granule cell layer (GCL). **c** In the molecular layer both of the inhibitory types, stellate cells (St) and basket cells (Ba) were efficiently transduced. Within the Purkinje cell layer (PCL), the calbindin (CB+) immunoreactivity (**d**) and the distinct branching pattern of the dendritic trees (**e**) confirmed the transduction of Purkinje cells. **f** Numerous labeled cells were found in the granule cell layer, where ~80 % of the transduced cells co-labeled for NeuN indicating that the abundant granule cells are transduced efficiently. *Scale bars* 500 µm (**b**) 25 µm (**c**, **d**, **f**) and 10 µm (**e**)

infection. Indeed, only Sindbis virus (Ghosh et al. 2011) has been reported to amplify sufficiently from a single particle to allow the visualization of long-ranging axonal structures from individual neurons in 3-week-old animals. However, extreme cytotoxicity and reduced efficacy in adult animals (Chen et al. 2000) hamper the practical use of Sindbis virus for the purpose of quantitative morphological tracing.

Our vector may be regarded as a viable alternative to classical single cell labeling approaches, such as those based on biocytin delivery via patch pipettes. The latter are limited by low success rates for recovering complete axonal morphologies [e.g., ~60 % (Oberlaender et al. 2012b)] and require histological post-processing to stain the biocytin-labeled structures. Moreover, reduced penetrability of axon bundles such as the white matter limits the success of tracing long-range axons using biocytin-labeling (where post-processing with immunological agents is required). RABV ΔG (VSV-G^{RtmC}), on the other hand, is not affected by any of these issues (Fig. 2). In addition to the aforementioned qualities, the large size of RABV ΔG (VSV-G^{RtmC}) particles limits diffusion, allowing very targeted infection of a spatially restricted brain volume. We propose that co-injection of RABV ΔG (VSV-G^{RtmC}) variants expressing different fluorescent markers, together with large-scale reconstruction of single-cell morphology, could aid the classification of neuron types within a specific brain region or nucleus.

Recently, a glycoprotein-deleted form of another closely related rhabdovirus, the vesicular-stomatitis-virus (rVSV), has also been used as a single-cycle (i.e., non-trans-synaptic) anterograde tracer (van den Pol et al. 2009). Despite strong morphological labeling following fluorescent marker

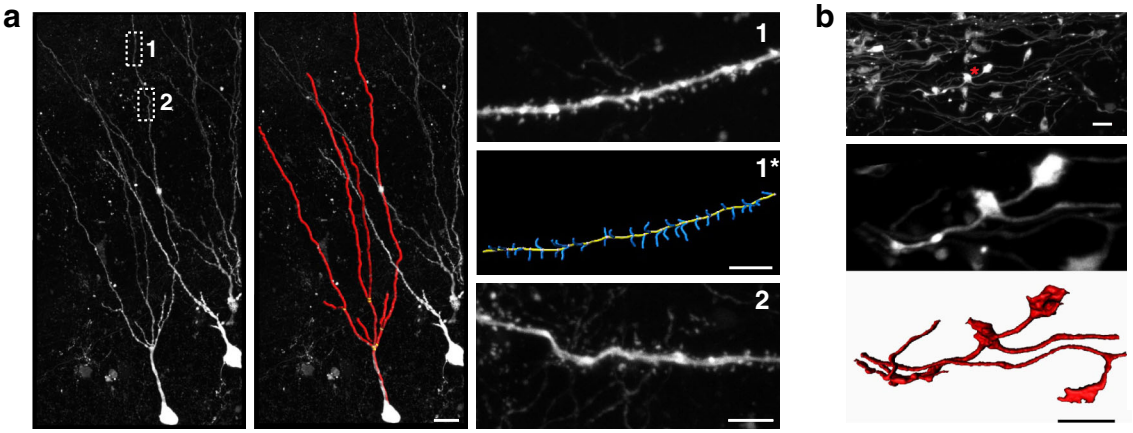

Fig. 5 Labeling and surface reconstruction in aged animals. RABV ΔG-mCherry(VSV-G^{RtmC}) infection of hippocampal dentate gyrus neurons in a 15-month-old APP/PS1 mouse—a mouse model for Alzheimer's disease—enables the fine-detailed reconstruction of dendrites and spines (**a**), as well as of axonal boutons (**b**). **a** Strong labeling facilitated automated reconstruction of the dendritic tree (*left* and *middle panel*; scale: 15 µm) and of dendritic spines (*right panels 1* and *1**; scale 5 µm) of a dentate gyrus cell using Imaris (Bitplane, Zurich, Switzerland). This labeling also revealed anatomical abnormalities like tortuous dendrites, which have previously been described as an effect of aging in humans [*right panel 2* (Tsamis et al. 2010]. **b** Similar to the dendrites/spines, the axons of granule cells (mossy fibers) and their boutons in the CA3 area of the hippocampus were strongly labeled (*upper* and *middle panel*). Automated surface reconstruction (Imaris) of an isolated mossy fiber bouton showing its fine morphological details (*lower panel*). *Scale bars* 5 µm

expression, the use of this virus is limited due to severe, fast-onset cytotoxic effects that cause shut-down of the host cell transcription and nuclear export (Faul et al. 2009). This cytotoxicity strongly restricts the time window for many anatomical/physiological studies to ~1 day post infection, even for attenuated variants of rVSV ΔG (Beier et al. 2011).

The presumed amphotropic qualities of the chimeric VSV-G envelope protein likely enable transduction of a wider range of species and cell types than those presented here. Of note, a similar VSV-G pseudotyped RABV ΔG vector has recently been described (Gomme et al. 2010). This vector was also shown to be anterograde (Wickersham et al. 2013), although it may have a slightly different tropism due to differences in the transmembrane domain of the glycoprotein-packaging construct. Our findings, together with the latter study, suggest novel applications for RABV ΔG in addition to its use as a retrograde (Wickersham et al. 2007a) or mono-trans-synaptic tracer (Wickersham et al. 2007b). For example, RABV ΔG (VSV-G^{RtmC}) may be used to define a spatially confined starter cell population for mono-trans-synaptic tracing. It may also be employed as a tool to manipulate/monitor neural circuit activity following the expression of, for example, calcium/voltage indicators or photo-activatable channels (Osakada et al. 2011). In addition, it can be readily combined with retrogradely transducing RABV variants. Unlike other previously reported combinations of anterograde and retrograde agents, the present approach enables the exploitation of two vectors with the same diffusion characteristics, high quality of labeling and short time course for expression as shown in Fig. 1d. Lastly, this tool together with other technologies, e.g., permitting dendritic or synaptic protein profiling (Ginger et al. 2013a; Micheva et al. 2010) or gross-scale reconstruction approaches (as described here), could greatly aid the classification of cell-type identity. In conclusion, the combination of different RABV variants with optical, physiological and computational approaches, offers a wide range of possibilities for the investigation of the structure–function relationship of neuronal circuits.

Methods

Engineering of the hybrid glycoprotein

The chimeric VSV/SAD G (VSV G^{RtmC}) cDNA was constructed to encode the ectodomain (aa 1–454) of VSV Indiana G (kindly provided by Dr. John K. Rose) fused to the entire transmembrane and cytoplasmic domain (amino acids 450–524) (Mebatsion et al. 1995) of RABV SAD G. This construct differs from the packaging construct employed by Wickersham et al. (2013), which contained the surface- and trans-membrane domain of the VSV glycoprotein and cytoplasmic domain of the RABV glycoprotein.

Virus production

The production of G-gene deficient RABV SAD ΔG-eGFP and SAD ΔG-mCherry was described previously (Wickersham et al. 2007a). SAD ΔG myr-TdTom was constructed in the same way to encode a protein in which two

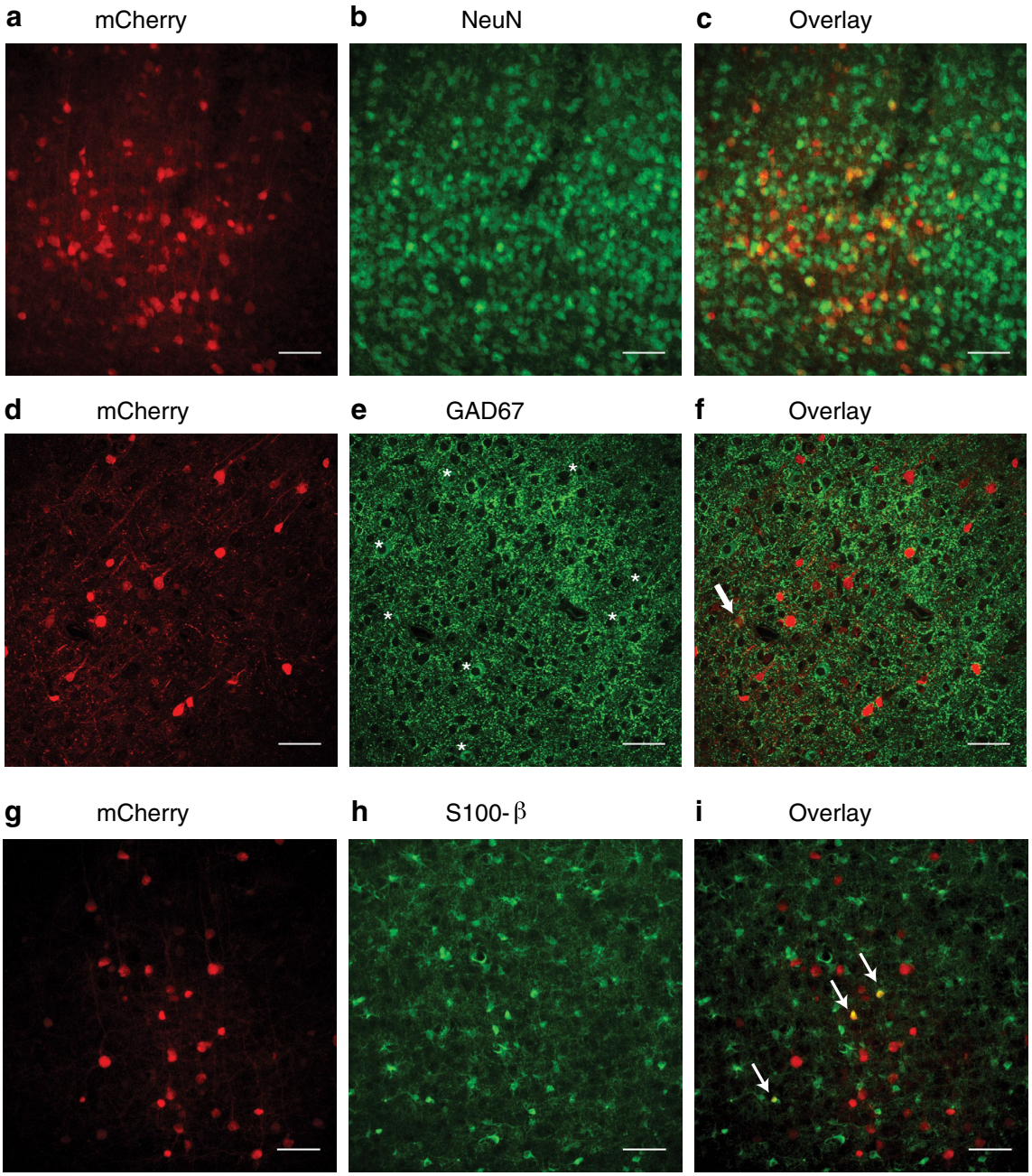

Fig. 6 Tropism of RABV ΔG (VSV-G^{RtmC}) in CNS. Determination of cell-type identity of RABV ΔG (VSV-G^{RtmC}) infected mCherry expressing cells in layer 5 of the barrel cortex (representative images in **a**, **d** and **g**) in 50-µm-thick sections using immunohistochemistry against NeuN (total neuron marker; **b**), GAD67 (marker of inhibitory interneurons; **e**) and S-100β (marker of astrocytes, **h**). Overlay of mCherry and cell-specific marker (**c**, **f** and **i**). Images are either max projections (**a**–**c**, **g**–**i**) derived from selected planes of a multi-plane image stack or a single plane (**d**–**f**) obtained from laser scanning confocal microscopy. *Stars* in panel **e** indicate GAD67 positive cells. A single mCherry-/GAD67 positive neuron is indicated by an *arrow* in (**f**). *Arrows* in panel **i** indicate mCherry-/S-100β positive cells. *Scale bars* 50 µm

tandem copies of a myristoylation signal are fused to tdTomato for membrane targeting (Trichas et al. 2008).

Stocks of VSV G^{RtmC}-pseudotyped rabies viruses [hereafter referred to as RABV ΔG XFP (VSV G^{RtmC})] were prepared essentially as described in (Rancz et al. 2011), with the exception that BSR T7/5 cells (Buchholz et al. 1999) were used instead of BHK-21 cells and pCAGGS VSV/SAD G was used as the transcomplementing plasmid. Cells were replated 24 h after infection with the initial starter stock and the supernatant media discarded and replaced with new media. VSV G^{RtmC}-pseudotyped virus was harvested 3 days post

infection. Titers of the different variants of pseudotyped rabies virus were in the range of 2×10^6–5×10^7 infectious particles/ml, estimated by serial dilution and infection of the BHK-21 cell line.

Stereotaxic injections

All experimental procedures were performed in accordance with French law and the European Directive covering the use of experimental animals (2010/63/EU) and approved by the Ethics Committee of Bordeaux (approval # 5012024-A). Stereotaxic injections were performed as previously described (Cetin et al. 2006) in C57Bl/6 J mice (aged 1–15 months) or in 15-month-old APP/PS1 mice [a mouse model for Alzheimer's disease (Reiserer et al. 2007)]. In brief, viral vectors were injected into the brains of isoflurane anesthetized and head-fixed mice using a 10-µl glass syringe fitted with a 35-gauge needle or a pulled glass pipette. Volume and speed of the injections were controlled using a WPI Ultra Micro Pump. The stereotaxic coordinates were as follows: (1) Thalamic ventral posteromedial (VPm) nucleus: anterior/posterior (A/P) −1.70 mm, lateral (L) 1.60 mm, dorso/ventral (D/V) 3.20 mm; (2) thalamic posteromedial (POm) nucleus: A/P −1.80 mm, L 1.25 mm, D/V 2.75 mm; (3) hippocampal dentate gyrus (DG): A/P −1.90 mm, L 1.20 mm, D/V 1.90 mm; (4) layer 5 (L5) of primary somatosensory barrel cortex (BC): A/P −0.94 mm, L 3.00 mm, D/V 0.80 mm; (5) cerebellum: A/P −5.68 mm, L 0.68 mm, D/V 1.70–0 mm (6) amygdala: A/P −0.82 mm, L 2.45 mm, D/V 4.75 mm; (7) substantia nigra: A/P −3.00 mm, L 1.56 mm, D/V 4.1 mm. A/P and L coordinates are given with respect to the bregma, D/V coordinates with respect to the brain surface. Injection volumes were 200–600 nl for RABV ΔG XFP (VSV G^{RtmC}), 400 nl for AAV (diluted 1/50) and 600 nl for lentivirus. Sparse labeling was achieved by diluting anterograde rabies virus to titers of $\sim 2 \times 10^4$ infectious particles/ml and injection of 250 nl, which resulted in injection of 5–10 infectious particles.

Mouse perfusion and brain sectioning

Mice were deeply anesthetized with a lethal dose of sodium pentobarbital and then transcardially perfused with 30 ml normal Ringer's solution (135 mM NaCl, 5.4 mM KCl, 1 mM $CaCl_2$, 1.8 mM $MgCl_2$, 5 mM HEPES, pH 7.4) followed by 100 ml of a 4 % PFA solution (prepared in 1× phosphate buffered saline (PBS, pH 7.4). Fixed brains were dissected and postfixed in 4 % PFA solution for either 24 h, or 6 h in the case where immunohistology was performed. Free-floating slices (50 µm) were cut using a vibratome (Leica).

Immunohistological determination of the cellular tropism of RABVΔG(VSV-G^{RtmC})

Cell types were identified using antibodies against NeuN (dilution: 1:500; Millipore, clone A60, MAB377) to mark neurons, the 67 kDa isoform of glutamate decarboxylase GAD67 (1:1,500 dilution; Millipore, clone 1G10.2, MAB5406) to label GABAergic neurons (Meyer et al. 2011), S100β (1:1,500; Sigma S2532) to mark astrocytes (Zuo et al. 2004), or against Iba1 (1:500; Wako Cat. #019-19741) to mark microglia (Schafer et al. 2012). NeuN and S100β were detected using Alexa488-conjugated goat anti-mouse H + L (Life technologies), and GAD67 was detected using Alexa647-conjugated goat anti-mouse (subtype IgG2A) (Life technologies).

Immunohistochemical protocols were adapted from Meyer et al. (2011). In brief, free-floating slices were blocked with MOM blocking reagent (Vector Labs) (1 h) in the presence of 0.5 % triton X-100, then for 30 min in 3 % BSA, 4 % NGS, 0.5 % triton in 1× PBS. Slices were incubated 40 h with the primary antibody in 3 % BSA, 2 % NGS in 1× PBS at 4 °C, washed two times with 0.1 M PB then two times with 0.1 M PB + 1 % NGS. Slices were then incubated 2 h at RT with the secondary antibody (1:500) in the presence of 0.3 % triton X-100, washed five times with 0.1 M PB, counter-stained with TO-PRO-3 to label nuclei (1:5,000; Life Technologies), and mounted in prolong gold mounting media. The number of RABV ΔG (VSV G^{RtmC}) transduced cells expressing cell-type specific markers was quantified by manually counting the immunohistochemically stained cells in confocal images stacks.

High-resolution microscopy, tracing and quantification

For reconstruction of thalamic neurons, images were acquired using a prototype confocal laser scanning system (based on LAS AF SP5, Leica Microsystems), equipped with a glycerol immersion objective (HCX PL APO 63x, 1.2 N.A.), a tandem scanning system (Resonance Scanner), spectral detectors with hybrid technology (GaAsP photocathode), and mosaic scanning software [Matrix Screener (beta-version), provided by Frank Sieckmann, Leica Microsystems]. Mosaic image stacks of volumes up to 2 mm × 2 mm × 0.05 mm (in thalamus) and 0.6 × 0.6 × 0.05 mm (in cortex) were acquired at a resolution of 0.094 µm × 0.094 µm × 0.5 µm per voxel (2.5× digital zoom, 8× line average, 8 kHz scanning speed, ∼20 × 20 and ∼6 × 6 fields of view in thalamus and cortex, respectively) for each of 12 consecutive 50-µm-thick brain sections. 3D reconstructions were performed using previously described automated tracing algorithms (Oberlaender et al. 2007). Automated tracings were proof-edited (Dercksen et al. 2012) and semi-automatically aligned

across brain sections (Dercksen et al. 2009) using Amira Visualization Software (Visage Imaging).

All remaining images were acquired using either a commercial confocal microscope (Leica SP5) or a commercial spinning disk system (Leica SP2). Hippocampal mossy fiber boutons were reconstructed from image stacks using the Imaris surface tool (Bitplane, Zurich, Switzerland). To compare the fluorescence intensities and signal-to-noise ratios of RABV ΔG (VSV G^{RtmC}), lentivirus- (LV), and adeno-associated virus (AAV) infected brain sections were imaged with identical microscopy settings. Image stacks were acquired at 16 bit-depth at a resolution of 141.47 nm × 141.47 nm × 125.89 nm per voxel (63× magnification, 1.7× digital zoom, 1024 × 1024 pixel per image, 3× line average, 700 Hz scanning speed). Cellular somata were detected automatically in these 3D image stacks using Imaris, and the maximum fluorescence intensity of the somata was quantified as arbitrary unit (0–65536 levels of grey) from 16 bit images. Background levels were calculated for each image stack as the average mean intensity value of several larger distributed areas devoid of any cellular processes (i.e., signal). For illustration purposes, the intensity levels of all three images in Fig. 1b were enhanced to the same extent. Cell counts for immunological cell-type characterizations were performed manually with the use of Amira Visualization Software (Visage Imaging) on confocal image stacks.

Fluorescence intensity comparison

Fluorescence intensities were compared using brains of mice injected at 4 months of age with either lentivirus (MND-eGFP-WPRE, a kind gift of Dr. N. Abrous), AAV 2/9 CAG eGFP-WPRE (Penn Vector Core), or RABV ΔG-eGFP(VSV G^{RtmC}). Injected animals were killed at 6 days post infection (RABV ΔG), 12 days post infection (lentivirus), or 22 days post infection (AAV). eGFP-labeled cells were imaged and analyzed as described above.

Statistics

Significance was evaluated using one-way ANOVA followed by a post hoc Tukey test for multiple comparisons using GraphPad Prism 6 software (San Diego, CA). *** $p < 0.001$. Data are represented as mean ± SEM.

Acknowledgments We thank Drs. Nuno Da Costa and Kevan Martin for fruitful discussion, Drs. Kamill Balint and Botond Roska for their kind and helpful advice on handling RABV, Drs. Aude Panatier and Axel Nimmerjahn for their advice about glial cells, Dr. Panatier for providing the S100ß antibody and Dr. Nora Abrous for providing the lentivirus. Imaging data was acquired using equipment of the Bordeaux Imaging Center (BIC) and the Max Planck Florida Institute. The AAV2/9 eGFP vector was obtained from the Penn Vector Core using materials made available by Dr. Hongkui Zeng, Ph.D. of the Allen Institute for Brain Science. This project has been funded with support from the European Commission (European Erasmus Mundus programme; M.G.H.). This publication reflects the views only of the authors, and the Commission cannot be held responsible for any use, which may be made of the information contained therein. This study was also supported by INSERM (A.F.), the PDBEB Programm CNC Coimbra (S.V.S.), LabEx BRAIN (M.G.H., A.F., M.G., C.M.), Conseil de la Region d'Aquitaine (A.F., M.G.), ANR (10-MALZ-0009; C.M.), DFG (SFB 870; K.K.C. and A.G.), the Bernstein Center for Computational Neuroscience in Tuebingen (funded by the German Federal Ministry of Education and Research (BMBF; FKZ: 01GQ1002)) (M.O.), Max Planck Institute for Biological Cybernetics, Tuebingen (M.O.), Max Planck Florida Institute for Neuroscience, Jupiter (J.M.G, M.O.), and the Werner Reichardt Center for Integrative Neuroscience, Tuebingen (M.O.).

References

Beier KT, Saunders A, Oldenburg IA, Miyamichi K, Akhtar N, Luo L, Whelan SP, Sabatini B, Cepko CL (2011) Anterograde or retrograde transsynaptic labeling of CNS neurons with vesicular stomatitis virus vectors. Proc Natl Acad Sci USA 108(37): 15414–15419

Buchholz UJ, Finke S, Conzelmann KK (1999) Generation of bovine respiratory syncytial virus (BRSV) from cDNA: BRSV NS2 is not essential for virus replication in tissue culture, and the human RSV leader region acts as a functional BRSV genome promoter. J Virol 73(1):251–259

Burns JC, Friedmann T, Driever W, Burrascano M, Yee JK (1993) Vesicular stomatitis virus G glycoprotein pseudotyped retroviral vectors: concentration to very high titer and efficient gene transfer into mammalian and nonmammalian cells. Proc Natl Acad Sci USA 90(17):8033–8037

Cahoy JD, Emery B, Kaushal A, Foo LC, Zamanian JL, Christopherson KS, Xing Y, Lubischer JL, Krieg PA, Krupenko SA, Thompson WJ, Barres BA (2008) A transcriptome database for astrocytes, neurons, and oligodendrocytes: a new resource for understanding brain development and function. J Neurosci 28(1):264–278

Callaway EM (2008) Transneuronal circuit tracing with neurotropic viruses. Curr Opin Neurobiol 18(6):617–623

Cetin A, Komai S, Eliava M, Seeburg PH, Osten P (2006) Stereotaxic gene delivery in the rodent brain. Nat Protoc 1(6):3166–3173

Chen BE, Lendvai B, Nimchinsky EA, Burbach B, Fox K, Svoboda K (2000) Imaging high-resolution structure of GFP-expressing neurons in neocortex in vivo. Learn Mem 7(6):433–441

Choi J, Young JA, Callaway EM (2010) Selective viral vector transduction of ErbB4 expressing cortical interneurons in vivo with a viral receptor-ligand bridge protein. Proc Natl Acad Sci USA 107(38):16703–16708

da Costa NM, Martin KA (2013) Sparse reconstruction of brain circuits: or, how to survive without a microscopic connectome. Neuroimage 80:27–36

Dercksen VJ, Weber B, Guenther D, Oberlaender M, Prohaska S, Hege HC (2009) Automatic Alignment of Stacks of Filament Data. IEEE Int Symp on Biomedical Imaging: From Nano to Macro (ISBI) 971-974

Dercksen VJ, Oberlaender M, Sakmann B, Hege HC (2012) Interactive visualization: a key prerequisite for reconstruction

of anatomically realistic neural networks. Proceedings of the 2009 Workshop on Visualization in medicine and life sciences (VMLS 09)

Deschenes M, Veinante P, Zhang ZW (1998) The organization of corticothalamic projections: reciprocity versus parity. Brain Res Brain Res Rev 28(3):286–308

Douglas RJ, Martin KA (2004) Neuronal circuits of the neocortex. Annu Rev Neurosci 27:419–451

Faul EJ, Lyles DS, Schnell MJ (2009) Interferon response and viral evasion by members of the family rhabdoviridae. Viruses 1(3):832–851

Finkelshtein D, Werman A, Novick D, Barak S, Rubinstein M (2013) LDL receptor and its family members serve as the cellular receptors for vesicular stomatitis virus. Proc Natl Acad Sci USA 110(18):7306–7311

Ghosh S, Larson SD, Hefzi H, Marnoy Z, Cutforth T, Dokka K, Baldwin KK (2011) Sensory maps in the olfactory cortex defined by long-range viral tracing of single neurons. Nature 472(7342): 217–220

Ginger M, Broser P, Frick A (2013a) Three-dimensional tracking and analysis of ion channel signals across dendritic arbors. Front Neural Circuits 7:61

Ginger M, Haberl M, Conzelmann KK, Schwarz MK, Frick A (2013b) Revealing the secrets of neuronal circuits with recombinant rabies virus technology. Front Neural Circuits 7:2

Gomme EA, Faul EJ, Flomenberg P, McGettigan JP, Schnell MJ (2010) Characterization of a single-cycle rabies virus-based vaccine vector. J Virol 84(6):2820–2831

Helmstaedter M (2013) Cellular-resolution connectomics: challenges of dense neural circuit reconstruction. Nat Methods 10(6): 501–507

Larsen DD, Wickersham IR, Callaway EM (2007) Retrograde tracing with recombinant rabies virus reveals correlations between projection targets and dendritic architecture in layer 5 of mouse barrel cortex. Front Neural Circuits 1:5

Lichtman JW, Denk W (2011) The big and the small: challenges of imaging the brain's circuits. Science 334(6056):618–623

Mebatsion T, Schnell MJ, Conzelmann KK (1995) Mokola virus glycoprotein and chimeric proteins can replace rabies virus glycoprotein in the rescue of infectious defective rabies virus particles. J Virol 69(3):1444–1451

Mebatsion T, Finke S, Weiland F, Conzelmann KK (1997) A CXCR4/CD4 pseudotype rhabdovirus that selectively infects HIV-1 envelope protein-expressing cells. Cell 90(5):841–847

Meyer HS, Schwarz D, Wimmer VC, Schmitt AC, Kerr JN, Sakmann B, Helmstaedter M (2011) Inhibitory interneurons in a cortical column form hot zones of inhibition in layers 2 and 5A. Proc Natl Acad Sci USA 108(40):16807–16812

Micheva KD, Busse B, Weiler NC, O'Rourke N, Smith SJ (2010) Single-synapse analysis of a diverse synapse population: proteomic imaging methods and markers. Neuron 68(4):639–653

Nathanson JL, Yanagawa Y, Obata K, Callaway EM (2009) Preferential labeling of inhibitory and excitatory cortical neurons by endogenous tropism of adeno-associated virus and lentivirus vectors. Neuroscience 161(2):441–450

Nhan HL, Callaway EM (2012) Morphology of superior colliculus- and middle temporal area-projecting neurons in primate primary visual cortex. J Comp Neurol 520(1):52–80

Oberlaender M, Bruno RM, Sakmann B, Broser PJ (2007) Transmitted light brightfield mosaic microscopy for three-dimensional tracing of single neuron morphology. J Biomed Opt 12(6): 064029

Oberlaender M, Boudewijns ZS, Kleele T, Mansvelder HD, Sakmann B, de Kock CP (2011) Three-dimensional axon morphologies of individual layer 5 neurons indicate cell type-specific intracortical pathways for whisker motion and touch. Proc Natl Acad Sci USA 108(10):4188–4193

Oberlaender M, de Kock CP, Bruno RM, Ramirez A, Meyer HS, Dercksen VJ, Helmstaedter M, Sakmann B (2012a) Cell type-specific three-dimensional structure of thalamocortical circuits in a column of rat vibrissal cortex. Cereb Cortex 22(10):2375–2391

Oberlaender M, Ramirez A, Bruno RM (2012b) Sensory experience restructures thalamocortical axons during adulthood. Neuron 74(4):648–655

Ohara S, Inoue K, Witter MP, Iijima T (2009) Untangling neural networks with dual retrograde transsynaptic viral infection. Front Neurosci 3(3):344–349

Osakada F, Mori T, Cetin AH, Marshel JH, Virgen B, Callaway EM (2011) New rabies virus variants for monitoring and manipulating activity and gene expression in defined neural circuits. Neuron 71(4):617–631

Parekh R, Ascoli GA (2013) Neuronal morphology goes digital: a research hub for cellular and system neuroscience. Neuron 77(6):1017–1038

Rancz EA, Franks KM, Schwarz MK, Pichler B, Schaefer AT, Margrie TW (2011) Transfection via whole-cell recording in vivo: bridging single-cell physiology, genetics and connectomics. Nat Neurosci 14(4):527–532

Reiserer RS, Harrison FE, Syverud DC, McDonald MP (2007) Impaired spatial learning in the APPSwe + PSEN1DeltaE9 bigenic mouse model of Alzheimer's disease. Genes Brain Behav 6(1):54–65

Schafer DP, Lehrman EK, Kautzman AG, Koyama R, Mardinly AR, Yamasaki R, Ransohoff RM, Greenberg ME, Barres BA, Stevens B (2012) Microglia sculpt postnatal neural circuits in an activity and complement-dependent manner. Neuron 74(4):691–705

Svoboda K (2011) The past, present, and future of single neuron reconstruction. Neuroinformatics 9(2–3):97–98

Trichas G, Begbie J, Srinivas S (2008) Use of the viral 2A peptide for bicistronic expression in transgenic mice. BMC Biol 6:40

Tsai PS, Kaufhold JP, Blinder P, Friedman B, Drew PJ, Karten HJ, Lyden PD, Kleinfeld D (2009) Correlations of neuronal and microvascular densities in murine cortex revealed by direct counting and colocalization of nuclei and vessels. J Neurosci 29(46):14553–14570

Tsamis IK, Mytilinaios GD, Njau NS, Fotiou FD, Glaftsi S, Costa V, Baloyannis JS (2010) Properties of CA3 dendritic excrescences in Alzheimer's disease. Curr Alzheimer Res 7(1):84–90

van den Pol AN, Ozduman K, Wollmann G, Ho WS, Simon I, Yao Y, Rose JK, Ghosh P (2009) Viral strategies for studying the brain, including a replication-restricted self-amplifying delta-G vesicular stomatis virus that rapidly expresses transgenes in brain and can generate a multicolor golgi-like expression. J Comp Neurol 516(6):456–481

Wickersham IR, Finke S, Conzelmann KK, Callaway EM (2007a) Retrograde neuronal tracing with a deletion-mutant rabies virus. Nat Methods 4(1):47–49

Wickersham IR, Lyon DC, Barnard RJ, Mori T, Finke S, Conzelmann KK, Young JA, Callaway EM (2007b) Monosynaptic restriction of transsynaptic tracing from single, genetically targeted neurons. Neuron 53(5):639–647

Wickersham IR, Sullivan HA, Seung HS (2013) Axonal and subcellular labelling using modified rabies viral vectors. Nat Commun 4:2332

Zuo Y, Lubischer JL, Kang H, Tian L, Mikesh M, Marks A, Scofield VL, Maika S, Newman C, Krieg P, Thompson WJ (2004) Fluorescent proteins expressed in mouse transgenic lines mark subsets of glia, neurons, macrophages, and dendritic cells for vital examination. J Neurosci 24(49):10999–11009

2.2. Connectivity Features in the *Fmr1*KO mouse

The following manuscript describes experiments that were performed to probe defects in the structural and functional connectivity in a mouse model of Fragile X Syndrome. This project was partially performed as EuroBioImaging project in the BioImaging Core for Magnetic Resonance Imaging in the group of Prof. Heerschap (UMC Radboud, Nijmegen). The experimental work was performed by:

Matthias Haberl: experimental design; antero- and retrograde virus production; viral tracer injections; analysis of tracer injections; preparation of all figures

Valerio Zerbi: design of MRI protocols; analysis of resting state functional MRI (rs-fMRI) and of diffusion tensor MRI (DT-MRI)

Andor Veltien: image acquisition of rs-fMRI and DT-MRI

Melanie Ginger: retrograde virus production

Manuscript N. 3

Manuscript in preparation for submission

Structural and functional connectivity deficits of the neuronal circuits in *Fmr1* knockout mouse model

Haberl M.[1,2,3], Zerbi V.[4], Veltien A.[4], Ginger M.[1,2],

Heerschap A.[4], Martin K.[3] and Frick A.[1,2]

2.2. Connectivity Features in the *Fmr1*KO mouse

The following manuscript describes experiments that were performed to probe defects in the structural and functional connectivity in a mouse model of Fragile X Syndrome. This project was partially performed as EuroBioImaging project in the BioImaging Core for Magnetic Resonance Imaging in the group of Prof. Heerschap (UMC Radboud, Nijmegen). The experimental work was performed by:

Matthias Haberl: experimental design; antero- and retrograde virus production; viral tracer injections; analysis of tracer injections; preparation of all figures

Valerio Zerbi: design of MRI protocols; analysis of resting state functional MRI (rs-fMRI) and of diffusion tensor MRI (DT-MRI)

Andor Veltien: image acquisition of rs-fMRI and DT-MRI

Melanie Ginger: retrograde virus production

Manuscript N. 3

Manuscript in preparation for submission

Structural and functional connectivity deficits of the neuronal circuits in *Fmr1* knockout mouse model

Haberl M.[1,2,3], Zerbi V.[4], Veltien A.[4], Ginger M.[1,2],

Heerschap A.[4], Martin K.[3] and Frick A.[1,2]

Abstract

Structural and functional wiring of the brain provides the fundamental basis that determines its capabilities and limitations. Fragile X syndrome, a frequent form of inherited mental retardation and cause of autism in humans, leads to learning and memory deficits, a high prevalence of autistic behavior, seizures, hypersensitivity to sensory stimuli and alterations in the processing of sensory information. Here, we probed alterations in the functional and structural connectivity, both locally and in the long-range, of neocortical circuits in the *Fmr1* KO mouse model. To measure these various connectivity aspects, we combined ultra-high-field *in vivo* diffusion tensor MRI, resting-state functional MRI and viral tracing. Our results show a hyper-connectivity phenotype for local neocortical circuits, but a hypo-connectivity for long-ranging ones. This anatomical data is matched by a functional decoupling of various neocortical regions from one another. We therefore identify Fragile X disease as a "connectopathy", which could explain altered sensory information processing in this disorder, and the complications of rescue strategies acting on molecular targets.

Introduction

Fragile X syndrome (FXS) is the most prevalent inherited mental retardation and most common single gene cause of autism spectrum disorder (ASD) in humans, occurring with a prevalence of 1/4000 in male and 1/8000 in female children[1]. Symptoms include learning and memory deficits, a high prevalence of autistic behavior, seizures, hypersensitivity to sensory stimuli and alterations/perturbations in the processing of sensory information[2]. The *Fmr1* knock-out (KO) mouse model[3] exhibits several neuropathologic features that are similar to those in human FXS patients, which suffer a loss of function of the *FMR1* gene[4]. While many studies focus on the misregulation of individual neuronal receptors or compartments our knowledge about the network organization is sparse. Today we only have some indications about small-scale network changes and we do not know how they are involved in the disease, or how they contribute to the cognitive and perceptional changes in FXS. At the cellular level, an altered anatomical connectivity has been proposed to play a role in both FXS and ASD[5]. Both dendritic spine morphology and axon outgrowth[6] are thought to be altered in *Fmr1* KO mice. Therefore altered brain circuits are believed to play an important role in FXS. Several reports indicated changes in the neocortical

short-range connectivity in *Fmr1* KO mice but often those appeared during a narrow time window and disappeared in adolescence[7-10]. This poses the question of whether wiring changes actually play a role in the adulthood in FXS? Here, a profound knowledge of deficits in the neuronal circuit wiring would be necessary to bridge the gap between alterations found on the molecular/micro-circuit level and behavioral/intellectual deficits.

Correct structural wiring is critical for maintaining normal brain function, like the processing of sensory information. Long-range connections between different brain areas are crucial for the faithful sequential transfer of sensory information in a feedforward and feedback manner. Short-ranging connections need to be intact to integrate and process the information step-wise in each area. We hypothesized that both, the connectivity within and in between brain areas might be altered in FXS given the deficits, which have been described previously in axonal outgrowth and spine morphologies. Yet, long-range wiring deficits underlying FXS have been largely unexplored as a potential mechanism underlying cognitive deficits. Therefore we set out to quantify brain-wide and local structural connectivity features in the *Fmr1* KO mouse model and correlate them to the functional connectivity.

Here we used diffusion tensor imaging (DTI) to measure structural integrity of the white matter in the *Fmr1* KO mice and found a reduced organization or number of axons within the fiber bundles of the corpus callosum below several cortical areas. Retrograde labeling from one adjacent and therefore presumably affected region, the primary visual cortex, revealed that in fact the number of long-ranging inputs to this area is reduced. Overall we find a shift towards more local and less long ranging input. Using resting state functional MRI (rs-fMRI) we found that in fact the structural changes correspond to a functional de-synchronization/decoupling of several brain areas, which are crucial for the processing of sensory, visual and auditory information.

Results

Altered diffusion tensor fractional anisotropy

We hypothesized that an altered network organization/connectivity in the neocortex could lead to the deficits that have been described in the processing of sensory information in FXS and ASD. Therefore we measured the large-scale anatomical connectivity of adult mice of the *Fmr1* KO FXS model[3] ultra-high-field MRI (11.7 T). We used diffusion tensor imaging (DTI) to measure structural connectivity parameters. In particular we measured the fractional anisotropy (FA) values, which allow an exploration of the organization and integrity of the structures in parallel oriented tissue. We found that the white matter is significantly affected in several parts of the brain (**Fig. 1**). In particular, the FA values were decreased in the corpus callosum below the visual cortex, auditory cortex and parts of the somatosensory cortex.

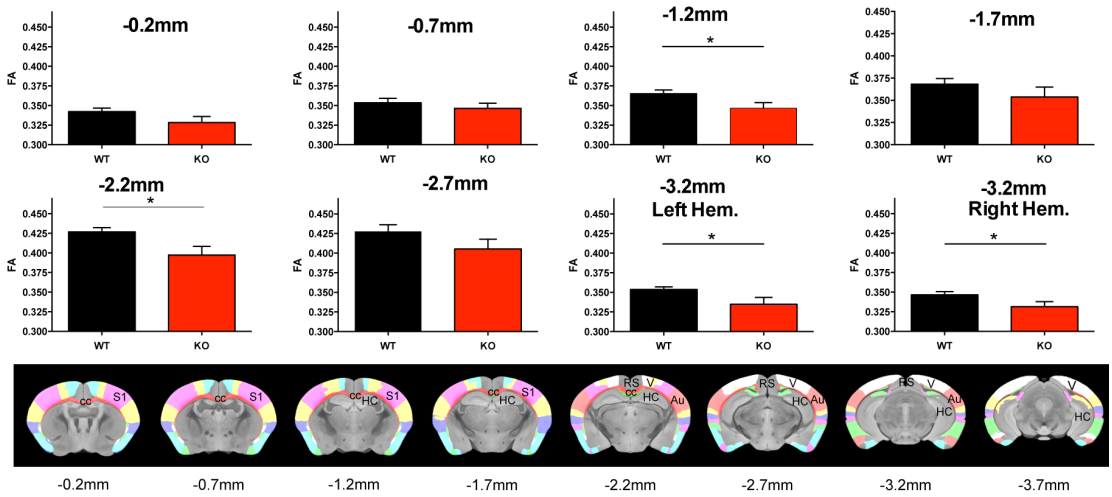

Fig 1. Reduced structural integrity of the corpus callosum in *Fmr1*KO mice

Diffusion tensor imaging (DTI) in the *Fmr1* KO mice shows a reduced fractional anisotropy in the white matter, indicating a reduction in the number of axons, or less organized fibers. The FA values of the corpus callosum were collectively measured in several horizontally planes from -0.2mm -2.7mm and separately from -3.2mm to -3.7mm from the bregma, with an interplane distance of 0.5mm (WT: n=12; *Fmr1*KO: n=8). The FA values were significantly reduced in *Fmr1* KO mice at -1.2mm (p=0.0274) -2.2mm (p=0.0178) and at -3.2mm (in both hemispheres; right: p=0.0423; left p=0.0314); unpaired t-test.

Local- and long-ranging structural input connectivity in *Fmr1* KO mice

Our results show that the organization of the white matter is structurally altered, and that the primary visual cortex (amongst others) may be strongly affected by these changes. To test whether this white matter defect is caused by a reorganization of anatomical connections, we quantified projections into the primary visual cortex. In particular, we investigated alterations in the local connectivity of the visual cortex versus long-ranging projections into this region. To address these questions, we employed a retrograde rabies virus (SADΔG-eGFP(SAD G)) injected into the primary visual cortex (V1). To control the precise location of the injection site and the diffusion of the virus in the tissue we co-injected a local/anterograde variant of the virus SADΔG-mCherry(VSV^{Ctm})[11]. The average diffusion of the virus in the tissue is ~200μm with a maximal distance of locally infected cells at ~500μm (**Table 1**) distance calculated from the center of mass of the infected cells. All labeled cells were introduced as fiducal markers into a 3D average brain model (MRI generated; 16μm resolution) of the C57/Bl6 mouse[12], to compute the Euclidian distance in the whole-brain from the injection site (**Fig. 2**). The average distance of input to the brain region is at ~1mm distance. A summary of the most important values calculated from the tracer injections can be found in **Table 1**. We found a reduced average distance of presynaptic cells in the *Fmr1* KO mice. Conversely the contribution of presynaptic cells from within the visual cortex is increased in the *Fmr1* KO mice.

Table 1. Quantification of the labeled cells

The center of mass of the anterogradely labeled cells determines the center of the injection site. The distance of the anterogradely labeled cells gives an indication about the maximum diffusion of rabies virus in the tissue. The distribution of the retrogradely labeled cells is indicated for cells in the Cortex, the Visual Cortex and the Primary Visual Cortex.

Key: Total: all retrogradely labeled cells; Cortex: all retrogradely labeled cells in the cortex; Vi (Visual Cortex): all retrogradely labeled cells in the primary and secondary visual cortex V1 (primary visual cortex): all retrogradely labeled cells in the primary and secondary visual cortex

	WT	**KO**
Anterogradely/Locally labeled cells		
Average distance from injection point (μm)	198,24 ± 11,97	219,22 ± 12,60

Max distance from injection point (μm)	475,62	370,03
Retrogradely labeled cells		
Total number of labeled cells	1173	1495
Max distance from injection point (μm)	5736,33	6625,49
Average distance from injection point (μm)	1191,33 ± 24,45	738,81 ± 20,96
Median (μm)	1003	410,8
Cortex		
Percentage of cells in Ctx, from Total (%)	95,82	92,37
Max distance from injection point (μm)	5341,76	5997,16
Average distance from Injection point (μm)	1127,68 ± 22,87	610,71 ± 17,82
Visual Cortex		
Percentage of cells in Vi, from Ctx (%)	76,25	89,50
Percentage of cells in Vi, from Total (%)	73,06	82,68
Max distance from injection point (μm)	2489,91	2580,75
Average distance from injection point (μm)	871,69 ± 18,79	434,35 ± 9,36
Primary Visual Cortex		
Percentage of cells in V1, from Vi (%)	63,83	88,19
Percentage of cells in V1, from Total (%)	46,63	72,91
Max distance from injection point (μm)	2311,47	2210,50
Average distance from injection point (μm)	647,96	365,67

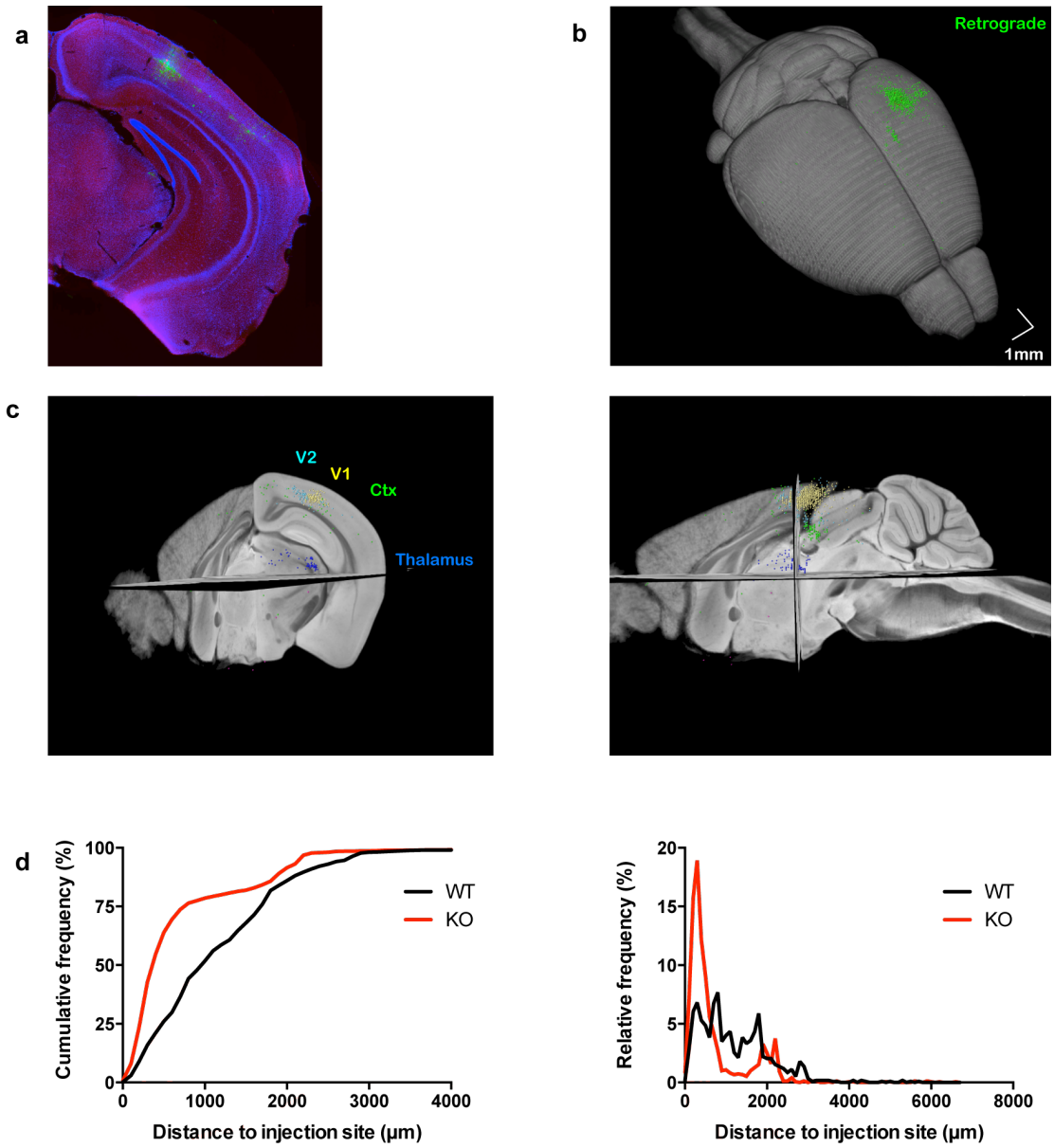

Fig. 2. Input to the primary visual cortex of *Fmr1* KO mice

(a) Example image displaying the injection site. (b) Overview of the 3D model with all retrogradely labeled cells in green. (c) Recoloring of the retrogradely labeled cells into, primary visual cortex, secondary visual cortex other cortical areas and the thalamus. (d) Distance of the retrogradely labeled cells to the injection site in the *Fmr1* KO mice and the WT mice. The relative number of cells (in % of total), plotted as cumulative and relative frequency per distance to the injection site, indicates a strong increase in the cells with less than 1mm distance.

Functional connectivity in the neocortex of *Fmr1* KO mice

To evaluate the relevance of the anatomical deficits we proceeded by assessing whether the structural alterations in *Fmr1* KO mice would

correspond/correlate to an altered functional connectivity (**Fig. 3**). Resting state functional MRI (rs-fMRI) measurements were performed in head-restrained *Fmr1* KO (n=7) and wild-type (n=10) mice under light isofluorane aneasthesia. We performed
135 rs-fMRI experiments to measure the functional connectivity of somatosensory, auditory, visual, and motor cortex and the dorsal and ventral hippocampus, as well as the subcortical areas (**Fig. 3**, **Supplementary Fig. S1**).

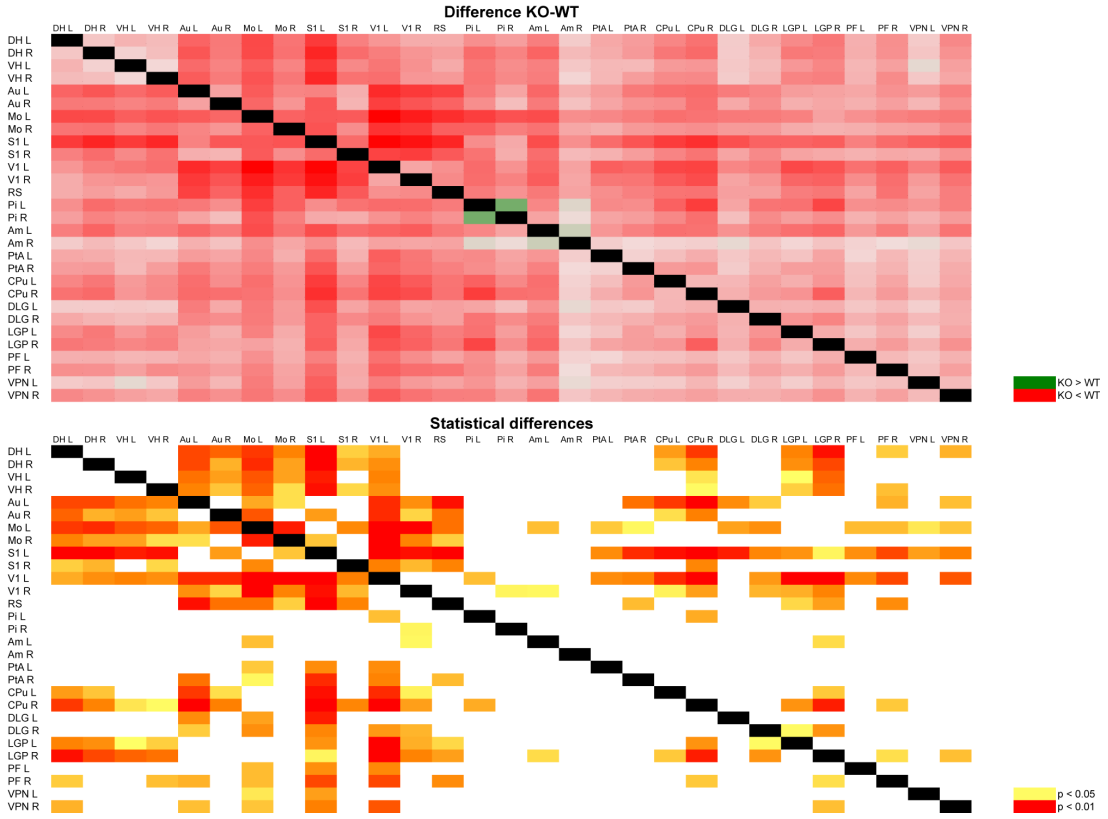

Fig 3. Functional decoupling of brain areas in *Fmr1*KO mice

Upper panel: Difference of the Z-scores of rs-fMRI measurements calculated as average Z-score of *Fmr1* KO mice minus average Z-score of WT mice. Lower panel: Statistically significant differences in the functional connectivity matrix are color coded for the p-value. Resting state fMRI measurements revealed a reduced functional connectivity between several brain areas in the *Fmr1* KO mice (n=7) compared to age-matched wild type mice (n=10). The functional decoupling affected largely connections from hippocampus to neocortical areas and the intracortical connectivity. The auditory cortex is less linked to the dorsal and ventral hippocampus, to the visual cortex and to the retrosplenial cortex. The connectivity between visual cortex and the motor and somatosensory cortices is also deficient. Overall all measured cortical areas appear to be strongly affected. None of the examined connections showed a statistically significant increased functional connectivity. The pre-dominant pattern is a

functional decoupling of numerous brain areas. Key: Dorsal hippocampus (DH), ventral hippocampus (VH), auditory cortex (Au), motor cortex (Mo), primary somatosensory cortex (S1), primary visual cortex (V1), retrosplenial cortex (RS), Piriform Cortex (Pi), Amygdala (Amy), Pretectal Area (PtA), Caudate Putamen (CPu), lateral geniculate nucleus (DLG), globus pallidus (LGP), parafascicular nucleus (PF), ventral posterolateral nucleus and ventral posteromedial nucleus (VPN). Right hemisphere (R), left hemisphere (L).

Discussion

We found converging connectivity changes in *Fmr1* KO mice, structurally on a whole-brain and single-cell-resolution level and a corresponding functional decoupling of several brain areas, in particular in the neocortex. Alterations in the way the brain is wired provide a reasonable explanation for deficits in the sensory information processing and could also be linked to learning deficits either by being cause or being effect.

In particular we found a reduced fractional anisotropy in several parts of the corpus callosum, which could indicate that either the number of axons running through these areas is reduced or that they are running less in parallel, e.g. they could be ascending more into the cortex. Since these measurements allow more than one interpretation we decided to inject viral tracers that allowed us to quantify the number of connections. The retrograde tracer allowed us to determine more specifically how these changes could be caused. When examining the connections arriving to the visual cortex we found a reduced number of neuronal input from long-ranging connections to V1 in the *Fmr1* KO mice. Conversely we found an increased number of local connections (<1mm of distance). This shift could lead to an imbalance in the cognitive processing of sensory information, by underrepresentation of external information in the cortex and overrepresentation of ongoing activity in the own brain area. We hypothesized that this overrepresentation of the local information and a reduction of input from other regions would cause the region to be more isolated and functionally decoupled from other brain areas. We tested this idea using resting state functional MRI and found that this decoupling in fact occurs between V1 and several other brain areas. Interestingly a reduced functional connectivity appears to be a widespread phenomenon, which we found between several cortical and subcortical areas. We conclude that connectivity changes are an important feature in FXS, which

should be further assessed. The altered communication of the sensory cortical areas might play an important role in the overall processing of sensory information in FXS and contribute largely to the cognitive and behavioral defects in the disease.

We consider that combining non-invasive measurements with a fine-scale dissection of circuit structure is an important step for a better understanding of the neuropathology. We expect that this work will pave the way in the future in two directions. First we hope it will lead to future studies in human FXS patients to determine the role that connectivity changes play in the human disease. And secondly we think this study should provide a useful framework/baseline, to test the effects of therapeutic agents for their ability to reverse wiring deficits in *Fmr1* KO. The prospect of those two directions would offer a mode for a fast MRI based-assessment of rescue approaches and facilitate the transition of strong candidate drugs to human patients, providing new objective criteria to evaluate their success.

Materials and Methods

Adult (9-12 weeks old) male *Fmr1* KO2 mice[3] in a C57BL/6 background and male wild-type littermates were used in all experiments. Genotypes were determined by a PCR analysis of DNA extracted from tail samples. All experiments and analysis were performed with the experimenter being blind to the genotype.

Virus production

RABV SAD ΔG-eGFP (RG) was produced as described previously[11]. VSV G^{RtmC}-pseudotyped SAD ΔG-mCherry was produced as described previously using BSR T7/5 cells[11].

Stereotaxic injections

All stereotactic injections and subsequent experiments were performed according to French law and the European Directive covering the use of experimental animals (2010/63/EU) and approved by the Ethics Committee of Bordeaux (approval #5012024-A). Stereotaxic injections were performed in *Fmr1* KO and WT mice at 10-12 weeks of age. The stereotactic injections of viral vectors were performed in isofluorane anesthetized and head-fixed mice using a 10μl glass syringe fitted with a 34-gauge needle or a pulled glass pipette. Injection volume and speed were controlled

using a WPI Ultra Micro Pump. The coordinates for the injections were (i) anterior/posterior (A/P) 3.0 mm, lateral (L) 0.94 mm, dorso/ventral (D/V) 0.5 mm for the primary visual cortex (V1). A/P and L coordinates are given with respect to the bregma, D/V coordinates with respect to the brain surface. Viral injections were performed with 200nl viral solution consisting of 1/10th anterograde rabies virus (VSV^{tm}) mCherry together with 9/10th retrograde (RG) eGFP rabies virus. Anterograde RABV was utilized to verify injection coordinates and to normalize the amount of injected viral solution. Subsequent comparisons between animals were done normalizing the number of retrogradely infected cells to the number of locally (anterogradely) labeled cells in the same animal. Ratios of the retrogradely labeled cells in different areas were calculated in relation to the total number of retrogradely labeled cells in the same animal.

Mouse brain slice preparation

Mice were perfused and brains sectioned as described previously[11]. Briefly, mice were administered a lethal dose of sodium pentobarbital and then trans-cardially perfused with 30ml normal Ringer's solution followed by 100ml of a 4% PFA solution in 1 X phosphate buffered saline (PBS). The mouse brains were dissected and postfixated in 4% PFA solution and slices were cut using a vibratome (Leica). For whole-forebrain sectioning brains where emerged in 10% Gelatine, post-fixed 2h in 4% PFA, sectioned in 50μm slices and mounted using Prolong Gold Antifade Reagent. Immunohistology was used for signal amplification for the axon quantification using dsRed antibody (polyclonal Rabbit) and Alexa 594 goat anti-rabbit.

Fluorescence microscopy and analysis

Images of the entire forebrain where acquired using a scanning mosaic widefield fluorescence acquisition system (Nanozoomer, Hamamatsu) equipped with a 20X 0.75 NA objective. Images were acquired by scanning each section at multiple (~5-6) z-positions with 8μm step size. Analysis of retrogradely and locally labeled cells was performed blind to the genotype by placing manually fiducal markers on the cell position. Images where segmented using the mouse brain atlas ('The Mouse Brain in Stereotaxic Coordinates', Paxinos and Franklin) and fiducal points where transformed into a 3D average brain atlas, using Vaa3D software[13], to compute the Euclidian

distance of each marker in the whole-brain in xyz directions from the injection site. The precise coordinates of each injection site was confirmed by calculating the center of mass of infected cells by the local tracer SADΔG-mCherry(VSV-G).

MR imaging

MRI was performed on mice from the same line of mice in adult male mice (9-12 weeks old). Breeding of the *Fmr1* KO mice[3] in a C57BL/6 background and wild-type littermates was continued in Nijmegen (Netherlands) in the same conditions. MRI measurements were performed with an 11.7 T BioSpec Avance III small animal MR system (Bruker BioSpin, Ettlingen, Germany) equipped with an actively shielded gradient set of 600 mT/m and operated by Paravision 5.1 software. We used a circular polarized volume resonator for signal transmission and an actively decoupled mouse brain quadrature surface coil for signal reception (Bruker BioSpin). During the MR experiments, low-dose isoflurane was used (3.5% for induction and ~1.5% for maintenance), slightly adjusted throughout the experiment to maintain a fast and stable breathing frequency (>130 bpm). The mice were placed in a stereotactic device in order to immobilize the head. Body temperature was measured with a rectal thermometer and maintained at 37° C by a heated air flow device.

After standard adjustments and shimming, **rsfMRI** datasets were acquired using a single shot spin echo sequence combined with echo-planar imaging (SE-EPI) sequence. Six hundred repetitions with a repetition time (TR) of 1.8s and echo time (TE) of 16.9ms were recorded for a total acquisition time of 18 minutes. Other imaging parameters: field of view = 25 × 25 mm; image matrix = 96 × 96; spatial resolution = 260 × 260 × 500 μm; number of slices = 9.

Diffusion of water was imaged as described previously[14,15]. In short, 22 axial slices covering the whole brain were acquired with a four-shot SE-EPI protocol. B0 shift compensation, navigator echoes and an automatic correction algorithm to limit the occurrence of ghosts and artefacts were implemented. Encoding b-factors of 0 s/mm^2 (b0 images; 5×) and 1000 s/mm^2 were used and diffusion-sensitizing gradients were applied along 30 non-collinear directions in three-dimensional space. Other imaging parameters: TR = 7.55 s; TE = 20ms; field of view = 20 × 20 mm; image matrix = 128 × 128; spatial resolution = 156 × 156 × 500 μm; total acquisition time = 18 min.

Functional connectivity measurements

The rsfMRI datasets were processed as described previously (Zerbi et al., J Neuoscience 2014 online); briefly, the data were first realigned using a least squares method and rigid-body transformation with Statistical Parametric Mapping (SPM) mouse toolbox (SPM5, University College London, [16]).

The mean SE-EPI images of each mouse were then used to generate and normalize the data into a study-specific template through linear affine and non-linear diffeomorphic transformation (ANTs. V1.9, http://picsl.upenn.edu/ANTS/). On the template, seventeen areas were selected in left and right hemisphere and back-transformed in each subject space using the inverse of the affine and diffeomorphic transformations. Brain regions where segmented based on based on a MRI atlas[12], and includes: dorsal hippocampus (DH), ventral hippocampus (VH), auditory cortex (Au), primary motor cortex (M1), somatosensory cortex (So), primary visual cortex (V1), retrosplenial cortex (RS), Piriform Cortex (Pi), Amygdala (Amy), Pretectal Area (PtA), Caudate Putamen (CPu), lateral geniculate nucleus (DLG), globus pallidus (LGP), parafascicular nucleus (PF), ventral posterolateral nucleus and ventral posteromedial nucleus (VPL, VPM). In-plane spatial smoothing (0.4×0.4mm) and temporal high-pass filtering (cut-off at 0.01Hz) were applied to compensate for small across-mouse misregistration and temporal low frequency noise using the FEAT tool of FSL (FSL 5.0, [17]). Functional connectivity (FC) between ROIs was calculated from the BOLD time series after movement regression using total correlation analyses implemented in FSLNets (FSLNets, V0.3, www.fmrib.ox.ac.uk/fsl). Pearson's correlation values were Fisher transformed to *Z*-scores for group comparisons and statistical analysis.

Diffusion tensor MRI parameters estimation

The calculation of the two commonly used DT-MRI parameters, mean diffusivity (MD) and fractional anisotropy (FA), was performed following a protocol as described previously[15]. Briefly, the diffusion images were first realigned with SPM mouse toolbox, to compensate for small movement artefacts; thereafter, the datasets were spatially normalized to a study-specific template through linear affine and non-linear diffeomorphic transformation using ANTs. Following these pre-processing

steps, the diffusion tensor was estimated for every voxel using the PATCH algorithm[18].

Regions of interest in several white matter (WM) and grey matter (GM) areas were drawn on the template image based on an anatomical atlas ('The mouse brain in stereotaxic coordinates', Keith B.J. Franklin, George Paxinos, 1997) and the resulting FA and MD values were measured for further statistical analyses.

Supplementary Material

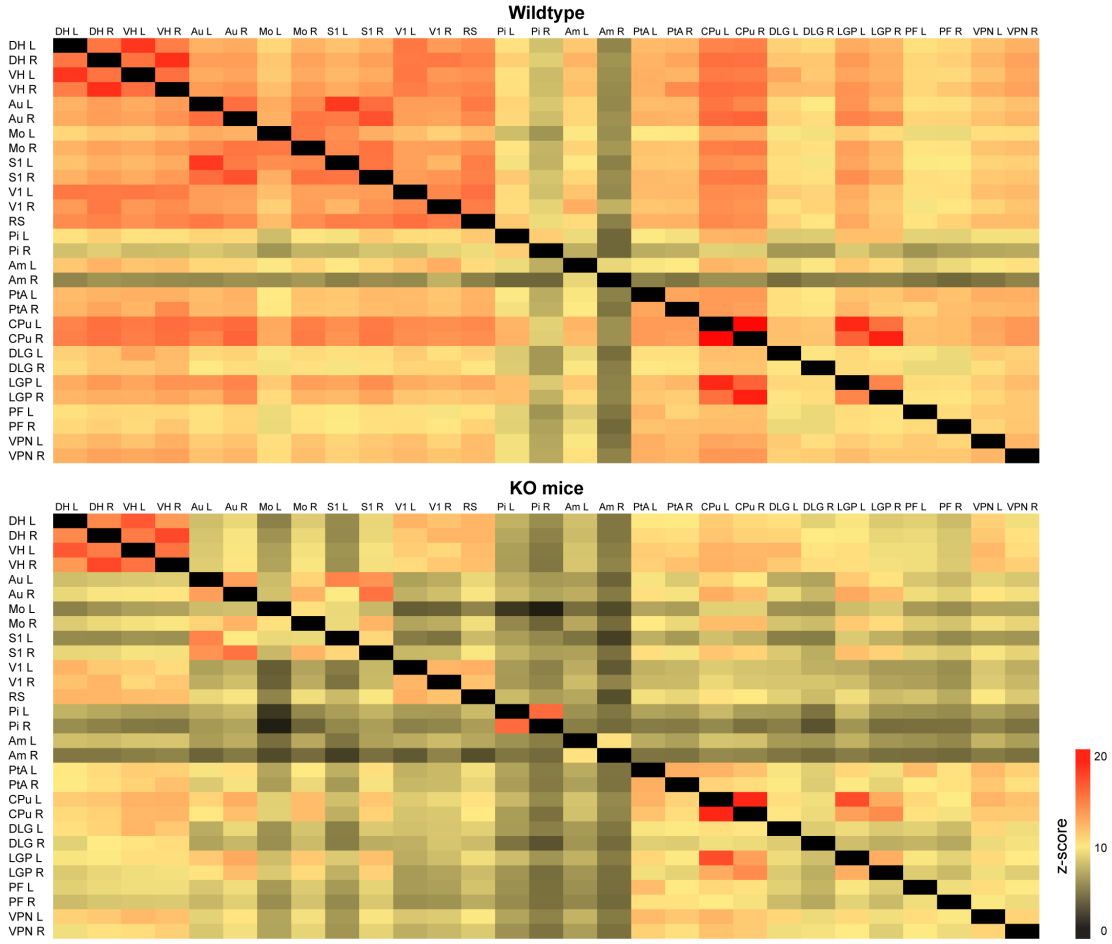

Supplementary Fig S1. Functional Connectivity Matrix of WT and *Fmr1*KO mice

Resting state fMRI measurements were performed in *Fmr1*KO mice (n=7) and age-matched wild type mice (n=10). The intracortical functional connectivity is very strong in the wildtype animals whereas it is less in the *Fmr1* KO mice. Key: Dorsal hippocampus (DH), ventral hippocampus (VH), auditory cortex (Au), motor cortex (Mo), primary somatosensory cortex (S1), primary visual cortex (V1), retrosplenial cortex (RS), Piriform Cortex (Pi), Amygdala

(Amy), Pretectal Area (PtA), Caudate Putamen (CPu), lateral geniculate nucleus (DLG), globus pallidus (LGP), parafascicular nucleus (PF), ventral posterolateral nucleus and ventral posteromedial nucleus (VPN). Right (R) and left hemisphere (L).

References

1. Bassell, G. J. & Warren, S. T. Fragile X Syndrome: Loss of Local mRNA Regulation Alters Synaptic Development and Function. *Neuron* **60,** 201–214 (2008).
2. Penagarikano, O., Mulle, J. G. & Warren, S. T. The pathophysiology of fragile x syndrome. *Annu Rev Genomics Hum Genet* **8,** 109–129 (2007).
3. Mientjes, E. J. *et al*. The generation of a conditional Fmr1 knock out mouse model to study Fmrp function in vivo. *Neurobiology of Disease* **21,** 549–555 (2006).
4. D'Hulst, C. & Kooy, R. F. Fragile X syndrome: from molecular genetics to therapy. *J. Med. Genet.* **46,** 577–584 (2009).
5. Belmonte, M. K. & Bourgeron, T. Fragile X syndrome and autism at the intersection of genetic and neural networks. *Nature Neuroscience* (2006).
6. Antar, L. N., Li, C., Zhang, H., Carroll, R. C. & Bassell, G. J. Local functions for FMRP in axon growth cone motility and activity-dependent regulation of filopodia and spine synapses. *Mol. Cell. Neurosci.* **32,** 37–48 (2006).
7. Bureau, I., Shepherd, G. M. G. & Svoboda, K. Circuit and Plasticity Defects in the Developing Somatosensory Cortex of Fmr1 Knock-Out Mice. *J Neurosc* **28,** 5178–5188 (2008).
8. Gibson, J. R., Bartley, A. F., Hays, S. A. & Huber, K. M. Imbalance of neocortical excitation and inhibition and altered UP states reflect network hyperexcitability in the mouse model of fragile X syndrome. *Journal of Neurophysiology* **100,** 2615–2626 (2008).
9. Testa-Silva, G. *et al*. Hyperconnectivity and slow synapses during early development of medial prefrontal cortex in a mouse model for mental retardation and autism. *Cerebral Cortex* **22,** 1333–1342 (2012).
10. Patel, A. B., Loerwald, K. W., Huber, K. M. & Gibson, J. R. Postsynaptic FMRP promotes the pruning of cell-to-cell connections among pyramidal neurons in the L5A neocortical network. *J Neurosc* **34,** 3413–3418 (2014).
11. Haberl, M. G. *et al*. An anterograde rabies virus vector for high-resolution large-scale reconstruction of 3D neuron morphology. *Brain Struct Funct* (2014). doi:10.1007/s00429-014-0730-z
12. Ullmann, J. F. P., Watson, C., Janke, A. L., Kurniawan, N. D. & Reutens, D. C. A segmentation protocol and MRI atlas of the C57BL/6J mouse neocortex. *NeuroImage* **78,** 196–203 (2013).
13. Peng, H., Bria, A., Zhou, Z., Iannello, G. & Long, F. Extensible visualization and analysis for multidimensional images using Vaa3D. *Nat Protoc* **9,** 193–208 (2014).
14. Harsan, L.-A. *et al*. In vivo diffusion tensor magnetic resonance imaging and fiber tracking of the mouse brain. *NMR Biomed* **23,** 884–896 (2010).
15. Zerbi, V. *et al*. Gray and white matter degeneration revealed by diffusion in an

Alzheimer mouse model. *Neurobiology of Aging* **34,** 1440–1450 (2013).
16. Sawiak, S. J., Wood, N. I., Williams, G. B., Morton, A. J. & Carpenter, T. A. Voxel-based morphometry with templates and validation in a mouse model of Huntington's disease. *Magnetic Resonance Imaging* **31,** 1522–1531 (2013).
17. Jenkinson, M., Beckmann, C. F., Behrens, T. E. J., Woolrich, M. W. & Smith, S. M. FSL. *NeuroImage* **62,** 782–790 (2012).
18. Zwiers, M. P. Patching cardiac and head motion artefacts in diffusion-weighted images. *NeuroImage* **53,** 565–575 (2010).

3. General Discussion and Future Perspectives

During this work we developed a new anterograde viral tracer, based on the glycoprotein-deleted variant of rabies virus, and tested its potential for studying neuronal circuits. We found that the rapid high-level expression of transgenes, and limited cytotoxicity is advantageous to delineate the neuronal morphology and to reconstruct neuromorphological features. Importantly the intense labeling is independent of the age of the animal, which provides an advantage over several other viral tracers that normally depend on cellular promoters (Gray et al., 2011; Hong et al., 2007). We tested the new anterograde tracer for bulk and sparse labeling. Diluting the virus and injecting only a few viral particles (<10) allowed us to sparsely label neurons *in vivo*, still achieving intense labeling and therefore facilitating subsequent reconstructions. Stereotactically co-injecting the anterograde variant together with the retrograde (not trans-synaptic) glycoprotein-deleted rabies virus allows us to study a brain region of interest in a combined fashion. We can thus precisely define the center of the injection site (as the center of mass of anterogradely labeled cells), meanwhile having the input of this region labeled together with the axonal projections coming from it, in a different color.

We took advantage of this approach and combined it in a quantitative way, together with non-invasive whole-brain measurements of structural and functional connectivity. We employed these techniques to study connectivity features in the *Fmr1* KO mouse model. We found alterations of both local- and long-range connections when comparing the *Fmr1* KO mice to WT littermates.

In particular, using DTI we found a reduced FA in the corpus callosum adjacent to several cortical areas. Those deficits in the WM integrity might be caused by a reduction in the number of axons in these areas, less in parallel-organized axons or a reduction in the myelination of the axons. Each of these interpretations could have strong implications for the function of long-ranging connections. Myelination provides an important mechanism for the signal transmission (Hildebrand et al., 1993) and recent evidence suggests that along individual axons the thickness of myelin can vary substantially (Tomassy et al., 2014). It would be possible that the regulation of myelination is disturbed in FXS, e.g. by changes in the oligodendrocytes, the type of glial cells that are responsible for the myelination in the CNS. In fact, evidence

suggests that - unlike earlier reports proposed - FMRP is not only expressed in oligodendrocyte progenitor cells and immature oligodendrocytes (Pacey and Doering, 2007; Wang et al., 2004), but also in mature oligodendrocytes (Giampetruzzi et al., 2013). Furthermore, also the mRNA of *Fmr1* was found in the corpus callosum of adult mice (Hinds et al., 1993). Furthermore *in vitro* studies showed that FMRP can act as a translational repressor of myelin basic protein (MBP), which is a crucial protein for the formation of myelin in the CNS (reviewed in (Boggs, 2006)). This however would suggest that a lack of FMRP in the oligodendrocytes would lead to an increase of MBP. An increased myelination would restrict the water diffusion, and should lead to increased rather than decreased FA values. More recent evidence from *in vivo* studies showed that the MBP and other myelin proteins are similar in the *Fmr1* KO mouse compared to wild type mice. Furthermore this study found that the FMRP concentrations in the oligodendrocytes *in vivo* are likely too small to act as translational repressor on MBP or other proteins, and that in comparison, the level of FMRP present in cortical neurons nearby the oligodendrocytes is much higher (Giampetruzzi et al., 2013).

We therefore consider that the reason for the reduction in FA reported here is most likely due to a mechanism altering neuronal features, rather than acting through the oligodendrocytes. To investigate the two possible neuronal mechanisms that might play a role in the reduced FA, we would need to quantify the number of axons, and also examine how they run in the tissue (parallel or dispersed). A decreased number of axons would, in the worst-case scenario, mean that the number of cells sending projections to the adjacent cortical areas is reduced. We therefore decided to quantify the number and the origin of cells projecting to one of the presumably affected cortical regions, the primary visual cortex (V1). When quantifying their average distance to the injection site we found less long-distance connections and that more of the input is coming from the immediate proximity (<1mm of distance). Overall, we see a hyper-connectivity phenotype for local neocortical circuits, but a hypo-connectivity for long-ranging ones. In the literature, a local change in connectivity has been described in several publications (Bureau et al., 2008; Patel et al., 2014; Testa-Silva et al., 2012), but very often this change was only seen transiently (Bureau et al., 2008; Testa-Silva et al., 2012). Whereas in other studies it was suggested that a change is due to a deficit in the pruning of synapses, which occurs between the 2nd

and the 5th postnatal week in mice (Patel et al., 2014). These somewhat contradictory results did not leave an indication how the connectivity of small-networks would be manifested in adult *Fmr1* KO mice. Here we found that both, the short- and long-range wiring is altered and conclude that the connectivity features might play an important role in sensory and cognitive deficits of adults with FXS.

The overall large number of neurons labeled in the short-range distance (>90% in both genotypes) might appear surprising at first. However, a recent study performed in macaque monkeys quantified the input into several visual areas as fraction of labeled neurons (FLN). The authors found that the FLN from subcortical areas makes only 1.3% of the total neurons labeled and that the long-ranging cortico-cortical connectivity is also low with 3% FLN. Local intrinsic connectivity on the other hand is extremely high with 80% FLN, while neighboring areas comprise 15% cumulative FLN (Markov et al., 2011). The authors concluded that the "high investment in local projections highlights the importance of local processing". This is a reasonable conclusion, considering the dominance of intrinsic connectivity over exterior input. Whereas the additional prominent connection strength from neighboring areas is another proof of the wiring efficacy of the brain, which is often described as the concept of small-world networks (Bullmore and Sporns, 2009; Watts and Strogatz, 1998). This implies that functionally related brain areas should be kept in close physical proximity to reduce the wiring costs for the organism.

We used rs-fMRI to further assess, in the *Fmr1*KO mouse model, whether the structural alterations in the KO mice would lead to an altered functional processing in the brain. We found that the resting-state functional connectivity was significantly reduced between numerous brain areas. Which led us to the conclusion that (i) the alteration in the connectivity is causing, or at least involved in functionally relevant changes in the neuronal network; (ii) that this phenomenon is not specific for V1 but rather widespread in the brain of *Fmr1* KO mice. We therefore propose that FXS in characterized by a strong component of connectivity deficits, which should be further explored to understand their role in the cognitive deficits.

3.1 Deficits of Connectivity in FXS as a Potential Biomarker

Hypersensitivity to visual, auditory, tactile, and olfactory stimulation is a feature that is common to both human FXS patients and *Fmr1* KO mice. We were therefore interested in studying connectivity changes to- and in between- the neocortical sensory areas. We examined which anatomical alterations occur in brain wiring and neuronal connectivity in FXS and what functional role they play in the brain. We found connectivity changes in *Fmr1* KO mice, structurally on a large- and fine-scale level, and a corresponding functional decoupling of several brain areas, in particular in the neocortex. Changes in the way the brain is wired provide a reasonable explanation for deficits in the sensory information processing and could also be linked to learning deficits, either by being the cause or being the effect of such change. We propose that the non-invasive measurements of brain connectivity – demonstrated here in the mouse – could be repeated in human patients. Our study thus points to suitable biomarkers that could be applied for testing the efficacy of therapeutic interventions. This could facilitate and improve the outcome of clinical trials, by testing their capability of reversing brain wiring deficits in FXS.

The recent discontinuation of several large-scale drug trials emphasizes the need for a better mechanistic understanding of FXS. Those drugs did not bring the anticipated advantageous effect on patients e.g. Arbaclofen (Seaside Therapeutics/Roche) or Mavoglurant/mGluR5 (AFQ056) (Novartis), even though they act on particularly well-described molecular targets (mGluR5 and GABAR). Alterations in the anatomical wiring provide a mechanism that could explain (i) the drastic effects found on the processing of sensory information in the neuronal circuits and (ii) the complications in rescue strategies aiming at curing molecular phenotypes. We believe that our work will not only strengthen our understanding of the pathologic deficits of FXS (and ASDs) but also that it will provide a framework for testing the effectiveness of novel therapeutic agents for their capability to reverse changes in the anatomical and functional wiring in FXS mice and in the future in human patients.

Importantly our study was specifically performed only in adult mice (9-12 weeks postnatal). Previous pre-clinical studies and tests have often been performed in cell cultures or young animals (e.g. starting chronic treatment in mice at 4-5 weeks (Michalon et al., 2012)). It is thus important to consider additional tests, both in vivo and ex vivo which evaluate intermediate measures like the capability of potential

therapeutics to reverse wiring deficits. Performing those trials in adult animals can provide better indications for clinical efficacy in adult FXS patients since neuronal wiring is much more plastic in the young animals or infants, where the brain is still undergoing strong rewiring and pruning effects. We suggest that our approach has the potential to become an analysis pipeline to test the new drug candidates. Such drug candidates can be identified at an increasing speed in large screenings for bioactive small molecules with a desirable effect (Dominguez et al., 2014). One potential compound for FXS is the recently identified small molecule (FRAX486) that acts by inhibiting a protein modulating the actin cytoskeleton dynamics (Dolan et al., 2013). The component has been used in adult mice and provided positive effects on several behavior deficits. It would therefore be interesting to test whether this drug would be efficient to reverse the connectivity features found here. To test this we could examine the same parameters of structural and functional connectivity in the adult mice with and without treatment.

A last point that should be considered is the complexity of FXS and the variability of associated phenotypes. The cause of this variability is not entirely clear but it likely depends on several other genetic or environmental factors. Therefore it seems reasonable that probably not all FXS patients are equally affected by changes in mGluR and GABA activity or connectivity features. Some patients develop strong epilepsy, which could be caused by an excitation/inhibition imbalance and might be corrected by targeting GABA receptors. Depending on the neurologic deficits in each patient might be treated for the combination of the most severe problems he/she experiences. All in all, rather than removing promising drugs from the market because they do not provide the benefit in a sufficiently large number of patients it would be better to develop a personalized medicine for FXS patients. Here large-scale wiring and functional connectivity have the advantage that they can be measured in the patient and predictions could be made how beneficial certain treatments might be.

3.2. Alternative Tracers

The most important aspects and limitations concerning mono-trans-synaptic tracing and anterograde viral tracing have been discussed in the Publications **N.1** and **N.2** respectively.

In spite of their numerous advantages, rabies virus derived vectors – even glycoprotein deleted forms – are still mostly limited by eventual cytotoxic side effects. This cytotoxicity is in part due to certain aspects of rabies virus biology. However the high level production of virally encoded genes, including transgenes, which is an advantage for tracing, may also contribute to this cytotoxicity.

Reducing the toxicity of RABV to permit long-term infection might therefore be achieved by reducing the expression levels of the rabies virus polymerase, which can for example be achieved by changing the position of the polymerase (L) gene of the rabies virus (Finke et al., 2000) to a different position further downstream. Another interesting target for manipulating the virus to reduce neurotoxicity could be the matrixprotein (M). This is an essential protein for the assembly of the virus, but at the same time it has a crucial regulatory role for the balance of virus transcription and replication. While a reduced M expression causes an increased transcription and reduced replication (Finke and Conzelmann, 2003; Finke et al., 2003) an increased M expression might reduce the transcription and therefore decrease the translation and make the infection less exhaustive for the cell metabolism.

In some cases, like long-term studies, alternative approaches might be favorable. While there are different options for anterograde viral vectors that exhibit very low toxicity, most notable AAVs, the options are more limited for retrograde vectors. To date most of them are either not single-cycle vectors, and cross further trans-synaptic steps to connected neurons, or are toxic to the cell or both. The most promising candidates as alternative retrograde vectors are (i) a retrograde serotype of the AAV (Towne et al., 2010) (ii) lentivirus pseudotyped with the rabies virus glycoprotein (Kato et al., 2007) and (iii) a Canine Adeno-Virus (CAV). Despite enormous efforts, the first two still exhibit a low retrograde efficacy and often lead to only a small number of retrogradely labeled cells or are mixed with somatically infected cells and further they were shown to work mainly for specific projections (Aschauer et al., 2013; Carpentier et al., 2012; Kato et al., 2014; Nelson et al., 2013). Meanwhile, CAV has been improved over the last years and it is now possible to

reach high titers and efficient retrograde tracing. To date there is only a limited number of studies that applied this technique this far to questions about the neural circuitry, even though the potential is promising. It has been shown that CAV is specific for neurons and does not infect glial cells (Soudais et al., 2001) has a large cloning capacity 27-kb and leads to a long-lasting transfection shown up to 1 year, but the expression levels seem to somewhat decrease over time (Soudais et al., 2004).

Notably CAV serotype 2 was recently combined with designer drug application technology (DREADD) (Boender et al., 2014), which might be of great interest to explore the effects of neuromodulators and alter them in long-term experiments. There is however some concern about pathway specific tropism (Senn et al., 2014) and the retrograde tracing properties (mono- versus polysynaptic) have not been evaluated extensively.

All of the viral vectors mentioned in chapter 3 are under constant development, to reduce toxicity, increase expression levels, increase packaging size, achieve cell type specificity and it is therefore difficult to specify a single best technique, each having its own merits and drawbacks, which need to be taken into consideration. Therefore the viral vector should be chosen carefully for a specific purpose, to find the best type for each experiment, considering all advantages and disadvantages.

3.3 Future Perspectives

Based on our findings we suggest the following long-term experimental plan:

(1) In order to verify the local hyperconnectivity, we have begun to quantify the local axonal arbors (i.e. the output) of bulk-infected neurons in the visual cortex. To quantify the axonal arbors of neurons we recently developed a novel anterograde RABV ΔG based method, conferring intense labeling of neuronal structures (Haberl et al., 2014). We are now using this approach with algorithms delineating the axonal arborization of the infected neurons (Broser et al., 2008). We are therefore combining anterograde RABV injections in V1 with confocal scanning microscopy in the same area over several layers, and the white matter. Automated tracing and quantification methods are applied to measure changes in the number and localization of axons. From this data we will establish an axonal density plot ranging from layer 1-6 and the white matter in *Fmr1* KO and in WT mice. This approach should provide an additional quantitative measure of the local connectivity of neocortical circuits of *Fmr1* KO mice and of the number of outgoing connections.

(2) We are currently measuring the spine density of excitatory neurons in the target area, in order to evaluate how changes in the local- and long-ranging connectivity could influence the density. We therefore started reconstructing sparsely labeled pyramidal neurons in layer 3 of adult *Fmr1* KO and WT mice. We are using 3D reconstruction software (Imaris, Bitplane) to quantify the number of spines per dendritic segment. We will then test whether the spine density changes occur in the second generation of the *Fmr1* KO mouse model. We will determine whether the spine density correlates with the calculated sum of changes of local pre-synaptic cells and long ranging pre- synaptic cells as well as the local axonal density.

(3) In the next step we will further define the local contribution of excitatory / inhibitory input to the observed changes by quantifying the number of retrogradely labeled GABAergic interneurons in the intra-areal fraction of labeled neurons. We will therefore use immunohistochemistry to stain GABAergic neurons and quantify the number of RABV labeled inhibitory neurons in both conditions. This will allow us to determine whether the local change of presynaptic neurons implies a change in the ratio of excitatory vs. inhibitory input.

(4) Once these experiments regarding the characterization of the connectivity phenotype in Fmr1KO mice are completed, this knowledge will provide a baseline for

testing the effect of different drugs on correcting alterations of the cortical wiring in FXS. Since we are correlating fine- structural measurements with non-invasive functional and structural magnetic-resonance imaging (MRI) we hope that the MRI measurements can be performed similarly on human patients. Since they can be performed repeatedly and provide another objective criteria to evaluate the efficacy of therapeutic agents.

4. References

Akins, M.R., Leblanc, H.F., Stackpole, E.E., Chyung, E., and Fallon, J.R. (2012). Systematic mapping of fragile X granules in the mouse brain reveals a potential role for presynaptic FMRP in sensorimotor functions. The Neuroscientist 520, 3687–3706.

Alexander, A.L., Lee, J.E., Lazar, M., and Field, A.S. (2007). Diffusion tensor imaging of the brain. Neurotherapeutics 4, 316–329.

Antar, L.N., Li, C., Zhang, H., Carroll, R.C., and Bassell, G.J. (2006). Local functions for FMRP in axon growth cone motility and activity-dependent regulation of filopodia and spine synapses. Mol. Cell. Neurosci. 32, 37–48.

Aschauer, D.F., Kreuz, S., and Rumpel, S. (2013). Analysis of transduction efficiency, tropism and axonal transport of AAV serotypes 1, 2, 5, 6, 8 and 9 in the mouse brain. PLoS ONE 8, e76310.

Ashley, C.T., Sutcliffe, J.S., Kunst, C.B., Leiner, H.A., Eichler, E.E., Nelson, D.L., and Warren, S.T. (1993). Human and murine FMR-1: alternative splicing and translational initiation downstream of the CGG-repeat. Nat. Genet. 4, 244–251.

Bagni, C., and Greenough, W.T. (2005). From mRNP trafficking to spine dysmorphogenesis: the roots of fragile X syndrome. Nat Rev Neurosci 6, 376–387.

Bakker, C.E., and Oostra, B.A. (2003). Understanding fragile X syndrome: insights from animal models. Cytogenet. Genome Res. 100, 111–123.

Bassell, G.J., and Warren, S.T. (2008). Fragile X Syndrome: Loss of Local mRNA Regulation Alters Synaptic Development and Function. Neuron 60, 201–214.

Basser, P.J., Mattiello, J., and LeBihan, D. (1994). MR diffusion tensor spectroscopy and imaging. Biophysical Journal 66, 259–267.

Bear, M.F. (2005). Therapeutic implications of the mGluR theory of fragile X mental retardation. Genes Brain Behav. 4, 393–398.

Bear, M.F., Huber, K.M., and Warren, S.T. (2004). The mGluR theory of fragile X mental retardation. Trends Neurosci 27, 370–377.

Berry-Kravis, E. (2002). Epilepsy in fragile X syndrome. Dev Med Child Neurol 44, 724–728.

Berry-Kravis, E., Knox, A., and Hervey, C. (2011). Targeted treatments for fragile X syndrome. J Neurodev Disord 3, 193–210.

Berry-Kravis, E., Raspa, M., Loggin-Hester, L., Bishop, E., Holiday, D., and Bailey, D.B. (2010). Seizures in fragile X syndrome: characteristics and comorbid diagnoses. Am J Intellect Dev Disabil 115, 461–472.

Bhakar, A.L., Dölen, G., and Bear, M.F. (2012). The pathophysiology of fragile X (and what it teaches us about synapses). Annu. Rev. Neurosci. 35, 417–443.

Bianconi, E., Piovesan, A., Facchin, F., Beraudi, A., Casadei, R., Frabetti, F., Vitale, L., Pelleri, M.C., Tassani, S., Piva, F., et al. (2013). An estimation of the number of cells in the human body. Ann. Hum. Biol. 40, 463–471.

Binzegger, T., Douglas, R.J., and Martin, K.A.C. (2004). A quantitative map of the circuit of cat primary visual cortex. J Neurosc 24, 8441–8453.

Boender, A.J., de Jong, J.W., Boekhoudt, L., Luijendijk, M.C.M., van der Plasse, G., and Adan, R.A.H. (2014). Combined use of the canine adenovirus-2 and DREADD-technology to activate specific neural pathways in vivo. PLoS ONE 9, e95392.

Boggs, J.M. (2006). Myelin basic protein: a multifunctional protein. Cell. Mol. Life Sci. 63, 1945–1961.

Braat, S., and Kooy, R.F. (2014). Insights into GABAAergic system deficits in fragile X syndrome lead to clinical trials. Neuropharmacology.

Broeder, den, M.J., van der Linde, H., Brouwer, J.R., Oostra, B.A., Willemsen, R., and Ketting, R.F. (2009). Generation and characterization of FMR1 knockout zebrafish. PLoS ONE 4, e7910.

Broser, P.J., Erdogan, S., Grinevich, V., Osten, P., Sakmann, B., and Wallace, D.J. (2008). Automated axon length quantification for populations of labelled neurons. Journal of Neuroscience Methods 169, 43–54.

Brown, V., Jin, P., Ceman, S., Darnell, J.C., O'Donnell, W.T., Tenenbaum, S.A., Jin, X., Feng, Y., Wilkinson, K.D., Keene, J.D., et al. (2001). Microarray identification of FMRP-associated brain mRNAs and altered mRNA translational profiles in fragile X syndrome. Cell 107, 477–487.

Bullmore, E., and Sporns, O. (2009). Complex brain networks: graph theoretical analysis of structural and functional systems. Nat Rev Neurosci 10, 186–198.

Bureau, I., Shepherd, G.M.G., and Svoboda, K. (2008). Circuit and Plasticity Defects in the Developing Somatosensory Cortex of Fmr1 Knock-Out Mice. J Neurosc 28, 5178–5188.

Bushong, E.A., Martone, M.E., Jones, Y.Z., and Ellisman, M.H. (2002). Protoplasmic astrocytes in CA1 stratum radiatum occupy separate anatomical domains. J Neurosc 22, 183–192.

Cahoy, J.D., Emery, B., Kaushal, A., Foo, L.C., Zamanian, J.L., Christopherson, K.S., Xing, Y., Lubischer, J.L., Krieg, P.A., Krupenko, S.A., et al. (2008). A transcriptome database for astrocytes, neurons, and oligodendrocytes: a new resource for understanding brain development and function. J Neurosc 28, 264–278.

Callaway, E.M. (2008). Transneuronal circuit tracing with neurotropic viruses. Curr Opin Neurobiol 18, 617–623.

Carpentier, D.C.J., Vevis, K., Trabalza, A., Georgiadis, C., Ellison, S.M., Asfahani, R.I., and Mazarakis, N.D. (2012). Enhanced pseudotyping efficiency of HIV-1 lentiviral vectors by a rabies/vesicular stomatitis virus chimeric envelope

glycoprotein. Gene Therapy 19, 761–774.

Ceman, S., O'Donnell, W.T., Reed, M., Patton, S., Pohl, J., and Warren, S.T. (2003). Phosphorylation influences the translation state of FMRP-associated polyribosomes. Hum. Mol. Genet. 12, 3295–3305.

Christie, S.B., Akins, M.R., Schwob, J.E., and Fallon, J.R. (2009). The FXG: a presynaptic fragile X granule expressed in a subset of developing brain circuits. J Neurosc 29, 1514–1524.

Clerx, L., Visser, P.J., Verhey, F., and Aalten, P. (2012). New MRI markers for Alzheimer's disease: a meta-analysis of diffusion tensor imaging and a comparison with medial temporal lobe measurements. J. Alzheimers Dis. 29, 405–429.

Conzelmann, K.K., and Schnell, M. (1994). Rescue of synthetic genomic RNA analogs of rabies virus by plasmid-encoded proteins. J Virol 68, 713–719.

Curia, G., Papouin, T., Séguéla, P., and Avoli, M. (2009). Downregulation of tonic GABAergic inhibition in a mouse model of fragile X syndrome. Cerebral Cortex 19, 1515–1520.

D'Hooge, R., Nagels, G., Franck, F., Bakker, C.E., Reyniers, E., Storm, K., Kooy, R.F., Oostra, B.A., Willems, P.J., and De Deyn, P.P. (1997). Mildly impaired water maze performance in male Fmr1 knockout mice. Nsc 76, 367–376.

D'Hulst, C., and Kooy, R.F. (2009). Fragile X syndrome: from molecular genetics to therapy. J. Med. Genet. 46, 577–584.

D'Hulst, C., De Geest, N., Reeve, S.P., Van Dam, D., De Deyn, P.P., Hassan, B.A., and Kooy, R.F. (2006). Decreased expression of the GABAA receptor in fragile X syndrome. Brain Research 1121, 238–245.

Darnell, J.C., Jensen, K.B., Jin, P., Brown, V., Warren, S.T., and Darnell, R.B. (2001). Fragile X mental retardation protein targets G quartet mRNAs important for neuronal function. Cell 107, 489–499.

Darnell, J.C., and Klann, E. (2013). The translation of translational control by FMRP: therapeutic targets for FXS. Nature Neuroscience 16, 1530–1536.

Darnell, J.C., and Richter, J.D. (2012). Cytoplasmic RNA-binding proteins and the control of complex brain function. Cold Spring Harb Perspect Biol 4, a012344.

Darnell, J.C., Van Driesche, S.J., Zhang, C., Hung, K.Y.S., Mele, A., Fraser, C.E., Stone, E.F., Chen, C., Fak, J.J., Chi, S.W., et al. (2011). FMRP stalls ribosomal translocation on mRNAs linked to synaptic function and autism. Cell 146, 247–261.

Debanne, D., Boudkkazi, S., Campanac, E., Cudmore, R.H., Giraud, P., Fronzaroli-Molinieres, L., Carlier, E., and Caillard, O. (2008). Paired-recordings from synaptically coupled cortical and hippocampal neurons in acute and cultured brain slices. Nat Protoc 3, 1559–1568.

Deng, P.-Y., Rotman, Z., Blundon, J.A., Cho, Y., Cui, J., Cavalli, V., Zakharenko,

S.S., and Klyachko, V.A. (2013). FMRP regulates neurotransmitter release and synaptic information transmission by modulating action potential duration via BK channels. Neuron 77, 696–711.

Dictenberg, J.B., Swanger, S.A., Antar, L.N., Singer, R.H., and Bassell, G.J. (2008). A direct role for FMRP in activity-dependent dendritic mRNA transport links filopodial-spine morphogenesis to fragile X syndrome. Dev. Cell 14, 926–939.

Dobkin, C., Rabe, A., Dumas, R., Idrissi, El, A., Haubenstock, H., and Brown, W.T. (2000). Fmr1 knockout mouse has a distinctive strain-specific learning impairment. Nsc 100, 423–429.

Dolan, B.M., Duron, S.G., Campbell, D.A., Vollrath, B., Shankaranarayana Rao, B.S., Ko, H.-Y., Lin, G.G., Govindarajan, A., Choi, S.-Y., and Tonegawa, S. (2013). Rescue of fragile X syndrome phenotypes in Fmr1 KO mice by the small-molecule PAK inhibitor FRAX486. Proc. Natl. Acad. Sci. U.S.a. 110, 5671–5676.

Dominguez, E., Galmozzi, A., Chang, J.W., Hsu, K.-L., Pawlak, J., Li, W., Godio, C., Thomas, J., Partida, D., Niessen, S., et al. (2014). Integrated phenotypic and activity-based profiling links Ces3 to obesity and diabetes. Nat. Chem. Biol. 10, 113–121.

Ellegood, J., Pacey, L.K., Hampson, D.R., Lerch, J.P., and Henkelman, R.M. (2010). Anatomical phenotyping in a mouse model of fragile X syndrome with magnetic resonance imaging. NeuroImage 53, 1023–1029.

Etessami, R., Conzelmann, K.K., Fadai-Ghotbi, B., Natelson, B., Tsiang, H., and Ceccaldi, P.E. (2000). Spread and pathogenic characteristics of a G-deficient rabies virus recombinant: an in vitro and in vivo study. J. Gen. Virol. 81, 2147–2153.

Finke, S., Cox, J.H., and Conzelmann, K.K. (2000). Differential transcription attenuation of rabies virus genes by intergenic regions: generation of recombinant viruses overexpressing the polymerase gene. J Virol 74, 7261–7269.

Finke, S., and Conzelmann, K.-K. (2003). Dissociation of rabies virus matrix proteanin functions in regulation of viral RNA synthesis and virus assembly. J Virol 77, 12074–12082.

Finke, S., Mueller-Waldeck, R., and Conzelmann, K.-K. (2003). Rabies virus matrix protein regulates the balance of virus transcription and replication. J. Gen. Virol. 84, 1613–1621.

Fishell, G., and Heintz, N. (2013). The neuron identity problem: form meets function. Neuron 80, 602–612.

Garber, K.B., Visootsak, J., and Warren, S.T. (2008). Fragile X syndrome. Eur. J. Hum. Genet. 16, 666–672.

Geschwind, D.H., and Levitt, P. (2006). Autism spectrum disorders: developmental disconnection syndromes. Curr Opin Neurobiol 17, 103–111.

Giampetruzzi, A., Carson, J.H., and Barbarese, E. (2013). FMRP and myelin protein expression in oligodendrocytes. Mol. Cell. Neurosci. 56, 333–341.

Gibson, J.R., Bartley, A.F., Hays, S.A., and Huber, K.M. (2008). Imbalance of neocortical excitation and inhibition and altered UP states reflect network hyperexcitability in the mouse model of fragile X syndrome. Journal of Neurophysiology 100, 2615–2626.

Ginger, M., Haberl, M., Conzelmann, K.-K., Schwarz, M.K., and Frick, A. (2013). Revealing the secrets of neuronal circuits with recombinant rabies virus technology. Front. Neural Circuits 7, 2.

Golgi, C. (1873). Sulla struttura della sostanza grigia del cervello. Gazzetta Medica Italiana Lombardia.

Goñi, J., van den Heuvel, M.P., Avena-Koenigsberger, A., Velez de Mendizabal, N., Betzel, R.F., Griffa, A., Hagmann, P., Corominas-Murtra, B., Thiran, J.-P., and Sporns, O. (2014). Resting-brain functional connectivity predicted by analytic measures of network communication. Proc. Natl. Acad. Sci. U.S.a. 111, 833–838.

Gonçalves, J.T., Anstey, J.E., Golshani, P., and Portera-Cailliau, C. (2013). Circuit level defects in the developing neocortex of Fragile X mice. Nature Neuroscience 16, 903–909.

Goraly, N.B., Eliez, S., and Hedeus, M. (2003). White matter tract alterations in fragile X syndrome: preliminary evidence from diffusion tensor imaging. American Journal of ….

Gothelf, D., Furfaro, J.A., Hoeft, F., Eckert, M.A., Hall, S.S., O'Hara, R., Erba, H.W., Ringel, J., Hayashi, K.M., Patnaik, S., et al. (2007). Neuroanatomy of fragile X syndrome is associated with aberrant behavior and the fragile X mental retardation protein (FMRP). Ann Neurol 63, 40–51.

Grahn, J.A., Parkinson, J.A., and Owen, A.M. (2008). The cognitive functions of the caudate nucleus. Progress in Neurobiology 86, 141–155.

Gray, S.J., Foti, S.B., Schwartz, J.W., Bachaboina, L., Taylor-Blake, B., Coleman, J., Ehlers, M.D., Zylka, M.J., McCown, T.J., and Samulski, R.J. (2011). Optimizing promoters for recombinant adeno-associated virus-mediated gene expression in the peripheral and central nervous system using self-complementary vectors. Hum. Gene Ther. 22, 1143–1153.

Greicius, M.D., and Kimmel, D.L. (2012). Neuroimaging insights into network-based neurodegeneration. Current Opinion in Neurology 25, 727–734.

Haas, B.W., Barnea-Goraly, N., Lightbody, A.A., Patnaik, S.S., Hoeft, F., Hazlett, H., Piven, J., and Reiss, A.L. (2009). Early white-matter abnormalities of the ventral frontostriatal pathway in fragile X syndrome. Dev Med Child Neurol 51, 593–599.

Haberl, M.G., Viana da Silva, S., Guest, J.M., Ginger, M., Ghanem, A., Mulle, C., Oberlaender, M., Conzelmann, K.-K., and Frick, A. (2014). An anterograde rabies virus vector for high-resolution large-scale reconstruction of 3D neuron morphology. Brain Struct Funct.

Hagerman, R.J., and Hagerman, P.J. (2002). The fragile X premutation: into the phenotypic fold. Curr. Opin. Genet. Dev. 12, 278–283.

Hall, S.S., Jiang, H., Reiss, A.L., and Greicius, M.D. (2013). Identifying large-scale brain networks in fragile X syndrome. JAMA Psychiatry 70, 1215–1223.

Hallahan, B.P., Craig, M.C., Toal, F., Daly, E.M., Moore, C.J., Ambikapathy, A., Robertson, D., Murphy, K.C., and Murphy, D.G.M. (2011). In vivo brain anatomy of adult males with Fragile X syndrome: an MRI study. NeuroImage 54, 16–24.

Harris, S.W., Hessl, D., Goodlin-Jones, B., Ferranti, J., Bacalman, S., Barbato, I., Tassone, F., Hagerman, P.J., Herman, H., and Hagerman, R.J. (2008). Autism profiles of males with fragile X syndrome. Am J Ment Retard 113, 427–438.

Hatton, D.D., Buckley, E., Lachiewicz, A., and Roberts, J. (1998). Ocular status of boys with fragile X syndrome: a prospective study. J Aapos 2, 298–302.

Hayashi, M.L., Rao, B.S.S., Seo, J.-S., Choi, H.-S., Dolan, B.M., Choi, S.-Y., Chattarji, S., and Tonegawa, S. (2007). Inhibition of p21-activated kinase rescues symptoms of fragile X syndrome in mice. Proc. Natl. Acad. Sci. U.S.a. 104, 11489–11494.

Hays, S.A., Huber, K.M., and Gibson, J.R. (2011). Altered neocortical rhythmic activity states in Fmr1 KO mice are due to enhanced mGluR5 signaling and involve changes in excitatory circuitry. J Neurosc 31, 14223–14234.

Hazlett, H.C., Poe, M.D., Lightbody, A.A., Gerig, G., Macfall, J.R., Ross, A.K., Provenzale, J., Martin, A., Reiss, A.L., and Piven, J. (2009). Teasing apart the heterogeneity of autism: Same behavior, different brains in toddlers with fragile X syndrome and autism. J Neurodev Disord 1, 81–90.

He, C.X., and Portera-Cailliau, C. (2013). The trouble with spines in fragile X syndrome: density, maturity and plasticity. Neuroscience 251, 120–128.

Henderson, C., Wijetunge, L., Kinoshita, M.N., Shumway, M., Hammond, R.S., Postma, F.R., Brynczka, C., Rush, R., Thomas, A., Paylor, R., et al. (2012). Reversal of disease-related pathologies in the fragile X mouse model by selective activation of GABAB receptors with arbaclofen. Sci Transl Med 4, 152ra128.

Hessl, D., Rivera, S.M., and Reiss, A.L. (2004). The neuroanatomy and neuroendocrinology of fragile X syndrome. Ment Retard Dev Disabil Res Rev 10, 17–24.

Heulens, I., D'Hulst, C., Braat, S., Rooms, L., and Kooy, R.F. (2010). Involvement and therapeutic potential of the GABAergic system in the fragile X syndrome. ScientificWorldJournal 10, 2198–2206.

Heulens, I., D'Hulst, C., Van Dam, D., De Deyn, P.P., and Kooy, R.F. (2012). Pharmacological treatment of fragile X syndrome with GABAergic drugs in a knockout mouse model. Behavioural Brain Research 229, 244–249.

Hildebrand, C., Remahl, S., Persson, H., and Bjartmar, C. (1993). Myelinated nerve

fibres in the CNS. Progress in Neurobiology 40, 319–384.

Hinds, H.L., Ashley, C.T., Sutcliffe, J.S., Nelson, D.L., Warren, S.T., Housman, D.E., and Schalling, M. (1993). Tissue specific expression of FMR-1 provides evidence for a functional role in fragile X syndrome. Nat. Genet. 3, 36–43.

Hinton, V.J., Brown, W.T., Wisniewski, K., and Rudelli, R.D. (1991). Analysis of neocortex in three males with the fragile X syndrome. Am. J. Med. Genet. 41, 289–294.

Hoeft, F., Lightbody, A.A., Hazlett, H.C., Patnaik, S., Piven, J., and Reiss, A.L. (2008). Morphometric spatial patterns differentiating boys with fragile X syndrome, typically developing boys, and developmentally delayed boys aged 1 to 3 years. Arch. Gen. Psychiatry 65, 1087–1097.

Hong, S., Hwang, D.-Y., Yoon, S., Isacson, O., Ramezani, A., Hawley, R.G., and Kim, K.-S. (2007). Functional analysis of various promoters in lentiviral vectors at different stages of in vitro differentiation of mouse embryonic stem cells. Mol. Ther. 15, 1630–1639.

Hou, L., Antion, M.D., Hu, D., Spencer, C.M., Paylor, R., and Klann, E. (2006). Dynamic translational and proteasomal regulation of fragile X mental retardation protein controls mGluR-dependent long-term depression. Neuron 51, 441–454.

Huber, K.M., Gallagher, S.M., Warren, S.T., and Bear, M.F. (2002). Altered synaptic plasticity in a mouse model of fragile X mental retardation. Proc. Natl. Acad. Sci. U.S.a. 99, 7746–7750.

Hunnicutt, B.J., Long, B.R., Kusefoglu, D., Gertz, K.J., Zhong, H., and Mao, T. (2014). A comprehensive thalamocortical projection map at the mesoscopic level. Nature Neuroscience 17, 1276–1285.

Jakobsson, J., and Lundberg, C. (2006). Lentiviral Vectors for Use in the Central Nervous System. Molecular Therapy 13, 484–493.

Kates, W.R., Abrams, M.T., Kaufmann, W.E., Breiter, S.N., and Reiss, A.L. (1997). Reliability and validity of MRI measurement of the amygdala and hippocampus in children with fragile X syndrome. Psychiatry Res 75, 31–48.

Kato, S., Inoue, K.-I., Kobayashi, K., Yasoshima, Y., Miyachi, S., Inoue, S., Hanawa, H., Shimada, T., Takada, M., and Kobayashi, K. (2007). Efficient gene transfer via retrograde transport in rodent and primate brains using a human immunodeficiency virus type 1-based vector pseudotyped with rabies virus glycoprotein. Hum. Gene Ther. 18, 1141–1151.

Kato, S., Kobayashi, K., and Kobayashi, K. (2014). Improved transduction efficiency of a lentiviral vector for neuron-specific retrograde gene transfer by optimizing the junction of fusion envelope glycoprotein. Journal of Neuroscience Methods 227, 151–158.

Kaufmann, W.E., Cortell, R., Kau, A.S.M., Bukelis, I., Tierney, E., Gray, R.M., Cox,

C., Capone, G.T., and Stanard, P. (2004). Autism spectrum disorder in fragile X syndrome: communication, social interaction, and specific behaviors. Am. J. Med. Genet. A 129A, 225–234.

Kelly, R.M., and Strick, P.L. (2000). Rabies as a transneuronal tracer of circuits in the central nervous system. Journal of Neuroscience Methods 103, 63–71.

Klemmer, P., Meredith, R.M., Holmgren, C.D., Klychnikov, O.I., Stahl-Zeng, J., Loos, M., van der Schors, R.C., Wortel, J., de Wit, H., Spijker, S., et al. (2011). Proteomics, ultrastructure, and physiology of hippocampal synapses in a fragile X syndrome mouse model reveal presynaptic phenotype. Journal of Biological Chemistry 286, 25495–25504.

Koekkoek, S.K.E., Yamaguchi, K., Milojkovic, B.A., Dortland, B.R., Ruigrok, T.J.H., Maex, R., De Graaf, W., Smit, A.E., VanderWerf, F., Bakker, C.E., et al. (2005). Deletion of FMR1 in Purkinje cells enhances parallel fiber LTD, enlarges spines, and attenuates cerebellar eyelid conditioning in Fragile X syndrome. Neuron 47, 339–352.

Kooy, R.F., D'Hooge, R., Reyniers, E., Bakker, C.E., Nagels, G., De Boulle, K., Storm, K., Clincke, G., De Deyn, P.P., Oostra, B.A., et al. (1996). Transgenic mouse model for the fragile X syndrome. Am. J. Med. Genet. 64, 241–245.

Kooy, R.F., Reyniers, E., Verhoye, M., Sijbers, J., Bakker, C.E., Oostra, B.A., Willems, P.J., and Van Der Linden, A. (1999). Neuroanatomy of the fragile X knockout mouse brain studied using in vivo high resolution magnetic resonance imaging. Eur. J. Hum. Genet. 7, 526–532.

Kooy, R.F. (2003). Of mice and the fragile X syndrome. Trends Genet. 19, 148–154.

Larson, J., Jessen, R.E., Kim, D., Fine, A.-K.S., and Hoffmann, du, J. (2005). Age-dependent and selective impairment of long-term potentiation in the anterior piriform cortex of mice lacking the fragile X mental retardation protein. J Neurosc 25, 9460–9469.

Li, J., Pelletier, M.R., Perez Velazquez, J.-L., and Carlen, P.L. (2002). Reduced cortical synaptic plasticity and GluR1 expression associated with fragile X mental retardation protein deficiency. Mol. Cell. Neurosci. 19, 138–151.

Li, Z., Zhang, Y., Ku, L., Wilkinson, K.D., Warren, S.T., and Feng, Y. (2001). The fragile X mental retardation protein inhibits translation via interacting with mRNA. Nucleic Acids Res. 29, 2276–2283.

Liao, L., Park, S.K., Xu, T., Vanderklish, P., and Yates, J.R. (2008). Quantitative proteomic analysis of primary neurons reveals diverse changes in synaptic protein content in fmr1 knockout mice. Proc. Natl. Acad. Sci. U.S.a. 105, 15281–15286.

Lightbody, A.A., and Reiss, A.L. (2009). Gene, brain, and behavior relationships in fragile X syndrome: evidence from neuroimaging studies. Developmental Disabilities Research ….

Loesch, D., and Hagerman, R. (2012). Unstable mutations in the FMR1 gene and the

phenotypes. Adv. Exp. Med. Biol. 769, 78–114.

Logothetis, N.K. (2008). What we can do and what we cannot do with fMRI. Nature 453, 869–878.

Markov, N.T., Misery, P., Falchier, A., Lamy, C., Vezoli, J., Quilodran, R., Gariel, M.A., Giroud, P., Ercsey-Ravasz, M., Pilaz, L.J., et al. (2011). Weight consistency specifies regularities of macaque cortical networks. Cerebral Cortex 21, 1254–1272.

McClure, C., Cole, K.L.H., Wulff, P., Klugmann, M., and Murray, A.J. (2011). Production and titering of recombinant adeno-associated viral vectors. JoVE e3348.

McLennan, Y., Polussa, J., Tassone, F., and Hagerman, R. (2011). Fragile x syndrome. Curr. Genomics 12, 216–224.

Mebatsion, T., Weiland, F., and Conzelmann, K.K. (1999). Matrix protein of rabies virus is responsible for the assembly and budding of bullet-shaped particles and interacts with the transmembrane spike glycoprotein G. J Virol 73, 242–250.

Merenstein, S.A., Sobesky, W.E., Taylor, A.K., Riddle, J.E., Tran, H.X., and Hagerman, R.J. (1996). Molecular-clinical correlations in males with an expanded FMR1 mutation. Am. J. Med. Genet. 64, 388–394.

Michalon, A., Sidorov, M., Ballard, T.M., Ozmen, L., Spooren, W., Wettstein, J.G., Jaeschke, G., Bear, M.F., and Lindemann, L. (2012). Chronic pharmacological mGlu5 inhibition corrects fragile X in adult mice. Neuron 74, 49–56.

Mientjes, E.J., Nieuwenhuizen, I., Kirkpatrick, L., Zu, T., Hoogeveen-Westerveld, M., Severijnen, L., Rifé, M., Willemsen, R., Nelson, D.L., and Oostra, B.A. (2006). The generation of a conditional Fmr1 knock out mouse model to study Fmrp function in vivo. Neurobiology of Disease 21, 549–555.

Miller, L.J., McIntosh, D.N., McGrath, J., Shyu, V., Lampe, M., Taylor, A.K., Tassone, F., Neitzel, K., Stackhouse, T., and Hagerman, R.J. (1999). Electrodermal responses to sensory stimuli in individuals with fragile X syndrome: a preliminary report. Am. J. Med. Genet. 83, 268–279.

Müller, R.-A., Shih, P., Keehn, B., Deyoe, J.R., Leyden, K.M., and Shukla, D.K. (2011). Underconnected, but how? A survey of functional connectivity MRI studies in autism spectrum disorders. Cerebral Cortex 21, 2233–2243.

Nelson, A., Schneider, D.M., Takatoh, J., Sakurai, K., Wang, F., and Mooney, R. (2013). A circuit for motor cortical modulation of auditory cortical activity. J Neurosc 33, 14342–14353.

Neves, G., Cooke, S.F., and Bliss, T.V.P. (2008). Synaptic plasticity, memory and the hippocampus: a neural network approach to causality. Nat Rev Neurosci 9, 65–75.

Nimchinsky, E.A., Oberlander, A.M., and Svoboda, K. (2001). Abnormal development of dendritic spines in FMR1 knock-out mice. J Neurosc 21, 5139–5146.

O'Donnell, W.T., and Warren, S.T. (2002). A decade of molecular studies of fragile X

syndrome. Annu. Rev. Neurosci. 25, 315–338.

Oh, S.W., Harris, J.A., Ng, L., Winslow, B., Cain, N., Mihalas, S., Wang, Q., Lau, C., Kuan, L., Henry, A.M., et al. (2014). A mesoscale connectome of the mouse brain. Nature 508, 207–214.

Olmos-Serrano, J.L., Paluszkiewicz, S.M., Martin, B.S., Kaufmann, W.E., Corbin, J.G., and Huntsman, M.M. (2010). Defective GABAergic neurotransmission and pharmacological rescue of neuronal hyperexcitability in the amygdala in a mouse model of fragile X syndrome. J Neurosc 30, 9929–9938.

Osakada, F., and Callaway, E.M. (2013). Design and generation of recombinant rabies virus vectors. Nat Protoc 8, 1583–1601.

Pacey, L.K.K., and Doering, L.C. (2007). Developmental expression of FMRP in the astrocyte lineage: implications for fragile X syndrome. Glia 55, 1601–1609.

Patel, A.B., Hays, S.A., Bureau, I., Huber, K.M., and Gibson, J.R. (2013). A target cell-specific role for presynaptic Fmr1 in regulating glutamate release onto neocortical fast-spiking inhibitory neurons. J Neurosc 33, 2593–2604.

Patel, A.B., Loerwald, K.W., Huber, K.M., and Gibson, J.R. (2014). Postsynaptic FMRP promotes the pruning of cell-to-cell connections among pyramidal neurons in the L5A neocortical network. J Neurosc 34, 3413–3418.

Peça, J., and Feng, G. (2012). Cellular and synaptic network defects in autism. Curr Opin Neurobiol 22, 866–872.

Pfeiffer, B.E., and Huber, K.M. (2007). Fragile X mental retardation protein induces synapse loss through acute postsynaptic translational regulation. J Neurosc 27, 3120–3130.

Pieretti, M., Zhang, F.P., Fu, Y.H., Warren, S.T., Oostra, B.A., Caskey, C.T., and Nelson, D.L. (1991). Absence of expression of the FMR-1 gene in fragile X syndrome. Cell 66, 817–822.

Reiss, A.L., Abrams, M.T., Greenlaw, R., Freund, L., and Denckla, M.B. (1995). Neurodevelopmental effects of the FMR-1 full mutation in humans. Nat Med 1, 159–167.

Reiss, A.L., Patel, S., Kumar, A.J., and Freund, L. (1988). Preliminary communication: neuroanatomical variations of the posterior fossa in men with the fragile X (Martin-Bell) syndrome. Am. J. Med. Genet. 31, 407–414.

Ronesi, J.A., Collins, K.A., Hays, S.A., Tsai, N.-P., Guo, W., Birnbaum, S.G., Hu, J.-H., Worley, P.F., Gibson, J.R., and Huber, K.M. (2012). Disrupted Homer scaffolds mediate abnormal mGluR5 function in a mouse model of fragile X syndrome. Nature Neuroscience 15, 431–40–S1.

Roy, C.S., and Sherrington, C.S. (1890). On the Regulation of the Blood-supply of the Brain. The Journal of Physiology 11, 85–158.17.

Sabaratnam, M., Vroegop, P.G., and Gangadharan, S.K. (2001). Epilepsy and EEG findings in 18 males with fragile X syndrome. Seizure 10, 60–63.

Seltzer, M.M., Baker, M.W., Hong, J., Maenner, M., Greenberg, J., and Mandel, D. (2012). Prevalence of CGG expansions of the FMR1 gene in a US population-based sample. Am. J. Med. Genet. B Neuropsychiatr. Genet. 159B, 589–597.

Senn, V., Wolff, S.B.E., Herry, C., Grenier, F., Ehrlich, I., Gründemann, J., Fadok, J.P., Müller, C., Letzkus, J.J., and Lüthi, A. (2014). Long-range connectivity defines behavioral specificity of amygdala neurons. Neuron 81, 428–437.

Siomi, H., Choi, M., Siomi, M.C., Nussbaum, R.L., and Dreyfuss, G. (1994). Essential role for KH domains in RNA binding: impaired RNA binding by a mutation in the KH domain of FMR1 that causes fragile X syndrome. Cell 77, 33–39.

Sotelo, C. (2003). Viewing the brain through the master hand of Ramón y Cajal.

Soudais, C., Laplace-Builhe, C., Kissa, K., and Kremer, E.J. (2001). Preferential transduction of neurons by canine adenovirus vectors and their efficient retrograde transport in vivo. Faseb J. 15, 2283–2285.

Soudais, C., Skander, N., and Kremer, E.J. (2004). Long-term in vivo transduction of neurons throughout the rat CNS using novel helper-dependent CAV-2 vectors. Faseb J. 18, 391–393.

Stoodley, C.J., and Schmahmann, J.D. (2009). Functional topography in the human cerebellum: a meta-analysis of neuroimaging studies. NeuroImage 44, 489–501.

Suhl, J.A., Chopra, P., Anderson, B.R., Bassell, G.J., and Warren, S.T. (2014). Analysis of FMRP mRNA target datasets reveals highly associated mRNAs mediated by G-quadruplex structures formed via clustered WGGA sequences. Hum. Mol. Genet.

Sutcliffe, J.S., Nelson, D.L., Zhang, F., Pieretti, M., Caskey, C.T., Saxe, D., and Warren, S.T. (1992). DNA methylation represses FMR-1 transcription in fragile X syndrome. Hum. Mol. Genet. 1, 397–400.

Tang, G., Gudsnuk, K., Kuo, S.-H., Cotrina, M.L., Rosoklija, G., Sosunov, A., Sonders, M.S., Kanter, E., Castagna, C., Yamamoto, A., et al. (2014). Loss of mTOR-Dependent Macroautophagy Causes Autistic-like Synaptic Pruning Deficits. Neuron 83, 1131–1143.

Tessier, C.R., and Broadie, K. (2008). Drosophila fragile X mental retardation protein developmentally regulates activity-dependent axon pruning. Development 135, 1547–1557.

Testa-Silva, G., Loebel, A., Giugliano, M., de Kock, C.P.J., Mansvelder, H.D., and Meredith, R.M. (2012). Hyperconnectivity and slow synapses during early development of medial prefrontal cortex in a mouse model for mental retardation and autism. Cerebral Cortex 22, 1333–1342.

Tomassy, G.S., Berger, D.R., Chen, H.-H., Kasthuri, N., Hayworth, K.J., Vercelli, A.,

Seung, H.S., Lichtman, J.W., and Arlotta, P. (2014). Distinct profiles of myelin distribution along single axons of pyramidal neurons in the neocortex. Science 344, 319–324.

Towne, C., Schneider, B.L., Kieran, D., Redmond, D.E., and Aebischer, P. (2010). Efficient transduction of non-human primate motor neurons after intramuscular delivery of recombinant AAV serotype 6. Gene Therapy 17, 141–146.

Tucker, B., Richards, R.I., and Lardelli, M. (2006). Contribution of mGluR and Fmr1 functional pathways to neurite morphogenesis, craniofacial development and fragile X syndrome. Hum. Mol. Genet. 15, 3446–3458.

Uhlhaas, P.J. (2013). Dysconnectivity, large-scale networks and neuronal dynamics in schizophrenia. Curr Opin Neurobiol 23, 283–290.

Van Dam, D., D'Hooge, R., Hauben, E., Reyniers, E., Gantois, I., Bakker, C.E., Oostra, B.A., Kooy, R.F., and De Deyn, P.P. (2000). Spatial learning, contextual fear conditioning and conditioned emotional response in Fmr1 knockout mice. Behavioural Brain Research 117, 127–136.

van der Molen, M.J.W., Stam, C.J., and van der Molen, M.W. (2014). Resting-state EEG oscillatory dynamics in fragile X syndrome: abnormal functional connectivity and brain network organization. PLoS ONE 9, e88451.

Verheij, C., de Graaff, E., Bakker, C.E., Willemsen, R., Willems, P.J., Meijer, N., Galjaard, H., Reuser, A.J., Oostra, B.A., and Hoogeveen, A.T. (1995). Characterization of FMR1 proteins isolated from different tissues. Hum. Mol. Genet. 4, 895–901.

Vélez-Fort, M., Rousseau, C.V., Niedworok, C.J., Wickersham, I.R., Rancz, E.A., Brown, A.P.Y., Strom, M., and Margrie, T.W. (2014). The Stimulus Selectivity and Connectivity of Layer Six Principal Cells Reveals Cortical Microcircuits Underlying Visual Processing. Neuron.

Wang, H., Ku, L., Osterhout, D.J., Li, W., Ahmadian, A., Liang, Z., and Feng, Y. (2004). Developmentally-programmed FMRP expression in oligodendrocytes: a potential role of FMRP in regulating translation in oligodendroglia progenitors. Hum. Mol. Genet. 13, 79–89.

Wang, X.-S., Peng, C.-Z., Cai, W.-J., Xia, J., Jin, D., Dai, Y., Luo, X.-G., Klyachko, V.A., and Deng, P.-Y. (2014). Activity-dependent regulation of release probability at excitatory hippocampal synapses: a crucial role of fragile X mental retardation protein in neurotransmission. Eur. J. Neurosci. 39, 1602–1612.

Watts, D.J., and Strogatz, S.H. (1998). Collective dynamics of “small-world” networks. Nature 393, 440–442.

Weiler, I.J., Irwin, S.A., Klintsova, A.Y., Spencer, C.M., Brazelton, A.D., Miyashiro, K., Comery, T.A., Patel, B., Eberwine, J., and Greenough, W.T. (1997). Fragile X mental retardation protein is translated near synapses in response to neurotransmitter activation. Proc. Natl. Acad. Sci. U.S.a. 94, 5395–5400.

Wickersham, I.R., Finke, S., Conzelmann, K.-K., and Callaway, E.M. (2007a). Retrograde neuronal tracing with a deletion-mutant rabies virus. Nature Methods 4, 47–49.

Wickersham, I.R., Lyon, D.C., Barnard, R.J.O., Mori, T., Finke, S., Conzelmann, K.-K., Young, J.A.T., and Callaway, E.M. (2007b). Monosynaptic restriction of transsynaptic tracing from single, genetically targeted neurons. Neuron 53, 639–647.

Wijetunge, L.S., Angibaud, J., Frick, A., Kind, P.C., and Nägerl, U.V. (2014). Stimulated emission depletion (STED) microscopy reveals nanoscale defects in the developmental trajectory of dendritic spine morphogenesis in a mouse model of fragile X syndrome. J Neurosc 34, 6405–6412.

Willemsen, R., Levenga, J., and Oostra, B.A. (2011). CGG repeat in the FMR1 gene: size matters. Clin. Genet. 80, 214–225.

Wilson, B.M., and Cox, C.L. (2007). Absence of metabotropic glutamate receptor-mediated plasticity in the neocortex of fragile X mice. Proc. Natl. Acad. Sci. U.S.a. 104, 2454–2459.

Wu, Z., Yang, H., and Colosi, P. (2010). Effect of genome size on AAV vector packaging. Mol. Ther. 18, 80–86.

Zalfa, F., Giorgi, M., Primerano, B., Moro, A., Di Penta, A., Reis, S., Oostra, B., and Bagni, C. (2003). The fragile X syndrome protein FMRP associates with BC1 RNA and regulates the translation of specific mRNAs at synapses. Cell 112, 317–327.

Zhang, Y.Q., Bailey, A.M., Matthies, H.J., Renden, R.B., Smith, M.A., Speese, S.D., Rubin, G.M., and Broadie, K. (2001). Drosophila fragile X-related gene regulates the MAP1B homolog Futsch to control synaptic structure and function. Cell 107, 591–603.

Zhao, M.-G., Toyoda, H., Ko, S.W., Ding, H.-K., Wu, L.-J., and Zhuo, M. (2005). Deficits in trace fear memory and long-term potentiation in a mouse model for fragile X syndrome. J Neurosc 25, 7385–7392.

Zingg, B., Hintiryan, H., Gou, L., Song, M.Y., Bay, M., Bienkowski, M.S., Foster, N.N., Yamashita, S., Bowman, I., Toga, A.W., et al. (2014). Neural Networks of the Mouse Neocortex. Cell 156, 1096–1111.

(1994). Fmr1 knockout mice: a model to study fragile X mental retardation. The Dutch-Belgian Fragile X Consortium. Cell 78, 23–33.

5. Annex

Manuscript N. 4

Use of Rhabdoviruses to Study Neural Circuitry

Melanie Ginger*, Guillaume Bony*,
Matthias Haberl & Andreas Frick
*Equal contributions.

Appearing in Biology and Pathogenesis of Rhabdo- and Filoviruses
by World Scientific Publishing Co.

Chapter 1

Use of Rhabdoviruses to Study Neural Circuitry

Melanie Ginger[†], Guillaume Bony[†], Matthias Haberl & Andreas Frick[*]

INSERM, Neurocentre Magendie, Physiopathologie de la plasticité neuronale, U862, Bordeaux, France.
[2]Univ. Bordeaux, Neurocentre Magendie, Physiopathologie de la plasticité neuronale, U862, Bordeaux, France.
[†]These authors contributed equally

andreas.frick@inserm.fr

The ability to completely map all synaptic connections (i.e. the connectome) of the brain would provide neuroscientists the possibility to test predictive hypotheses about the brain organization/behavioral capability, compare variations between two brains and find common denominators between species. Yet, the techniques to take on such a challenging task in the mammalian brain (with ~10^{11}-10^{15} synapses depending on the species) are just evolving. Large research and funding efforts are underway devoted to the unravelling of the synaptic connectivity of individual neurons, specific neuron types, and of neural circuits to link their function to the underlying structure. Modern methodological approaches from a variety of disciplines are applied to tackle the immense complexity of the task. Amongst those approaches, recombinant neurotropic viruses of the rhabdoviridae family (in particular rabies virus and vesicular stomatitis virus) have become important tools. Advances in molecular biology, mouse genetics and in virology have increased the repertoire of tools available for defining the initial targets for infection as well as permitting improved tracing of synaptically connected neurons. At the same time, new constructs enhance our ability to manipulate circuits and to monitor their activity. Recombinant neurotropic viruses based strategies, together with optogenetic, electrophysiological, imaging methods and behavioural tasks enable previously unimaginable experiments. In this chapter, we will summarize the most recent advances in the use of recombinant rhabdoviruses for understanding the function and structure of neuronal circuitry.

1. Introduction

Recent years have seen a surge of interest in mapping the functional architecture of the brain. Magnetic resonance imaging approaches have greatly contributed to the overall map of distinct brain regions and the functional (non-directional) interaction of these regions (e.g.(1)). According to the Allen Brain Atlas (http://www.alleninstitute.org/) there are more than 700 brain structures and we are only at the beginning of our quest to understand the precise synaptic organization within and between these neural circuits. Entire maps of the synaptic connectivity of these neural circuits would enable the possibility to decipher their role in defined behavioral tasks. This endeavor is evidenced by large-scale initiatives such as the Human Brain Project, as well as the plethora of articles describing connectivity data at a nano-, meso- and macroscopic level (2-4). The evolution of sophisticated chemical and optical approaches (e.g. CLARITY, two-photon tomography, array tomography (5-7) - permitting the visualization of functional circuits on a brain-wide scale - are an essential part of this initiative. However, the characterization of the anatomical wiring diagram on such a scale also requires tools for marking and identifying interconnected neurons. Traditionally this has been performed using two main tracing approaches, based on either chemical/biochemical tracers, or on neurotropic viruses. Whilst each method has a number of strengths and limitations, the crucial advantages of several neurotropic viruses are their highly synapse-specific inter-neuronal transfer and self-amplifying nature, thereby enabling the visualization of fine-detailed morphological features of strictly synaptically connected neurons
(e.g. (8-10)). In addition to the ability to visualize neuronal circuits, the capacity to control and monitor their activity is also essential for understanding their function. This latter aspect is almost exclusively within the domain of neurotropic viruses, due to their amenability to genetic manipulation.

Most studies of neuronal circuit organization have exploited two main classes of virus –the alpha herpes viruses and rhabdoviruses (11, 12). The focus of this chapter is the use of recombinant rhadoviruses for the

dissection of the structure and function of neuronal circuits. Alternative approaches employing, for example alpha herpes viruses or chemical/biochemical tracers are reviewed elsewhere (e.g. (11, 13-17)).

2. Rhabdoviruses for the Analysis of Neuronal circuits

2.1 Rabies and vesicular stomatitis viruses

Certain rhabdoviruses, such as rabies virus (RABV) and the vesicular stomatitis virus (Indiana strain; VSV) are ideally suited to studies of neuronal circuit organization due to their ability to infect the nervous system (18). To the best of our knowledge, however, the only rhabdoviruses that have thus far been used for circuit analysis are and the closely related lyssavirus, rabies virus. Conceivably, other lyssaviruses might also be useful for studies in the nervous system due to their infectious properties. Rabies virus (RABV) has a long history of use as a transneuronal tracer and is thus, in many ways, the prototypic neurotropic tracer. Through the pioneering work of Strick, Ugolini and colleagues, much is known about the specific features of this tracer, in particular it's exclusively retrograde, trans-synaptic spread and the high level expression of its gene products (reviewed in (9, 11)). The native RABV is a poly-synaptic trans-synaptic tracer, meaning that after it has crossed synapses of the first-order neurons it will continue to do so, thereby infecting second- and then higher-order neurons (Fig. a, b). Although this property has certain advantages for addressing particular experimental questions (for example the flow of information from the CNS to the periphery) it is also a limitation, not in the least because of the convergent nature of many circuits (11, 19). Indeed, over the course of the trans-synaptic crossing and infection it becomes impossible to distinguish first-order from second- or high-order connected neurons.

Vesicular stomatitis virus (VSV) is a relative new-comer to the field of neuronal circuit analysis and it is uncertain whether wild-type forms are trans-synaptic in nature, or if they spread by diffusion (20, 21) reviewed in (22). Recent studies, using recombinant forms of VSV have indicated that they are also trans-synaptic. Glycoprotein-deleted forms of both

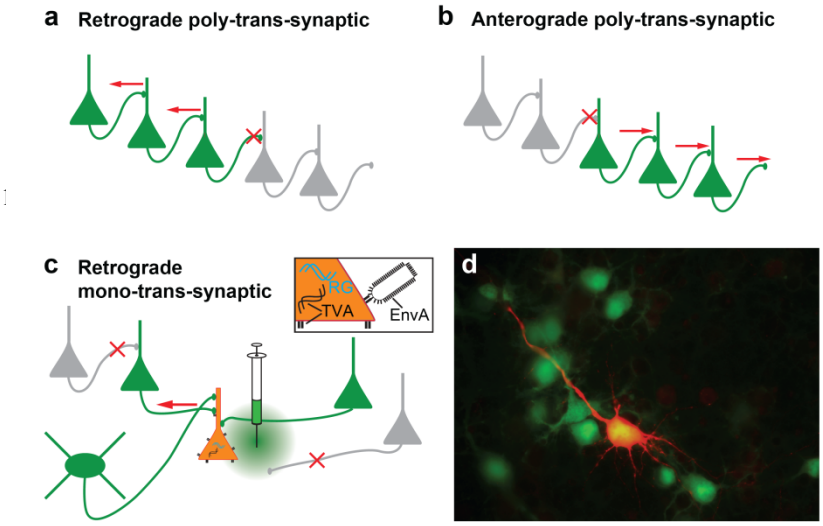

Schematic representation of different tracing possibilities
A) A retrograde poly-synaptic tracer moves from the dendrite of the post-synaptic neuron to the axon of the pre-synaptic, whereas an anterograde tracer (B) moves from the axon of a presynaptic neuron to the dendrites of a post-synaptic neuron. In both cases tracing is not limited to a single order synapse – the tracer continues to spread to the next neuron in a chain of synaptically-connected neurons. C) A mono-synaptic retrograde tracer, on the other hand, is only capable of crossing first order synapses from a postsynaptic neuron (orange) to those immediately presynaptic to it (green). D) Photomicrograph of a network of neurons traced in this manner. The single source cell (red/yellow) is connected to the presynaptic neurons in green. Panel C adapted from (9).

VSV and RABV have been described (22-26), demonstrating not only the important role of the envelope glycoprotein in trans-synaptic spread, but also the diversity of applications feasible with these glycoprotein-deleted vectors. We will therefore dedicate our discussion mostly to the potential of recombinant glycoprotein-deleted forms of both RABV and VSV for studying the physical wiring diagram of defined circuits, and for monitoring and manipulating their activity.

2.2 Glycoprotein-deleted rhabdoviruses

To overcome the limitations of 'classical' poly-synaptic viral tracers, a novel strategy was developed that restricted tracing to first order or 'mono-synaptic' synapses (8, 11). This strategy, which has come to be known as monosynaptic trans-synaptic tracing (or mono-trans- synaptic tracing, for short) was a consequence of several critical developments/innovations from the field of virus biology:
(1) The ability to rescue infectious rhabdovirus particles entirely from transfected DNA and thus manipulate the rhabdovirus genome (27-30).

(2) The finding that the infectious properties of glycoprotein-deleted forms of rhabdovirus (RbdΔG) could be rescued by either trans-complementation with their own glycoprotein or hybrid glycoproteins from other viral species (8, 23, 25, 31-34).
(3) The demonstration that RbdΔG is incapable of trans neuronal spreading (8, 22-24, 26).
(4) The development of the EnvA/TVA targeting system (35-37), which has also been used in cancer biology (38) and which permits targeting approaches which circumvent the natural tropism of a virus. Note that an avian virus receptor for subgroup B and its related glycoprotein (EnvB/TVB) has also been used in some studies (39-41).

As a result of further innovations, namely the introduction of a fluorescent marker into the viral genome (24)and approaches for trans-complementing the missing glycoprotein, the prototypic monosynaptic trans-synaptic tracing approach was developed (8). Since this approach was first developed for RABV, and has now been very well characterized using this virus, we will devote a larger part of our discussion to this work.

3 Mono-trans-synaptic tracing using RABV ΔG

Essentially this approach involves the production of a pseudotyped form of RABVΔG employing a hybrid glycoprotein containing sequences pertaining to the extracellular domain of a bird virus glycoprotein (avian sarcoma and leukosis virus EnvA glycoprotein). The resulting pseudotyped vector, RABV ΔG XFP(EnvA) (where XFP is any fluorescence marker) is incapable of infecting mammalian cells (8). Ectopic expression of the receptor for the EnvA glycoprotein (TVA) together with a trans-complementing rabies virus glycoprotein (RG), however, is sufficient to permit infection of a limited population of neurons. Since these neurons (or source cells) express RG, the production of infectious RABV ΔG particles in these cells permits trans-neuronal crossing, driving subsequent labeling of both the source cells and those immediately pre-synaptic to the source cell population (Fig. c, d).

Because of the constraints of the aforementioned tracing approach, the only neurons infected are the source cells and their first order pre-synaptic partners (source cells are distinguished by the expression of an additional fluorescent marker). The major consequence is of this development is the loss of ambiguity with the analysis of transneuronal tracing experiments. It is not only possible to discern the identity of the source cell population, but it also, for the most part, eliminates the problem of convergent connectivity patterns.

To understand the importance of this development, it is important to understand that the unequivocal synaptic pairing of neurons can only otherwise be demonstrated by paired electrophysiological recordings or by electron microscopy (EM). Light-mediated activation of the presynaptic neuron, for example by the expression of a light-sensitive ion channel such as channel rhodopsin (ChR2) in the presynaptic cell, can be used to infer connectivity. However other methods such as light activation, paired with electrophysiological recordings are needed to confirm this finding. While EM and paired electrophysiological recordings remain the gold standard for proving connectivity, they are unsuited to brain-wide circuit discovery or global circuit mapping approaches. The development of this mono-synaptically restricted tracing approach was this a major boon for field of circuit analysis.

Innovative targeting strategies (see below) permit the experimenter to determine, with more or less specificity, the identity of the target cell population. This permits not only the extraction of detailed information about the cell-type composition of certain circuits, but in certain cases, the elucidation of entirely novel connectivity patterns (e.g. (42-44)). A second major advantage is the ability to both map and manipulate the circuit under investigation. Thirdly, although this point remains the issue of some debate, this strategy also removes the aspect of ambiguity, which might theoretically arise, if certain circuits would be traced with more efficiency than others (see below). Lastly, the deletion of the glycoprotein has the effect of enhancing the survival of infected neurons,

reducing cytotoxicity (45, 46), and perhaps improving expression of the transgene (46).

3.1 Different strategies for mono-trans-synaptic tracing

As mentioned previously, the great advantage of the mono-trans-synaptic tracing approach is the ability to determine the identity of the source or starter cell population. In effective terms, this means devising a means of delivering the machinery required for mono-trans-synaptic tracing (i.e. TVA, RG and additional fluorescent marker) and limiting the expression of these factors to a more-or-less defined population of neurons. Various approaches have been developed to achieve this and may be roughly grouped into three main strategies – the use of accessory viruses, DNA transfection approaches or the use of transgenic animals. For a more detailed discussion of this issue, the reader is referred to a recent review (9, 47-49).

3.1.1 The use of accessory viruses to determine the source cell population.

The wide range of expression vectors used in modern neuroscience have, in most cases, provided ample possibilities for addressing the problem of targeting the sources cell population. These vectors can be adapted, for example by the use of a cell-type specific promoter, to target initial infection and thus mono-trans-synaptic tracing to a particular neuron type (50). More frequently, the use of a Cre-restricted expression vector is used, in conjunction with a transgenic or knock-in mouse expressing Cre in a particular neuron type (e.g. (51-56). In other cases, a more complex strategy involving a conditional bi-transgenic mouse line and an adeno associated virus (AAV) vector expressing TVA/RG under the control of a tetracycline-dependent promoter has been employed (57, 58). It has also been possible to take advantage of the inherent properties of certain certain vectors. For example retrovirus-mediated expression limits, with certain caveats (see (43)), the expression of TVA, RG and fluorescent marker encoding transgenes to proliferating neurons, a characteristic of early progenitors or neuroblasts. This approach permits

the tracing of *de novo* circuits formed as adult-born neurons integrate into an existing network (as described in (42, 43, 59)). AAV serotype 6 (AAV6) and herpes simplex virus (HSV), on the other hand, have the quality of being retrogradely transported. Approaches in which RG-expressing AAV6 and HSV vectors are coinjected with an alternatively pseudotyped form of RABV ΔG, which also has exclusively retrograde properties (see below) have permitted mono-trans-synaptic tracing from source cell population defined by their 'projection/connectivity signature' rather than by their molecular identity (60-62)
(63, 64). In this case the EnvA/TVA system is unnecessary because spatial targetting is used to limit infection to a specific population of projection neurons. Lastly, accessory vectors have been repackaged using novel pseudotyping strategies to limit their tropism to particular cellular populations (e.g. as described in (39, 40)).

3.1.2 Transfection approaches to delineate the source cell population.

In contrast to the aforementioned approaches permitting the 'bulk' targeting of populations of neurons, single cell transfection techniques can be used to identify neurons providing inputs into an individual neuron. To achieve this, expression plasmids encoding the tracing components are introduced using either two-photon-guided electroporation or whole cell patch-clamp mediated transfection (65, 66). Although painstaking, and difficult to achieve, such approaches enable the unambiguous identification of neurons presynaptic to a defined individual neuron. In combination with instance whole-cell recordings they provide unparalleled information about both the physiology and the connectivity matrix of a particular neuron.

In addition to the targeting of single neurons, *in vivo* transfection approaches as also highly suited to the targeting of specific populations of neurons, through, for example, the use of *in utero*- or early postnatal electroporation techniques. This approach has been used to target, as source cells, the neuronal progenitors of either olfactory bulb granule cells (67), or layer 2/3 pyramidal neurons in the neocortex (68). Further

specificity was achieved by spatial and temporal separation of the initial electroporation event and subsequent RABV ΔG(EnvA) infection.

3.1.3 The use of transgenic mouse for targeting of a source cell population.

A more generic option for source cell targeting is the use of a transgenic mouse line expressing TVA and RG, or TVA alone in a conditional manner. Both proteins can be placed under the control of a tetracycline-regulatable promoter (69) limiting their expression to a selccted cell populations by the choice of an appropriate tetracycline trans-activator driver line (tTA). This has enabled, for example, mono-trans-synaptic tracing from a defined population of neurons of the medial entorhinal cortex (70). Similarly, a floxed-STOP mouse line delivering either TVA, RG and fluorescent marker or TVA and RG, both in a Cre-dependent manner has been used to permit targeted tracing in combination with specific Cre driver lines (44, 59). The advantage of these approaches is that there is no need for two surgical procedures – RABV ΔG (EnvA) can be injected in a single operation. However, this approach is best suited to the analysis of long-range connections rather than local connections. Lastly, mice expressing TVA only in a Cre dependent manner (71) or through the use of a highly restricted promoter have also been described (43). In these two cases RG was delivered separately through the use of accessory virus. This measure was designed to limit false positives through lower levels of ectopic TVA expression.

3.2 Recent advances in mono-trans-synaptic tracing technology

Although the advances in mono-trans-synaptic tracing technology have recently been summarized in review form (9), we feel that the flurry of new work implicating this technology and arising over the last year merits an updated assessment of the current 'state of the art'.

Mono-trans-synaptic tracing may be used to address a multitude of questions, as well as providing a means of confirming findings from

other mapping approaches or for the discovery of novel connectivity patterns. Here we highlight the most interesting aspects of recent studies.

3.2.1.Dissecting the relationship between structure and function

The distribution of inputs can be used to extract information about the underlying functionality of a circuit. For example, there are two major outputs in the striatum and mono-trans-synaptic tracing from these two cell populations identified an asymmetry of inputs from cortical and subcortical brain areas respectively (53). There are also examples in which RABVΔG and mono-trans-synaptic tracing have been used to describe neuronal subpopulations within a well-defined brain nucleus based on their projection diagram (see (56, 72)). In the latter, the authors described a novel di-synaptic circuit transmitting sensory information from the retina to the visual cortex via an intermediate structure in the thalamus. Interestingly, this circuit was spatially segregated - in both the neocortex and thalamus – from a parallel circuit bringing different visual information from the retina to the visual cortex.

In addition, it is also possible to incorporate genetically encoded sensors into the RABV ΔG genome to monitor circuit modulation (for example see (64)). Elaborate toolboxes —encompassing mono-trans-synaptic tracing, retrograde tracing, classical tracers, optogenetics, pharmacology and behaviour studies — can now be put to use, as exemplified by Lammel et al (73). Importantly, these tools (e.g. RABV ΔG-mediated expression of ChR2) can even be used to mediate a behavioural response at the neuronal population level (73).

3.2.2 The use of mono-trans-synaptic tracing as an aid to circuit discovery.

Betley et al (56) demonstrate the utility of the mono-trans-synaptic approach for aiding circuit discovery. Another remarkable possibility with RABV ΔG is to identify the inputs of a specific neuron type. Indeed, the brain is made of a large number of structures, each composed of a vast amount of neuron types. For example, the cortex contain more

than ten interneuron subtypes (74) and nine excitatory neuron subtypes (75). Using transgenic mice, with or without additional vectors, it is possible to target a specific cell type for primary infection, such as parvalbumin positive interneurons or mitral cells in the olfactory bulb (55) or vasoactive-intestinal peptide positive interneurons of the primary visual cortex (58). Such approaches have also been used to target mono-trans-synaptic tracing to a specific layers of the entorhinal cortex, an important structure for spatial learning paradigms (70).

The mono-trans-synaptic tracing technology has also been applied successfully to the identification of spinal cord circuits. For example, the segregation and topography of premotor circuits associated with specific muscle targets has been shown (60-62).

3.2.3 Analysis of circuit remodelling

One approach, for which this technique is ideally suited, is the analysis of circuit remodelling, following, for example activity or normal developmental programmes.
Arenkiel et al (67) showed that odour stimulation resulted in enhanced tracing, resulting from an increased input onto olfactory bulb newborn neurons of odour-stimulated mice, as well as remodeling of their dendritic morphology. Novel connections from long range-inhibitory neurons were observed with adult-born neurons of the olfactory bulb (43). Interestingly, this study also suggested that migrating neuroblasts form transient connections with neurons of the rostral migrating stream and subependymal zone as they migrate to the OB. The integration of adult neurons into hippocampal circuits have also been described (42, 43, 59) albeit over different time-scales. Athough common patterns immerge, a number of novel connectivity diagrams were reported such as a transient input from CA3 (42), novel inputs from a region adjoining the ventral tegmental area (59) and early connection with neurons in the subgranular zone of the dentate gyrus (43).

Takatoh et al (44) used a modified mono-trans-synaptic tracing approach to map the premotor circuits involved in the control of coordinated whisking by premotor neurons. They analyzed the premotor neuron distribution at two distinct developmental stages, before and after the onset of whisking (i.e. postnatal day 11-14), and they were able to identify a developmental addition of projecting neurons in the premotor circuitry, which could explain the emergence of whisking. These brainstem premotor neurons also received input from the motor cortex, an area that has long been implicated in the control of whisking behaviour. Thus this study not only extended our knowledge of the circuits involved in the control of sensory information gathering, but also demonstrated age-dependent circuit remodeling using the mono-trans-synaptic tracing technique.

3.2.4 Confirming the wiring diagram

In addition to the aforementioned uses of this technology, RABV ΔG-mediated mono-trans-synaptic tracing may be used to confirm connectivity information obtained from other approaches. For example, the identity of the presynaptic layer 5 cell type providing input into layer 2/3 pyramidal neurons of the somatosensory neocortex (68) has been previously described using electrophysiological and optogenetic methods (reviewed in (76)). In addition, mono-trans-synaptic tracing has been used to confirm novel connectivity patterns discovered using other methods (see (51, 63, 77, 78). Farrow et al. (79) used mono-trans-synaptic tracing to confirm the identity of an inhibitory neuron providing presynaptic input to a defined class of ganglion cells. The identity of the presynaptic neuron was inferred by prior pharmacological experiments and by knowledge of the anatomical landscape of the retina. Undoubtedly, the intense morphological labeling conferred by the high level expression of RABV ΔG encoded fluorescence marker was an important aspect permitting the reconstruction of long-range axons from these neurons which extend over 1mm in the retina.

4. Other Tracing Strategies Using RABV ΔG

4.1 RABV ΔG as a single cycle retrograde tracer

In addition to its use for mono-trans-synaptic tracing, RABV ΔG, pseudotyped with its native glycoprotein, or that of a closely related RABV strain (RABV ΔG RG), acts as a classical retrograde tracer (23, 24, 46). RABV ΔG (RG) infects axon terminals (24) and is retrogradely transported to the cell body and dendrites of target neurons in the same manner as wild-type replication competent forms. However in the absence of trans-complementation, it remains confined to the initially infected neuron – thus acting as a 'single cycle' tracer (80). This enables the identification and also the concurrent modulation, monitoring and/or manipulation of neurons based on their projection characteristics. This approach has been used to label specific projection neurons of the somatosensory cortex of rodents and visual cortex of monkeys and cats (81-83). Concurrent injection of RABV ΔG variants expressing different fluorophores has been used to map the inputs from lateral entorhinal cortex to olfactory bulb and anterior piriform cortex in order to understand how connectivity shapes odour discrimination (84). Retrogradely-targeted RABVΔG has also been used to express ChR2 to study the post-synaptic elements of circuits involving defined projection neurons (85-87). RABV ΔG (RG) expressing Cre can be used to created conditional loss- or gain-of-function in defined projection neurons. Using such an approach, for example, Dölen et al (88) ablated oxytocin receptor function in a particular population of neurons projecting to the nucleus accumbens. Retrograde tracing approaches have also been used to confirm results obtained using mono-trans-synaptic tracing approaches (e.g. (44, 53, 55). However care is needed interpreting such findings due to the lack of precise knowledge regarding the identity of the neurons receiving these inputs. Finally, a novel kind of retrograde tracing approach was recently described in which target neurons expressing TVA were infected with RABV ΔG (EnvA) via their axon projections (89). While lacking the specificity of infection mediated via the axon terminals, it permits the un-ambiguous discrimination of TVA-expressing neurons based on their projection characteristics.

4.2 RABV ΔG as a single cycle antergrade tracer

The ability to pseudotype RABV ΔG using an alternative envelope protein permits the development of new vectors with altered tropism (e.g. (31, 32)). To extend this observation, we pseudotyped RABV ΔG with a chimeric glycoprotein containing the ectodomain of the VSV glycoprotein (VSV-G) and transmembrane- and cytoplasmic domain of RG (10). In doing so, we wished to target infection to neuronal cell bodies rather than their axons, permitting infection of neurons located at the site of infection. Indeed, we found that RBAV ΔG pseudotyped in this manner can act as an anterograde tracer rather than a retrograde tracer. Comparable findings were reported using a similar vector (pseudotyped with a chimeric glycoprotein containing the ecto- and transmembrane domains of VSVG and cytoplasmic domain of RG (90, 91). These vectors have a range of advantages, namely rapid, Golgi-like labeling of neuronal structures at the site of injection and compatibility with retrograde RABV ΔG forms, permitting reciprocal tracing of projection both to- and from a region (10, 91). Importantly, these vectors are suitable for use in aged animals, making them amenable to use in aging or neurodegeneration studies(10). This feature is not possible with most neurotropic vectors. Lastly, we were able to demonstrate that RABV ΔG can amplify from a single particle, conferring sufficient labeling to permit automated single neuron reconstruction approaches (10). The axon labeling achieved using this vector was superior to that achieved using intracellular introduction of biocytin – a method that has traditionally been use as a gold standard for single neuron reconstruction (16). This vector has a strong tropism for excitatory neurons but also permits the transduction of astrocytes (10) extending the range of cell types that can be transduced using RABV ΔG.

5. RABV as a Poly-synaptic Tracer

This subject has been the topic of numerous reviews ((13-15, 92)). We will therefore briefly highlight a number of interesting and innovative studies using this approach. Ohara et al (93) developed a recombinant form of the attenuated RABV strain, the HEP-flury strain, modified to express the envelope glycoprotein derived from the CVS strain, as well

as a number of fluorescent markers. These recombinant virus variants can be injected into different brain structures to examine convergent circuits in two colors (93-95). To overcome the difficulties in resolving first-order from higher-order connections in a polysynaptic tracing experiment, wild-type RABV was co-injected with cholera-toxin, a classical retrograde tracer (96). A complementary approach was previously suggested by López et al (97), who injected conventional biochemical tracers together with RABV to label inputs to- and from the thalamus. Finally, a recently developed single-cell targeting technique using a recombinant poly-synaptic RABV (98) may point the way to new strategies for the targeting of individual neurons.

6. Vesicular Stomatitis Virus as a Tracer of Neuronal Circuits

Although lesser known in neuroscience research, vesicular stomatitis virus (VSV) is also eminently suited to certain neuronal tracing applications. Possessing a broader tropism than RABV, it is also capable of infecting neuronal cells. Recombinant forms, suitable to genetic manipulation, permit the construction of a variety of vectors. Although capable of spreading in the CNS (20, 99), the specific trans-synaptic nature of its spread has only recently been confirmed using recombinant forms of the vector (26, 100, 101). Similar to RABV, glycoprotein deleted forms of VSV (VSVΔG) have been developed (22, 25, 26, 34). VSV readily accepts foreign transgenes and is also amenable to pseudotyping approaches (e.g. (22, 26, 34, 101, 102). VSV ΔG encoding eGFP and pseudotyped with its own glycoprotein was capable of infecting a broad range of cells in the CNS and resulted in confined focal infection, suggesting that like RABV, the glycoprotein gene is also responsible to trans-synaptic spreading. Recent studies confirm this finding and suggest that the nature of the glycoprotein can determine the direction of spreading of the recombinant virus (26, 100). Interestingly, this VSV can be engineered to spread in both an anterograde and retrograde direction permitting analysis of both inputs to and outputs from a target region (100). VSV ΔG can also be also be used to trace mono-synaptically connected circuits, however thus far this has only been demonstrated for the retrograde direction *in vivo*. The use of VSV

ΔG vectors pseudotyped with the avian sarcoma and leukosis virus (EnvA) glycoprotein permit specific targeting of a defined starter cell population, as established for RABV ΔG. Traced neurons exhibit fine morphological labeling, as has been demonstrated for RABV. The advantage of this system over RABV ΔG-mediated tracing/expression system is the extreme rapidity of transgene expression (within ~1h of infection (22, 100)). This vector is thus well suited to experiments *in vitro* systems such as cultured tissue where a rapid result is needed at a particular development time-point. In may thus also be useful in acute slices. The disadvantage, however, is the rapid toxicity. Calcium imaging experiments (calcium dynamics are used as a surrogate measure for electrical activity) showed that neurons infected with VSV ΔG were indistinguishable from WT neurons 24 post inoculation in brain slices prepared from infected mice (22). Similar findings were reported by Beier et al (100), however by 2 days post infection, electrophysiological properties of infected neurons had become aberrant, thus demonstrating a very narrow time-window for physiological experiments (100).

A novel circuit tracing approach has also been demonstrated in which the specificity of tracing is limited at the level of the pre-synaptic neuron (101) VSV ΔG has been engineered to express a chimeric glycoprotein containing extracellular sequences derived from the EnvA glycoprotein. This restricted tracing to presynaptic neurons expressing TVA (in this case engineered by Cre dependent expression using a ChAT-Cre, conditional TVA bitransgenic mouse). This vector was then pseudotyped with the rabies virus glycoprotein to permit axon infection and long-range retrograde transport of the pseudotyped vector. Following injection into the lateral geniculate nucleus (a nucleus essential for processing visual information from the retina (and which receives inputs from a wide range of retinal ganglion cells, RGC), trans-synaptic tracing was limited to starburst amacrine cells (SACs) immediate presynaptic to RGCs. Using this technique, Beier et al, described novel elements of the RGC-SAC circuitry. They also extended their description of the specificity of trans-synaptic tracing using VSV. In spite of the extensive overlap of neuronal processes, there was no infection of neurons with closely apposed structures. However, this approach may be limited to

certain types of synapses, because no tracing was observed via dendro-dendritic synapses.

7. Caveats

Although this is an extremely powerful approach, a number of caveats remain. Firstly, the long-standing principles about the specificity of tracing using the RABV (13, 92, 103) are derived mostly from studies using native (non-recombinant) forms of the virus, mostly derived from the Challenge Virus Standard (CVS). As noted (13) it is possible that other strains differ in their trans-neuronal tracing qualities. To date, almost all mono- trans- synaptic tracing studies have been performed with glycoprotein-deleted recombinant RABV derived from the highly attenuated Street Alabama Dufferin-derived strain, SAD B19. The trans-neuronal tracing qualities of this virus have now been evaluated in numerous brains regions and the following features immerge. Glycoprotein deleted SAD B19-based mono-trans-synaptic tracing is, in all but one example (see below), exclusively retrograde. Tracing occurs in an entirely synapse-specific manner (65, 67). A number of synapses of various modalities are crossed, including certain 'non-canonical' synapses such as dendro-dendritic synapse (but see also below). There is no evidence of the infection of 'fibers of passage' (e.g. (43)) although certain studies (44, 67) suggest that glial cells may be infected. The significance of the later observation has not fully been investigated. In our own work in the neocortex and hippocampus, we find no evidence of the infection of glial cells using EnvA-pseudotyped RABV ΔG of SAD B19 origin, but each brain area may be different. Finally, it is an oft-cited 'fact' that peripheral innoculation leads to transduction of motor neuron endplates, but not sensory neurons(15, 92). Recent studies show that this is not necessarily true for either SAD-B19 derived vectors or wildtype CVS-strains (44, 104, 105). Recent experiments using vectors derived from glycoprotein-deleted forms of the HEP-Flury strain of show that it can also function as an effective trans-neuronal tracer when *trans*-complemented with exogenously expressed glycoprotein (Mori and Morimoto, 2014). The specificity of tracing with this novel vector has not be characterized in detail and it is difficult to extrapolate these characteristics from other studies using this strain (e.g. (93, 95)) because

in the latter case the vector has been engineered to express a CVS-derived glycoprotein.

In spite of its enormous potential, mono-transynaptic tracing, like any other experimental approach, also has its limitations. Factors relating to the nature of the rabies negative-sense single-stranded RNA genome preclude the use of certain genetic tools possible with other neurotropic viruses (reviewed in (9, 11). Undersampling of presynaptic populations (55, 65) and the restricted time window (less than postnatal day 11) for use of the SAD B19-derived forms for tracing from the peripheral nervous system (60) are all significant factors to consider in the design of a tracing experiment. Most perturbing is the observation that this approach sometimes fails to reveal known synaptic connections. For example Wall et al (53) reported a dramatic under-labelling of striatal-inputs from substantia nigra pars compacta. This nucleus represents an important source of dopaminergic input to the striatum – a finding that was confirmed by injection of a non-trans-synaptic retrograde RABVΔG tracer (see also below). Wall and colleagues (53) speculate that the unusual structure of this synapse, which features a large extracellular space, may impede trans-synaptic tracing. Deshpande et al (43) observed a similar perplexing lack of tracing of between adult born neurons of the OB and mitral cells. This may reflect an aspect of their atypical dendro-dendritic synapses synapse or may represent some feature inherent to this type of new-born neurons, that the synapse lacks an essential molecule for trans-synaptic crossing. The molecules required for trans-synaptic crossing have not entirely been defined, although certain candidate molecules have been proposed (namely nicotinic acetylcholine receptor, neuronal cell adhesion molecule, low affinity nerve growth factor receptor (106)). It is thus possible that certain molecules may absent or present in limiting quantities in certain synapses. Another potential limitation, is that RABV ΔG particles cross synapses in a stochastic manner and that neurons with multiple inputs onto a source cell have a greater chance of being labeled in a given time window than those with sparse inputs (44). Another unanswered question is whether the probability of trans-synaptic crossing could linked to synaptic strength. This question is difficult to test experimentally, but evidence in its favour

comes from the finding that trans-synaptic tracing was more favourable in animals trained on a running wheel that sedentary animals. Although one study has shown that the activity of a synapse does not play a role in the efficiency of crossing (67), this may also strongly depend on the cell type involved. Lastly, rabies virus has been considered to be a gold standard for trans-neuronal tracing because of its obligate retrograde mode of passage. However, recent finding suggest that in certain cases this may not be the case. Zampieri et al.(105) showed that not only can RABV ΔG infect peripheral sensory neurons, but it is also capable, in certain cases, of anterograde transport. In so doing, they were able to dissect circuits involving sensory neurons, motor neurons and certain inhibitory neurons of the peripheral nervous. Reassuringly, perhaps, they demonstrated that anterograde transport is limited to the peripheral nervous system and does not occur in the CNS. The authors speculate that this may be due to different cytoskeletal dynamics in sensory neurons (c.f. CNS neurons). It is important to note, however, that this was demonstrated in P4 mice and is yet to be demonstrated in mature animals. VSV on the other hand has a limited history as a trans-synaptic tracer. Thus more studies are required to unequivocally establish its properties. It is important to note that although capable of crossing synapses in both the anterograde and retrograde direction, mono-trans-synaptic tracing has not yet been demonstrated in vivo. Lastly, it will be important to demonstrate whether attenuated forms of VSV such as those possessing the M15R mutation (107) can be used for physiological studies in vivo.

8. Perspectives

Recent developments in the field of RABV ΔG technology convincingly establish the importance and power of this tool for neural circuit mapping. Combined with other imaging, physiological, and behavioral approaches, it promises to open new avenues of research permitting a greater understanding of the mammalian connectome and its function. RABV ΔG is applicable to a range of experimental paradigms and permits not only the study of circuit structure, but also the ability to manipulate or monitor its function. VSV ΔG is a relatively new tracer

and its capabilities remain to be tested. It is likely that certain features of this vector namely the rapidity of replication and potential for anterograde mono-trans-synaptic tracing *in vivo* and ease of accepting alternative glycoproteins will lead to its preferred use in certain experimental questions.

A number of new targeting vectors and RABV ΔG variants have greatly extended the capabilities of the RABV ΔG toolbox. Many of these innovations may also be possible with VSV. The development of RABV variant expressing calcium sensors (64, 108), glutamate sensors (64), ChR2 (73), subcellular markers (91) and Cre recombinase (88, 108) extends the spectrum of approaches possible using this technology. In addition, the demonstration, for the first time that mono-trans-synaptic tracing may be targeted to non-rodent species greatly enhances the potential of this approach (50). RABV and VSV have been shown to have a very broad host range, including all mammalian species, birds and even insects (reviewed in (18)). Thus given the appropriate targeting strategy, experiments in other model systems ranging from perhaps drosophila to primates may soon be possible. The concomitant use of optical approaches (109, 110) will also greatly increase the potential of this technology for high-throughput screening approaches, making these vectors suitable for the global understanding of circuit level defects in models of pathology. Taken together these tools shows great promise for improving our understanding of neuronal circuit organisation/function as well as its plastic modification during physiological processes or in disease.

9. References

1. **Mori S**, **Zhang J**. 2006. Principles of diffusion tensor imaging and its applications to basic neuroscience research. Neuron **51**:527–539.
2. **Van Essen DC**, **Smith SM**, **Barch DM**, **Behrens TEJ**, **Yacoub E**, **Ugurbil K**, **WU-Minn HCP Consortium**. 2013. The WU-Minn Human Connectome Project: an

overview. Neuroimage **80**:62–79.

3. **Helmstaedter M**, **Briggman KL**, **Turaga SC**, **Jain V**, **Seung HS**, **Denk W**. 2013. Connectomic reconstruction of the inner plexiform layer in the mouse retina. Nature **500**:168–174.
4. **Bohland JW**, **Wu C**, **Barbas H**, **Bokil H**, **Bota M**, **Breiter HC**, **Cline HT**, **Doyle JC**, **Freed PJ**, **Greenspan RJ**, **Haber SN**, **Hawrylycz M**, **Herrera DG**, **Hilgetag CC**, **Huang ZJ**, **Jones A**, **Jones EG**, **Karten HJ**, **Kleinfeld D**, **Kötter R**, **Lester HA**, **Lin JM**, **Mensh BD**, **Mikula S**, **Panksepp J**, **Price JL**, **Safdieh J**, **Saper CB**, **Schiff ND**, **Schmahmann JD**, **Stillman BW**, **Svoboda K**, **Swanson LW**, **Toga AW**, **Van Essen DC**, **Watson JD**, **Mitra PP**. 2009. A proposal for a coordinated effort for the determination of brainwide neuroanatomical connectivity in model organisms at a mesoscopic scale. PLoS Comput. Biol. **5**:e1000334.
5. **Busse B**, **Smith S**. 2013. Automated analysis of a diverse synapse population. PLoS Comput. Biol. **9**:e1002976.
6. **Ragan T**, **Kadiri LR**, **Venkataraju KU**, **Bahlmann K**, **Sutin J**, **Taranda J**, **Arganda-Carreras I**, **Kim Y**, **Seung HS**, **Osten P**. 2012. Serial two-photon tomography for automated ex vivo mouse brain imaging. Nat. Methods **9**:255–258.
7. **Chung K**, **Deisseroth K**. 2013. CLARITY for mapping the nervous system. Nat. Methods **10**:508–513.
8. **Wickersham IR**, **Lyon DC**, **Barnard RJO**, **Mori T**, **Finke S**, **Conzelmann K-K**, **Young JAT**, **Callaway EM**. 2007. Monosynaptic restriction of transsynaptic tracing from single, genetically targeted neurons. Neuron **53**:639–647.
9. **Ginger M**, **Haberl M**, **Conzelmann K-K**, **Schwarz MK**, **Frick A**. 2013. Revealing the secrets of neuronal circuits with recombinant rabies virus technology. Frontiers in Neural Circuits **7**:2.
10. **Haberl M**, **Viana da Silva S**, **Guest M**, **Ginger M**,

Ghanem A, **Mulle C**, **Oberlaender**, **Conzelmann KK**, **Frick A**. An anterograde rabies virus vector for high-resolution
large-scale reconstruction of 3D neuron morphology. Brain Structure and Function. In Press

11. **Callaway EM**. 2008. Transneuronal circuit tracing with neurotropic viruses. Current Opinion in Neurobiology **18**:617–623.
12. **Ekstrand MI**, **Enquist LW**, **Pomeranz LE**. 2008. The alpha-herpesviruses: molecular pathfinders in nervous system circuits. Trends Mol Med **14**:134–140.
13. **Kelly RM**, **Strick PL**. 2000. Rabies as a transneuronal tracer of circuits in the central nervous system. J. Neurosci. Methods **103**:63–71.
14. **Dum RP**, **Strick PL**. 2013. Transneuronal tracing with neurotropic viruses reveals network macroarchitecture. Current Opinion in Neurobiology **23**:245–249.
15. **Ugolini G**. 2011. Rabies virus as a transneuronal tracer of neuronal connections. Advances in virus research **79**:165–202.
16. **Parekh R**, **Ascoli GA**. 2013. Neuronal morphology goes digital: a research hub for cellular and system neuroscience. Neuron **77**:1017–1038.
17. **Lanciego JL**, **Wouterlood FG**. 2011. A half century of experimental neuroanatomical tracing. J. Chem. Neuroanat. **42**:157–183.
18. **Koyuncu OO**, **Hogue IB**, **Enquist LW**. 2013. Virus infections in the nervous system. Cell Host Microbe **13**:379–393.
19. 2012. New technologies for imaging synaptic partners 1–7.
20. **Lundh B**. 1990. Spread of vesicular stomatitis virus along the visual pathways after retinal infection in the mouse. Acta Neuropathol. **79**:395–401.
21. **van den Pol AN**, **Reuter JD**, **Santarelli JG**. 2002. Enhanced cytomegalovirus infection of developing brain independent of the adaptive immune system. Journal of

Virology **76**:8842–8854.

22. **van den Pol AN**, **Ozduman K**, **Wollmann G**, **Ho WSC**, **Simon I**, **Yao Y**, **Rose JK**, **Ghosh P**. 2009. Viral strategies for studying the brain, including a replication-restricted self-amplifying delta-G vesicular stomatis virus that rapidly expresses transgenes in brain and can generate a multicolor golgi-like expression. J. Comp. Neurol. **516**:456–481.
23. **Etessami R**, **Conzelmann KK**, **Fadai-Ghotbi B**, **Natelson B**, **Tsiang H**, **Ceccaldi PE**. 2000. Spread and pathogenic characteristics of a G-deficient rabies virus recombinant: an in vitro and in vivo study. The Journal of general virology **81**:2147–2153.
24. **Wickersham IR**, **Finke S**, **Conzelmann K-K**, **Callaway EM**. 2007. Retrograde neuronal tracing with a deletion-mutant rabies virus. Nat. Methods **4**:47–49.
25. **Chandran K**, **Sullivan NJ**, **Felbor U**, **Whelan SP**, **Cunningham JM**. 2005. Endosomal proteolysis of the Ebola virus glycoprotein is necessary for infection. Science **308**:1643–1645.
26. **Beier KT**, **Arpiarr S**, **OLdenburg IA**, **Miyamichi K**, **Akhtar N**, **Luo L**, **Whelan SPJ**, **Sabatini B**, **Cepko CL**. 2011. Anterograde or retrograde transsynaptic labeling of CNS neurons with vesicular stomatitis virus vectors. Proc Natl Acad Sci USA **108**:15414–15419.
27. **Conzelmann KK**, **Schnell M**. 1994. Rescue of synthetic genomic RNA analogs of rabies virus by plasmid-encoded proteins. Journal of Virology **68**:713–719.
28. **Schnell MJ**, **Mebatsion T**, **Conzelmann KK**. 1994. Infectious rabies viruses from cloned cDNA. The EMBO Journal **13**:4195–4203.
29. **Lawson ND**, **Stillman EA**, **Whitt MA**, **Rose JK**. 1995. Recombinant vesicular stomatitis viruses from DNA. Proc Natl Acad Sci USA **92**:4477–4481.
30. **Whelan SP**, **Ball LA**, **Barr JN**, **Wertz GT**. 1995. Efficient recovery of infectious vesicular stomatitis virus entirely from cDNA clones. Proc Natl Acad Sci USA **92**:8388–

8392.

31. **Mebatsion T**, **Finke S**, **Weiland F**, **Conzelmann KK**. 1997. A CXCR4/CD4 pseudotype rhabdovirus that selectively infects HIV-1 envelope protein-expressing cells. Cell **90**:841–847.

32. **Mebatsion T**, **Conzelmann KK**. 1996. Specific infection of CD4+ target cells by recombinant rabies virus pseudotypes carrying the HIV-1 envelope spike protein. Proc Natl Acad Sci USA **93**:11366–11370.

33. **Mebatsion T**, **Schnell MJ**, **Conzelmann KK**. 1995. Mokola virus glycoprotein and chimeric proteins can replace rabies virus glycoprotein in the rescue of infectious defective rabies virus particles. Journal of Virology **69**:1444–1451.

34. **Schnell MJ**, **Johnson JE**, **Buonocore L**, **Rose JK**. 1997. Construction of a novel virus that targets HIV-1-infected cells and controls HIV-1 infection. Cell **90**:849–857.

35. **Young JA**, **Bates P**, **Varmus HE**. 1993. Isolation of a chicken gene that confers susceptibility to infection by subgroup A avian leukosis and sarcoma viruses. Journal of Virology **67**:1811–1816.

36. **Federspiel MJ**, **Bates P**, **Young JA**, **Varmus HE**, **Hughes SH**. 1994. A system for tissue-specific gene targeting: transgenic mice susceptible to subgroup A avian leukosis virus-based retroviral vectors. Proc Natl Acad Sci USA **91**:11241–11245.

37. **Bates P**, **Young JA**, **Varmus HE**. 1993. A receptor for subgroup A Rous sarcoma virus is related to the low density lipoprotein receptor. Cell **74**:1043–1051.

38. **Fisher GH**, **Orsulic S**, **Holland E**, **Hively WP**, **Li Y**, **Lewis BC**, **Williams BO**, **Varmus HE**. 1999. Development of a flexible and specific gene delivery system for production of murine tumor models. Oncogene **18**:5253–5260.

39. 2011. Monosynaptic inputs to ErbB4-expressing inhibitory neurons in mouse primary somatosensory cortex.

519:3402–3414.

40. **Choi J**, **Young JAT**, **Callaway EM**. 2010. Selective viral vector transduction of ErbB4 expressing cortical interneurons in vivo with a viral receptor-ligand bridge protein. Proc Natl Acad Sci USA **107**:16703–16708.
41. **Osakada F**, **Callaway EM**. 2013. Design and generation of recombinant rabies virus vectors. Nat Protoc **8**:1583–1601.
42. **Vivar C**, **Potter MC**, **Choi J**, **Lee J-Y**, **Stringer TP**, **Callaway EM**, **Gage FH**, **Suh H**, **van Praag H**. 2012. Monosynaptic inputs to new neurons in the dentate gyrus. Nat Commun **3**:1107.
43. **Deshpande A**, **Bergami M**, **Ghanem A**, **Conzelmann K-K**, **Lepier A**, **Götz M**, **Berninger B**. 2013. Retrograde monosynaptic tracing reveals the temporal evolution of inputs onto new neurons in the adult dentate gyrus and olfactory bulb. Proceedings of the National Academy of Sciences **110**:E1152–61.
44. **Takatoh J**, **Nelson A**, **Zhou X**, **Bolton MM**, **Ehlers MD**, **Arenkiel BR**, **Mooney R**, **Wang F**. 2013. New modules are added to vibrissal premotor circuitry with the emergence of exploratory whisking. Neuron **77**:346–360.
45. **Wickersham IR**, **Sullivan HA**, **Seung HS**. 2010. Production of glycoprotein-deleted rabies viruses for monosynaptic tracing and high-level gene expression in neurons. Nat Protoc **5**:595–606.
46. **Ohara S**, **Sato S**, **Oyama K**, **Tsutsui K-I**, **Iijima T**. 2013. Rabies virus vector transgene expression level and cytotoxicity improvement induced by deletion of glycoprotein gene. PLoS ONE **8**:e80245.
47. **Luo L**, **Callaway EM**, **Svoboda K**. 2008. Genetic dissection of neural circuits. Neuron **57**:634–660.
48. **Arenkiel BR**, **Ehlers MD**. 2009. Molecular genetics and imaging technologies for circuit-based neuroanatomy. Nature **461**:900–907.
49. **Packer AM**, **Roska B**, **Häusser M**. 2013. Targeting

neurons and photons for optogenetics. Nat. Neurosci. **16**:805–815.

50. **Liu Y-J**, **Ehrengruber MU**, **Negwer M**, **Shao H-J**, **Cetin AH**, **Lyon DC**. 2013. Tracing inputs to inhibitory or excitatory neurons of mouse and cat visual cortex with a targeted rabies virus. Curr. Biol. **23**:1746–1755.
51. **Kohara K**, **Pignatelli M**, **Rivest AJ**, **Jung H-Y**, **Kitamura T**, **Suh J**, **Frank D**, **Kajikawa K**, **Mise N**, **Obata Y**, **Wickersham IR**, **Tonegawa S**. 2014. Cell type-specific genetic and optogenetic tools reveal hippocampal CA2 circuits. Nat. Neurosci. **17**:269–279.
52. **Watabe-Uchida M**, **Zhu L**, **Ogawa SK**, **Vamanrao A**, **Uchida N**. 2012. Whole-brain mapping of direct inputs to midbrain dopamine neurons. Neuron **74**:858–873.
53. **Wall NR**, **La Parra De M**, **Callaway EM**, **Kreitzer AC**. 2013. Differential innervation of direct- and indirect-pathway striatal projection neurons. Neuron **79**:347–360.
54. **Wall NR**, **Wickersham IR**, **Cetin A**, **La Parra De M**, **Callaway EM**. 2010. Monosynaptic circuit tracing in vivo through Cre-dependent targeting and complementation of modified rabies virus. Proc Natl Acad Sci USA **107**:21848–21853.
55. **Miyamichi K**, **Shlomai-Fuchs Y**, **Shu M**, **Weissbourd BC**, **Luo L**, **Mizrahi A**. 2013. Dissecting local circuits: parvalbumin interneurons underlie broad feedback control of olfactory bulb output. Neuron **80**:1232–1245.
56. **Betley JN**, **Cao ZFH**, **Ritola KD**, **Sternson SM**. 2013. Parallel, redundant circuit organization for homeostatic control of feeding behavior. Cell **155**:1337–1350.
57. **Miyamichi K**, **Amat F**, **Moussavi F**, **Wang C**, **Wickersham I**, **Wall NR**, **Taniguchi H**, **Tasic B**, **Huang ZJ**, **He Z**, **Callaway EM**, **Horowitz MA**, **Luo L**. 2010. Cortical representations of olfactory input by trans-synaptic tracing. Nature **472**:191–196.
58. **Fu Y**, **Tucciarone JM**, **Espinosa JS**, **Sheng N**, **Darcy DP**, **Nicoll RA**, **Huang ZJ**, **Stryker MP**. 2014. A cortical

circuit for gain control by behavioral state. Cell **156**:1139–1152.

59. **Li Y**, **Stam FJ**, **Aimone JB**, **Goulding M**, **Callaway EM**, **Gage FH**. 2013. Molecular layer perforant path-associated cells contribute to feed-forward inhibition in the adult dentate gyrus. Proceedings of the National Academy of Sciences **110**:9106–9111.
60. 2010. Monosynaptic Rabies Virus Reveals Premotor Network Organization and Synaptic Specificity of Cholinergic Partition Cells **68**:456–472.
61. **Tripodi M**, **Stepien AE**, **Arber S**. 2011. Motor antagonism exposed by spatial segregation and timing of neurogenesis. Nature **479**:61–66.
62. **Pivetta C**, **Esposito MS**, **Sigrist M**, **Arber S**. 2014. Motor-circuit communication matrix from spinal cord to brainstem neurons revealed by developmental origin. Cell **156**:537–548.
63. **Yonehara K**, **Balint K**, **Noda M**, **Nagel G**, **Bamberg E**, **Roska B**. 2011. Spatially asymmetric reorganization of inhibition establishes a motion-sensitive circuit. Nature **469**:407–410.
64. **Yonehara K**, **Roska B**. 2013. Motion detection: neuronal circuit meets theory. Cell **154**:1188–1189.
65. 2010. Targeting Single Neuronal Networks for Gene Expression and Cell Labeling In Vivo **67**:562–574.
66. 2011. Transfection via whole-cell recording in vivo: bridging single-cell physiology, genetics and connectomics **14**:527–532.
67. **Arenkiel BR**, **Hasegawa H**, **Yi JJ**, **Larsen RS**, **Wallace ML**, **Philpot BD**, **Wang F**, **Ehlers MD**. 2011. Activity-induced remodeling of olfactory bulb microcircuits revealed by monosynaptic tracing. PLoS ONE **6**:e29423.
68. **Mori T**, **Morimoto K**. 2014. Rabies virus glycoprotein variants display different patterns in rabies monosynaptic tracing. Front Neuroanat **7**:47.
69. 2010. Transgenic targeting of recombinant rabies virus

reveals monosynaptic connectivity of specific neurons. **30**:16509–16513.

70. **Rowland DC**, **Weible AP**, **Wickersham IR**, **Wu H**, **Mayford M**, **Witter MP**, **Kentros CG**. 2013. Transgenically targeted rabies virus demonstrates a major monosynaptic projection from hippocampal area CA2 to medial entorhinal layer II neurons. J. Neurosci. **33**:14889–14898.

71. **Sun Y**, **Nguyen A**, **Nguyen J**, **Le L**, **Saur D**, **Choi J**, **Callaway EM**, **Xu X**. Cell-Type-Specific Circuit Connectivity
of Hippocampal CA1 Revealed through Cre-Dependent Rabies Tracing. Cell Rep. In Press.

72. **Cruz-Martín A**, **El-Danaf RN**, **Osakada F**, **Sriram B**, **Dhande OS**, **Nguyen PL**, **Callaway EM**, **Ghosh A**, **Huberman AD**. 2014. A dedicated circuit links direction-selective retinal ganglion cells to the primary visual cortex. Nature **507**:358–361.

73. **Lammel S**, **Lim BK**, **Ran C**, **Huang KW**, **Betley MJ**, **Tye KM**, **Deisseroth K**, **Malenka RC**. 2012. Input-specific control of reward and aversion in the ventral tegmental area. Nature **491**:212–217.

74. **Markram H**, **Toledo-Rodriguez M**, **Wang Y**, **Gupta A**, **Silberberg G**, **Wu C**. 2004. Interneurons of the neocortical inhibitory system. Nature Reviews Neuroscience **5**:793–807.

75. **Oberlaender M**, **de Kock CPJ**, **Bruno RM**, **Ramirez A**, **Meyer HS**, **Dercksen VJ**, **Helmstaedter M**, **Sakmann B**. 2012. Cell type-specific three-dimensional structure of thalamocortical circuits in a column of rat vibrissal cortex. Cereb. Cortex **22**:2375–2391.

76. **Feldmeyer D**. 2012. Excitatory neuronal connectivity in the barrel cortex. Front Neuroanat **6**:24.

77. **Knobloch HS**, **Charlet A**, **Hoffmann LC**, **Eliava M**, **Khrulev S**, **Cetin AH**, **Osten P**, **Schwarz MK**, **Seeburg PH**, **Stoop R**, **Grinevich V**. 2012. Evoked axonal oxytocin

release in the central amygdala attenuates fear response. Neuron **73**:553–566.

78. 2010. Genetic dissection of an amygdala microcircuit that gates conditioned fear **468**:270–276.
79. **Farrow K**, **Teixeira M**, **Szikra T**, **Viney TJ**, **Balint K**, **Yonehara K**, **Roska B**. 2013. Ambient illumination toggles a neuronal circuit switch in the retina and visual perception at cone threshold. Neuron **78**:325–338.
80. 2011. Chapter 9 - Rabies Virus as a Research Tool and Viral Vaccine Vector, 1st ed. Elsevier Inc.
81. **Nhan HL**, **Callaway EM**. 2012. Morphology of superior colliculus- and middle temporal area-projecting neurons in primate primary visual cortex. J. Comp. Neurol. **520**:52–80.
82. **Larsen DD**. 2008. Retrograde tracing with recombinant rabies virus reveals correlations between projection targets and dendritic architecture in layer 5 of mouse barrel cortex. Frontiers in Neural Circuits **1**.
83. **Connolly JD**, **Hashemi-Nezhad M**, **Lyon DC**. 2012. Parallel feedback pathways in visual cortex of cats revealed through a modified rabies virus. J. Comp. Neurol. **520**:988–1004.
84. **Chapuis J**, **Cohen Y**, **He X**, **Zhang Z**, **Jin S**, **Xu F**, **Wilson DA**. 2013. Lateral entorhinal modulation of piriform cortical activity and fine odor discrimination. J. Neurosci. **33**:13449–13459.
85. **Apicella AJ**, **Wickersham IR**, **Seung HS**, **Shepherd GMG**. 2012. Laminarly orthogonal excitation of fast-spiking and low-threshold-spiking interneurons in mouse motor cortex. J. Neurosci. **32**:7021–7033.
86. **Kiritani T**, **Wickersham IR**, **Seung HS**, **Shepherd GMG**. 2012. Hierarchical connectivity and connection-specific dynamics in the corticospinal-corticostriatal microcircuit in mouse motor cortex. Journal of Neuroscience **32**:4992–5001.
87. **Kress GJ**, **Yamawaki N**, **Wokosin DL**, **Wickersham IR**, **Shepherd GMG**, **Surmeier DJ**. 2013. Convergent cortical

innervation of striatal projection neurons. Nat. Neurosci. **16**:665–667.

88. **Dölen G**, **Darvishzadeh A**, **Huang KW**, **Malenka RC**. 2013. Social reward requires coordinated activity of nucleus accumbens oxytocin and serotonin. Nature **501**:179–184.

89. **Huang C-C**, **Sugino K**, **Shima Y**, **Guo C**, **Bai S**, **Mensh BD**, **Nelson SB**, **Hantman AW**. 2013. Convergence of pontine and proprioceptive streams onto multimodal cerebellar granule cells. Elife **2**:e00400.

90. **Gomme EA**, **Faul EJ**, **Flomenberg P**, **McGettigan JP**, **Schnell MJ**. 2010. Characterization of a single-cycle rabies virus-based vaccine vector. Journal of Virology **84**:2820–2831.

91. **Wickersham IR**, **Sullivan HA**, **Seung HS**. 2013. Axonal and subcellular labelling using modified rabies viral vectors. Nat Commun **4**:2332.

92. **Ugolini G**. 2008. Use of rabies virus as a transneuronal tracer of neuronal connections: implications for the understanding of rabies pathogenesis. Dev Biol (Basel) **131**:493–506.

93. **Ohara S**, **Inoue K-I**, **Yamada M**, **Yamawaki T**, **Koganezawa N**, **Tsutsui K-I**, **Witter MP**, **Iijima T**. 2009. Dual transneuronal tracing in the rat entorhinal-hippocampal circuit by intracerebral injection of recombinant rabies virus vectors. Front Neuroanat **3**:1.

94. **Ohara S**, **Inoue K-I**, **Witter MP**, **Iijima T**. 2009. Untangling neural networks with dual retrograde transsynaptic viral infection. Front Neurosci **3**:344–349.

95. **Ohara S**, **Sato S**, **Tsutsui K-I**, **Witter MP**, **Iijima T**. 2013. Organization of multisynaptic inputs to the dorsal and ventral dentate gyrus: retrograde trans-synaptic tracing with rabies virus vector in the rat. PLoS ONE **8**:e78928.

96. **Suzuki L**, **Coulon P**, **Sabel-Goedknegt EH**, **Ruigrok TJH**. 2012. Organization of cerebral projections to identified cerebellar zones in the posterior cerebellum of

the rat. J. Neurosci. **32**:10854–10869.

97. **López IP**, **Salin P**, **Kachidian P**, **Barroso-Chinea P**, **Rico AJ**, **Gómez-Bautista V**, **Conte-Perales L**, **Coulon P**, **Goff LK-L**, **Lanciego JL**. 2010. The added value of rabies virus as a retrograde tracer when combined with dual anterograde tract-tracing. J. Neurosci. Methods **194**:21–27.

98. **Nguyen TD**, **Wirblich C**, **Aizenman E**, **Schnell MJ**, **Strick PL**, **Kandler K**. 2012. Targeted single-neuron infection with rabies virus for transneuronal multisynaptic tracing. J. Neurosci. Methods **209**:367–370.

99. **van den Pol AN**, **Dalton KP**, **Rose JK**. 2002. Relative neurotropism of a recombinant rhabdovirus expressing a green fluorescent envelope glycoprotein. Journal of Virology **76**:1309–1327.

100. **Beier KT**, **Saunders AB**, **OLdenburg IA**, **Sabatini BL**, **Cepko CL**. 2013. Vesicular stomatitis virus with the rabies virus glycoprotein directs retrograde transsynaptic transport among neurons in vivo. Frontiers in Neural Circuits **7**:11.

101. **Beier KT**, **Borghuis BG**, **El-Danaf RN**, **Huberman AD**, **Demb JB**, **Cepko CL**. 2013. Transsynaptic tracing with vesicular stomatitis virus reveals novel retinal circuitry. J. Neurosci. **33**:35–51.

102. **Beier KT**, **Arpiarr S**, **Odenburg IA**, **Miyamichi K**, **Akhtar N**, **Luo L**, **Whelan SPJ**, **Sabatini B**, **Cepko CL**. 2012. Correction for Beier et al., Anterograde or retrograde transsynaptic labeling of CNS neurons with vesicular stomatitis virus vectors. Proceedings of the National Academy of Sciences **109**:9219–9219.

103. **Ugolini G**. 1995. Specificity of rabies virus as a transneuronal tracer of motor networks: transfer from hypoglossal motoneurons to connected second-order and higher order central nervous system cell groups. J. Comp. Neurol. **356**:457–480.

104. **Velandia-Romero ML**, **Castellanos JE**, **Martínez-Gutiérrez M**. 2013. In vivo differential susceptibility of sensory neurons to rabies virus infection. J. Neurovirol.

105. **Zampieri N**, **Jessell TM**, **Murray AJ**. 2014. Mapping sensory circuits by anterograde transsynaptic transfer of recombinant rabies virus. Neuron **81**:766–778.

106. **Lafon M**. 2005. Rabies virus receptors. J. Neurovirol. **11**:82–87.

107. **Publicover J**, **Ramsburg E**, **Rose JK**. 2004. Characterization of nonpathogenic, live, viral vaccine vectors inducing potent cellular immune responses. Journal of Virology **78**:9317–9324.

108. 2011. New Rabies Virus Variants for Monitoring and Manipulating Activity and Gene Expression in Defined Neural Circuits **71**:617–631.

109. **Niedworok CJ**, **Schwarz I**, **Ledderose J**, **Giese G**, **Conzelmann K-K**, **Schwarz MK**. 2012. Charting monosynaptic connectivity maps by two-color light-sheet fluorescence microscopy. Cell Rep **2**:1375–1386.

110. **Dodt H-U**, **Leischner U**, **Schierloh A**, **Jährling N**, **Mauch CP**, **Deininger K**, **Deussing JM**, **Eder M**, **Zieglgänsberger W**, **Becker K**. 2007. Ultramicroscopy: three-dimensional visualization of neuronal networks in the whole mouse brain. Nat. Methods **4**:331–336.